Electronic Supplementary Material (ESI) for Polymer Chemistry.

SUPPORTING INFORMATION

Facile construction of functional poly(monothiocarbonate)s copolymers under mild operating conditions

Thomas Habets,[a] Fabiana Siragusa,[a] Alejandro J. Müller,[b] Quentin Grossman,[c] Davide Ruffoni,[c] Bruno Grignard,[a] Christophe Detrembleur [a]*

[a] Center for Education and Research on Macromolecules (CERM), CESAM Research Unit, University of Liege, Sart-Tilman B6a, Quartier Agora, 4000 Liege, Belgium.

[b] POLYMAT and Department of Polymers and Advanced Materials: Physics, Chemistry and Technology, Faculty of Chemistry, University of the Basque Country UPV/EHU, 20018 Donostia-San Sebastián, Spain; IKERBASQUE, Basque Foundation for Science, Plaza Euskadi 5, Bilbao 48009, Spain

[c] Mechanics of Biological and Bioinspired Materials Laboratory, Department of Aerospace and Mechanical Engineering, University of Liege, 4000 Liege, Belgium

Table of contents

1. Materials and Instrumentation

Materials

All chemicals were used as received. 1,4-Butanedithiol (97%), 1,4-Diaminobutane (99%), 1,8-Diazabicyclo[5.4.0]undec-7-ene (DBU, 99%), 1-Propanethiol (99%), 2-Furanmethanethiol (98%), 2,2′-(Ethylenedioxy)diethanethiol (95%), 3-Mercaptopropionic acid (99%), Benzylamine (99%), Benzyl mercaptan (99%), Cyclohexylamine (99%), m-Xylylenediamine (99%) were purchased from Sigma Aldrich. Propylamine (99%) was purchased from Fluka. Cyclohexane-1,4-diamine (99%), Methanesulphonic acid (98%) were purchased from Fluorochem. 1,4-Benzenedimethanethiol (98%) was purchased from TCI. Formic acid (85%) was purchased from Mobilab.

4,4-dimethyl-5-methylene-1,3-dioxolan-2-one (αCC)[1], 4,4′-(ethane-1,2-diyl)bis(4-methyl-5-methylene-1,3-dioxolan-2-one) (bisαCC)[1] and 3-benzyl-4-hydroxy-4,5,5-trimethyloxazolidin-2-one[2] were synthesized according to procedures described elsewhere.

Dialysis membrane Spectra/Por 7 (MWCO 1 kD) was purchased from Repligen.

Instrumentation

Nuclear magnetic resonance (NMR) spectroscopy. ^{1}H- and ^{13}C-NMR analyses were performed on a Bruker 400 MHz spectrometer at 25 °C in the Fourier transform mode. 16 scans for ^{1}H spectra and 512 scans for ^{13}C spectra were recorded. ^{1}H- and ^{13}C-NMR analyses for the DBU-oxazolidone interaction experiments were performed on a Bruker Ultrashield Plus 700 MHz spectrometer at 25 °C in the Fourier transform mode. 16 scans for ^{1}H spectra and 32 scans for ^{13}C spectra were recorded.

Size exclusion chromatography (SEC). Number-average molecular weight (Mn) and dispersity (D) of the polymers were determined by size exclusion chromatography (SEC) in dimethylformamide (DMF) containing LiBr (0.025 M) at 55 °C (flow rate: 1 mL/min) with a Waters chromatograph equipped with three columns (PSS gram 1000Å (x2), 30 Å) and a precolumn, a dual absorbance detector (Waters 2487) and a refractive index detector (Waters 2414).

Thermogravimetric analysis (TGA). TGA analysis was performed on a TGA2 instrument from Mettler Toledo. *Determination of degradation temperature.* Around 5 to 10 mg of sample was heated at 10 °C/min from 30 to 50 °C and flushed for 10 min at 50 °C. The sample was then heated at 20 °C/min until 600 °C. All the experiment was conducted under nitrogen atmosphere (20 mL/min). *Determination of dehydration temperature.* Around 5 to 10 mg of sample was heated at 2 °C/min from 30 to 250 °C. All the experiment was conducted under nitrogen atmosphere (20 mL/min).

Differential scanning calorimetry (DSC). DSC analysis was performed on a DSC 250 (TA Instruments). All the experiments were performed under ultrapure nitrogen flow. Samples of 4–6 mg were used and placed in hermetic aluminum pans. *Analysis of hydroxyoxazolidone copolymers.* The sample was heated from 25 to 90 °C at a rate of 10 °C/min and cooled to -40°C at a rate of 10 °C/min. The temperature modulated segment was set with an amplitude of 2 °C with a period of 60 seconds. The sample was then heated to 200 °C at a rate of 2 °C/min. The glass transition temperatures were determined using the reversing heat flow curve. *Analysis of dehydrated polymers.* The sample was heated from 25 to 140 °C at a rate of 10 °/min, cooled to -80 °C at a rate of 10 °C/min, and heated to 160 °C at a rate of 10 °C/min.

Fourier Transform Infrared Spectra (F-TIR). FTIR measurements were carried out on a Nicolet IS5 spectrometer (Thermo Fisher Scientific) equipped with a diamond attenuated transmission

reflectance (ATR) device. 32 scans were recorded for each sample over the range 4000-500 cm^{-1} with a normal resolution of 4 cm^{-1}.

Lap-Shear Tests. Lap shear adhesion measurements were conducted on a MTS Criterion Model 43 system equipped with a 1 kN load cell with a displacement rate of 5 mm min^{-1}. A homemade setup was designed for avoiding failure in brittle samples on sample locking when aluminum substrates were used (Figure S123). The lap shear strength was calculated using the formula:

$$\tau = \frac{F}{A}$$

where τ is the lap shear strength (mPa), F is the applied force (N) and A the overlapped area (constant in this study as 150 mm^2). Each sample was measured three times.

2. Model reactions

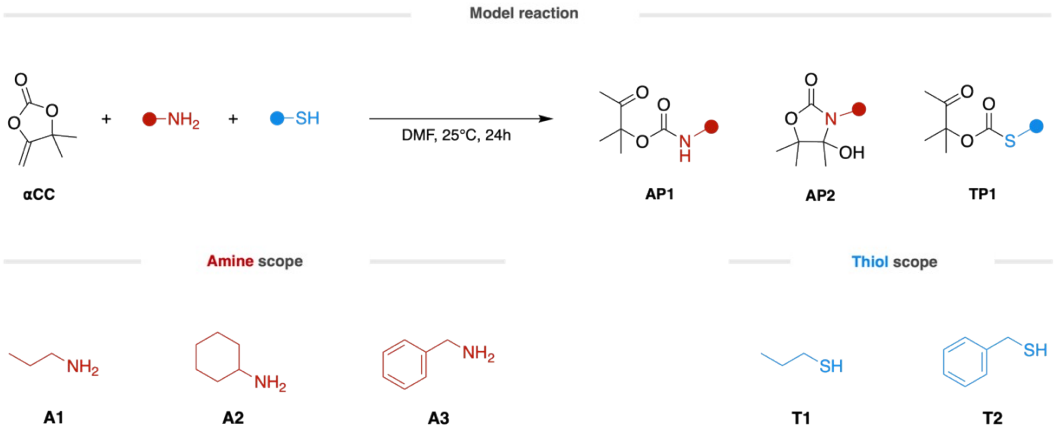

Scheme S1 – Substrate scope for the model reaction of αCC with amines and thiols.

Model reactions between αCC and a scope of different monofunctional amines **A1-3** and thiols **T1-2** have been carried out under different conditions. The kinetics were monitored by ^{1}H-NMR spectroscopy by sampling over time (1 min, 30 min, 1h, 2h, 4h, 24h).

General procedure

αCC (512 mg, 4 mmol, 2 eq.), the thiol (2 mmol, 1 eq.) and DMF (2 mL) were added to a reaction tube. Then, the amine (2 mmol, 1 eq.) was added and the reaction medium was stirred at 25°C under N_2 atmosphere. When used, DBU (0.08 mmol, 0.04 eq.) was added after all other components.

The NMR samples were prepared by mixing 100 µL of the reaction medium, a drop of formic acid to quench the reaction, and 700 µL of DMSO-d_6. The tube was then stored at -20°C prior analysis

The conversion in αCC, amine, thiol, and the oxo-urethane **AP1** cyclization (into **AP2**) were calculated following the respective equations:

$$\text{conv}(\alpha CC)\ (\%) = 1 - \frac{\text{I}(\alpha CC)}{\text{I}(\alpha CC) + \text{I(AP1)} + \text{I(AP2)} + \text{I(TP1)}}$$

$$\text{conv(amine)}\ (\%) = \frac{(\ \text{I(AP1)} + \text{I(AP2)}\ ) \times 2}{\text{I}(\alpha CC) + \text{I(AP1)} + \text{I(AP2)} + \text{I(TP1)}}$$

$$\text{conv(thiol)}\ (\%) = \frac{\text{I(TP1)} \times 2}{\text{I}(\alpha CC) + \text{I(AP1)} + \text{I(AP2)} + \text{I(TP1)}}$$

$$\text{cyclization(amine)}\ (\%) = \frac{\text{I(AP2)}}{\text{I(AP1)} + \text{I(AP2)}}$$

where *conv* is the conversion, *cyclization* the cyclization, *I* the normalized integration.

The peaks selected for the integration are attributed to their respective compounds and can be found below for each model reaction. Peaks relative to solvents appear at 2.5 ppm (DMSO-d_6), 2.73 and 2.89 ppm (DMF).

Model reaction with **A1** and **T1**

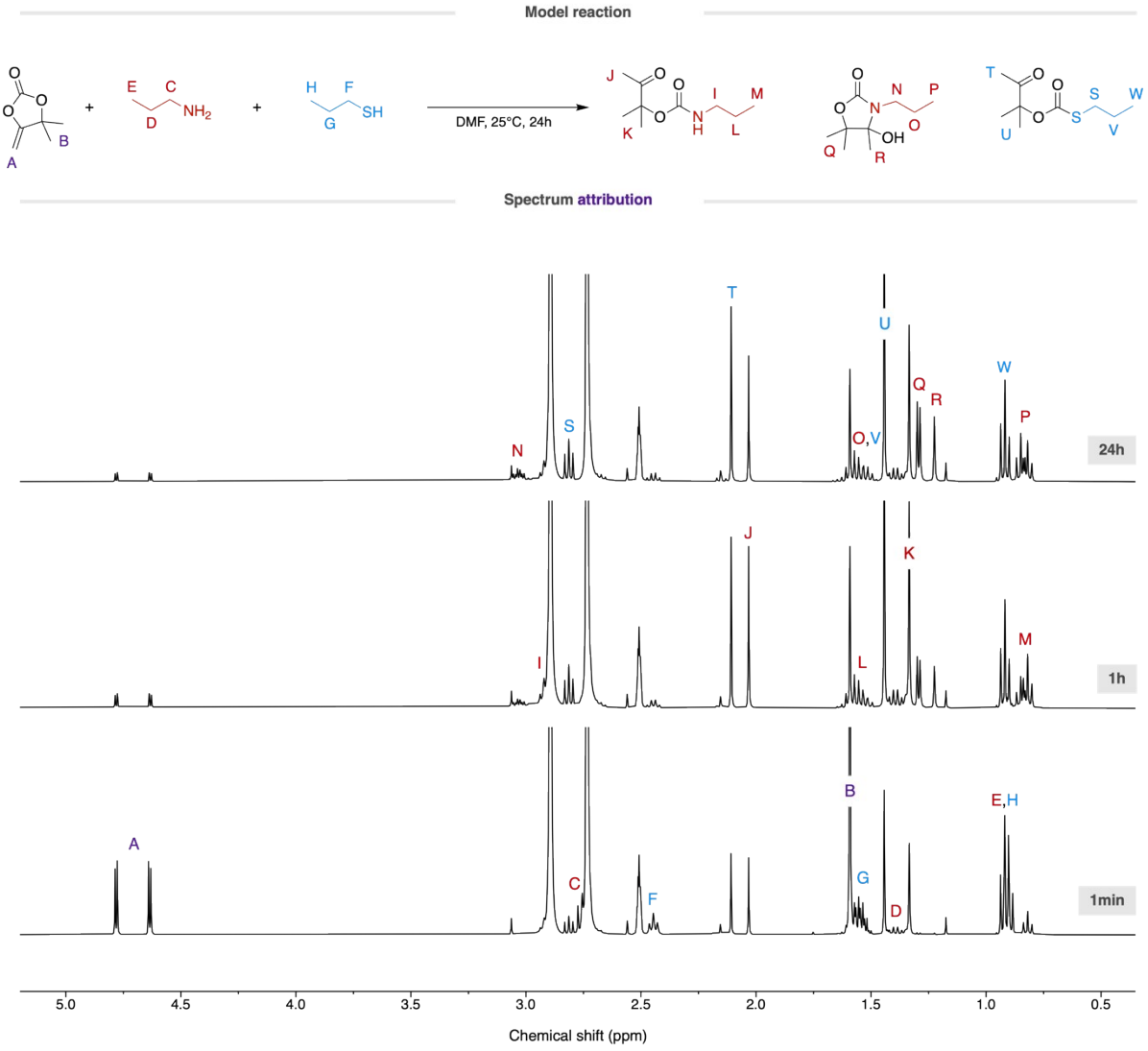

Figure S1 – Kinetic study of the model reaction between αCC, **A1**, and **T1** followed by ^{1}H-NMR spectroscopy (400 MHz, DMSO-d_6).

Compound	Peak	δ (ppm)
αCC	A	4.64
AP1	J	2.04
AP2	R	1.23
TP1	T	2.11

Model reaction with **A2** and **T1**

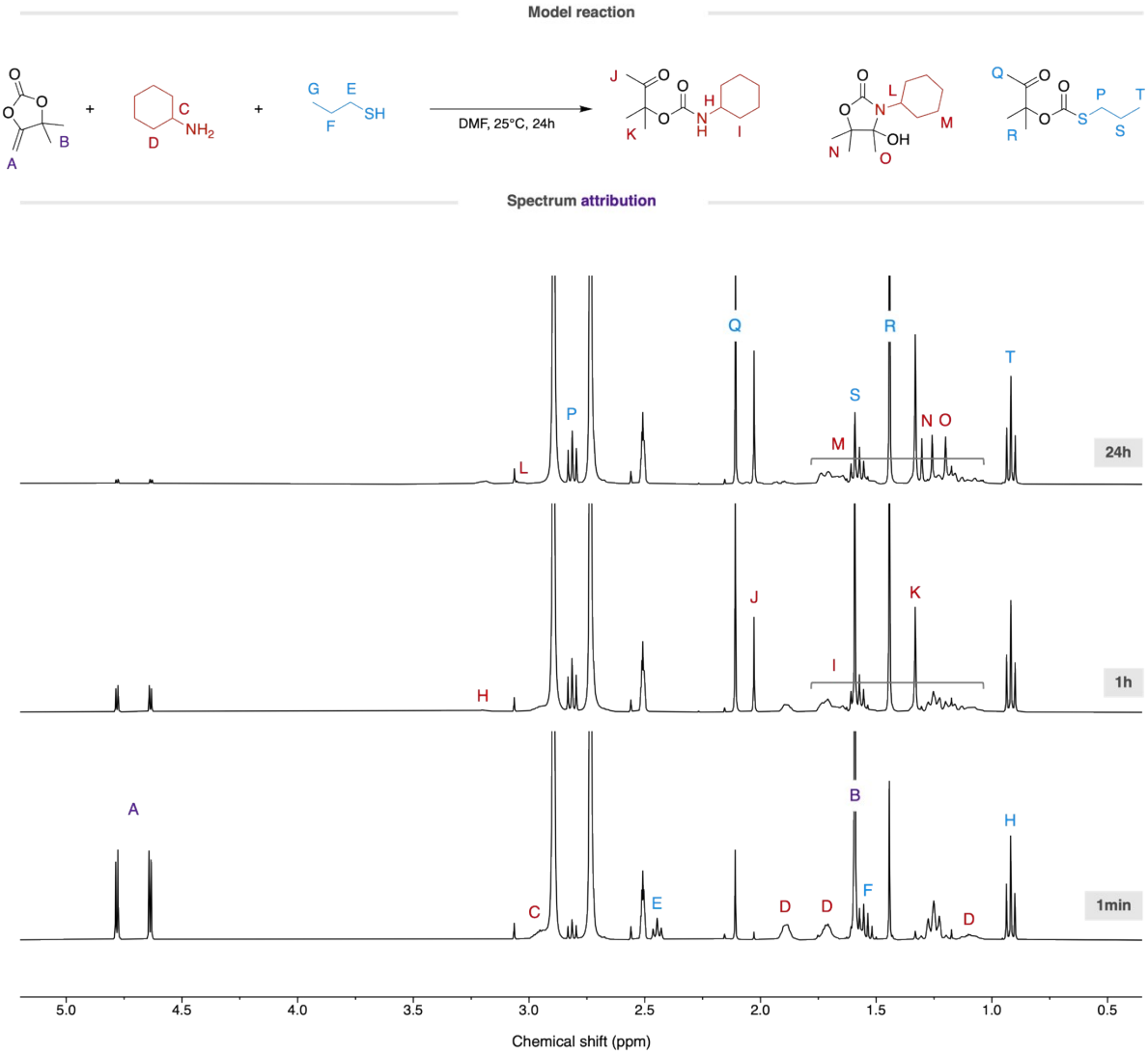

Figure S2 – Kinetic study of the model reaction between αCC, **A2**, and **T1** followed by ^{1}H-NMR spectroscopy (400 MHz, DMSO-d_6).

Compound	Peak	δ (ppm)
αCC	A	4.64
AP1	J	2.03
AP2	O	1.20
TP1	Q	2.11

Model reaction with **A3** and **T1**

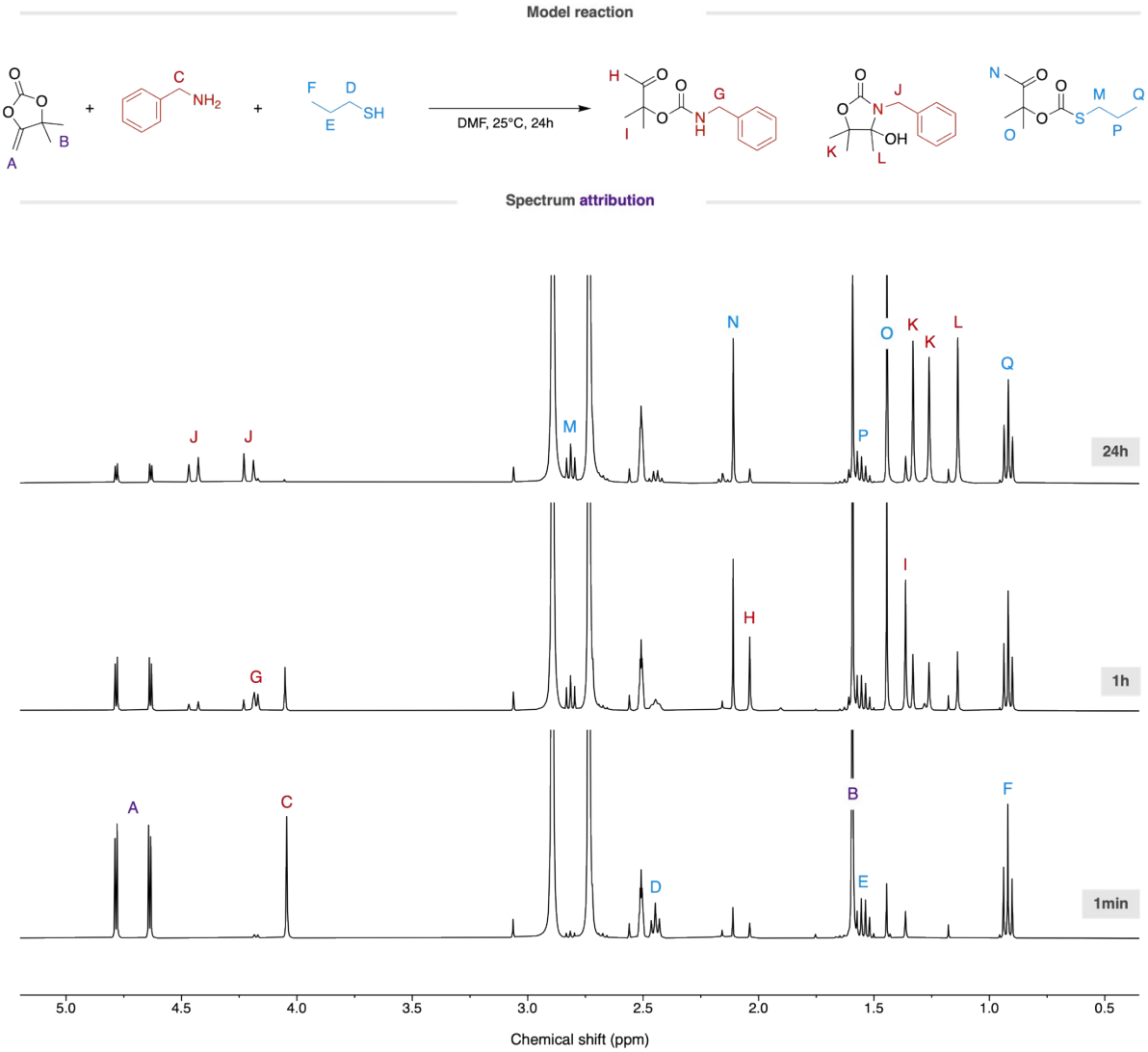

Figure S3 – Kinetic study of the model reaction between αCC, **A3**, and **T1** followed by ^{1}H-NMR spectroscopy (400 MHz, DMSO-d_6).

Compound	Peak	δ (ppm)
αCC	A	4.64
AP1	H	2.04
AP2	L	1.14
TP1	N	2.11

Model reaction with **A1** and **T2**

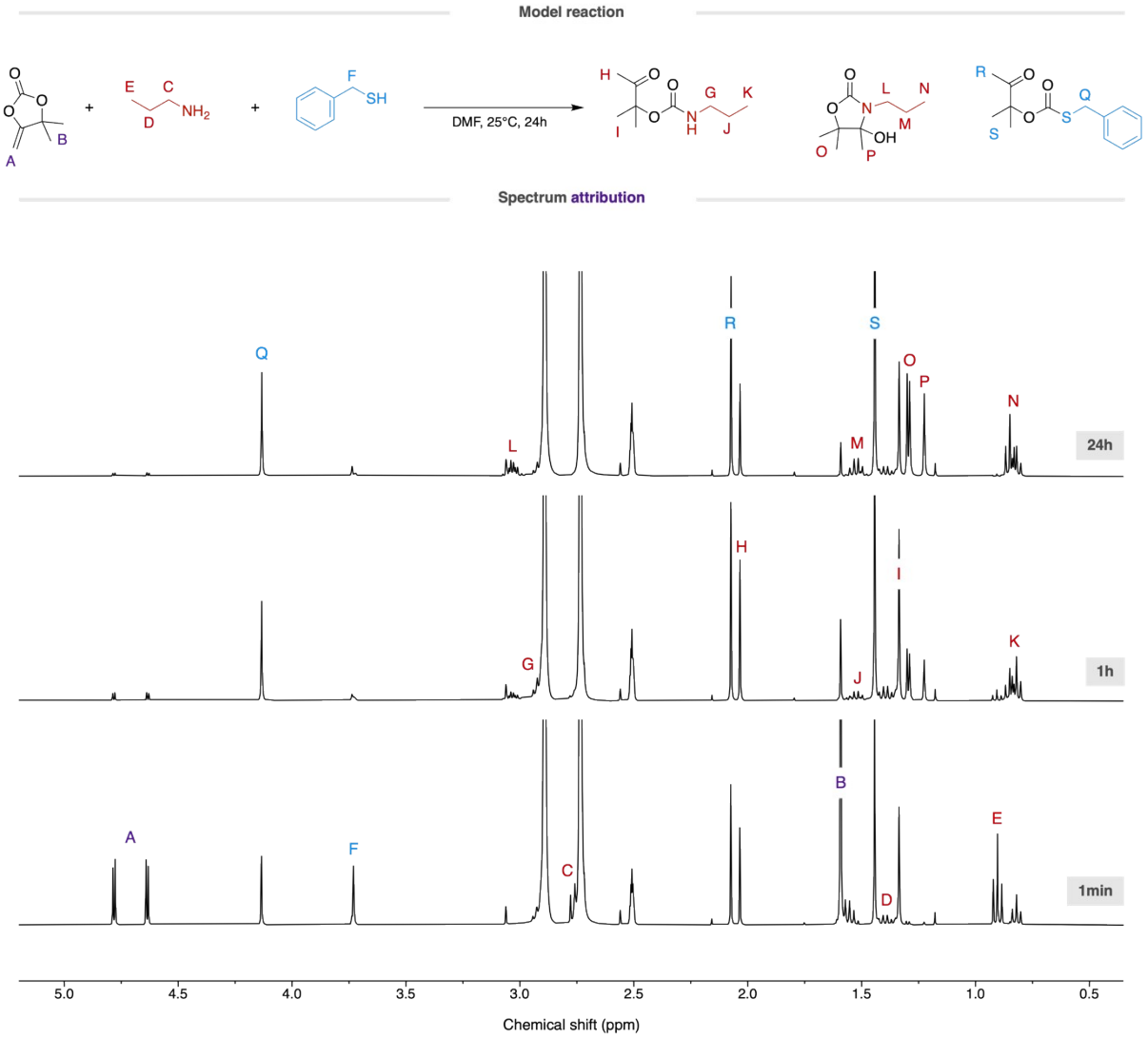

Figure S4 – Kinetic study of the model reaction between αCC, **A1**, and **T2** followed by ^{1}H-NMR spectroscopy (400 MHz, DMSO-d_6).

Compound	Peak	δ (ppm)
αCC	A	4.64
AP1	H	2.03
AP2	P	1.22
TP1	R	2.07

Model reaction with **A2** and **T2**

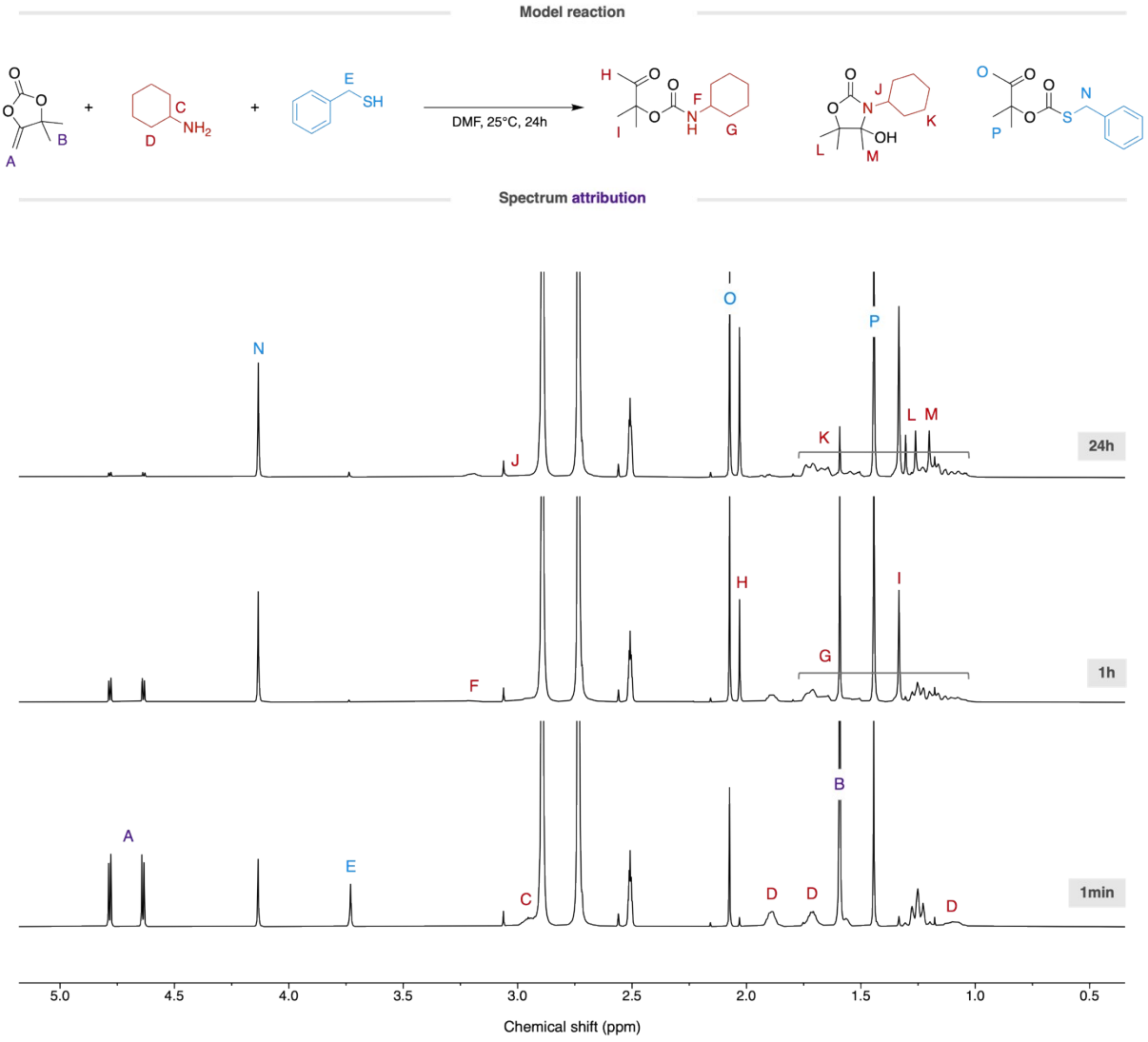

Figure S5 – Kinetic study of the model reaction between αCC, **A2**, and **T2** followed by ^{1}H-NMR spectroscopy (400 MHz, DMSO-d_6).

Compound	Peak	δ (ppm)
αCC	A	4.64
AP1	H	2.03
AP2	M	1.20
TP1	O	2.07

Model reaction with **A3** and **T2**

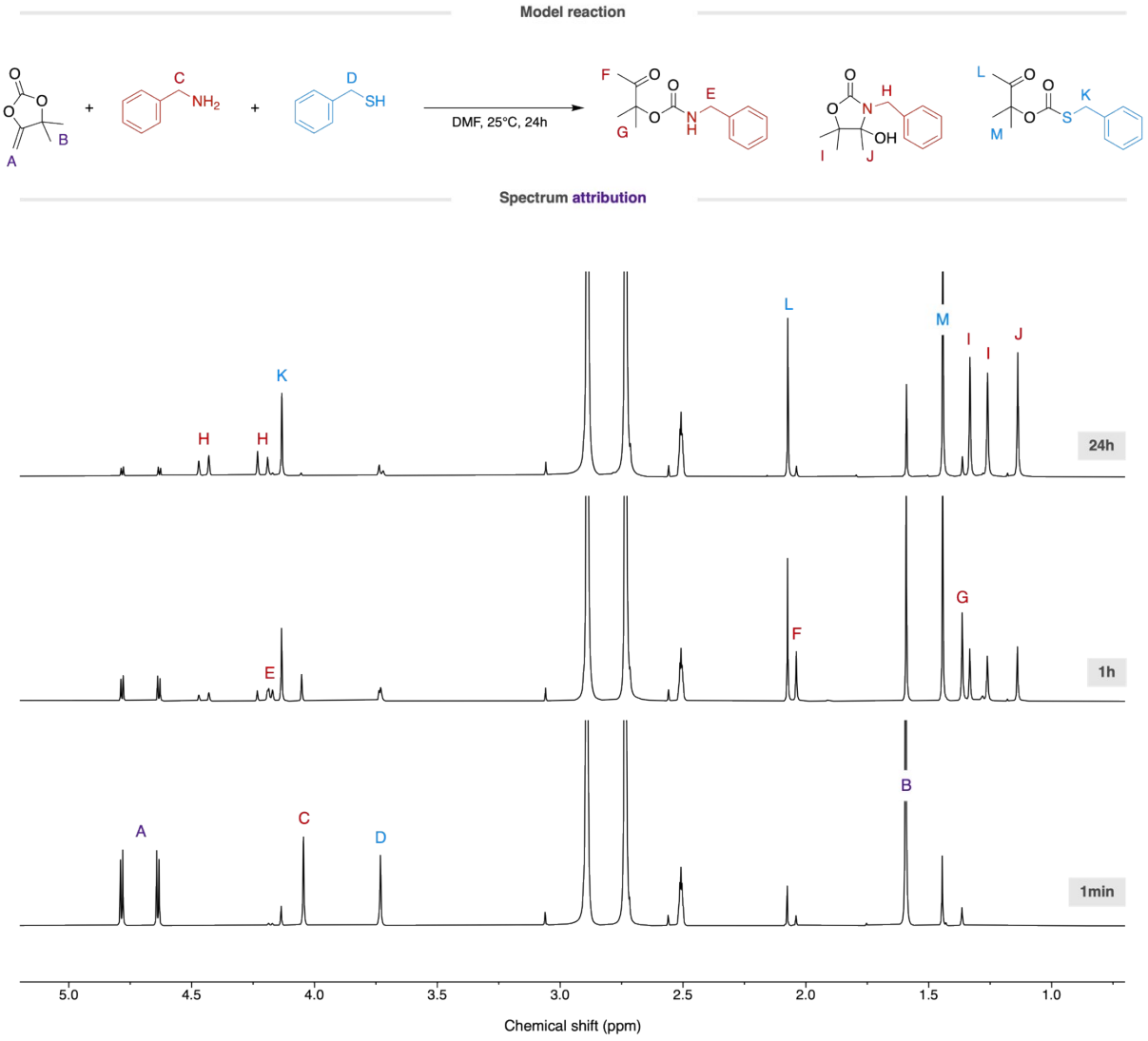

Figure S6 – Kinetic study of the model reaction between αCC, **A3**, and **T2** followed by ^{1}H-NMR spectroscopy (400 MHz, DMSO-d_6).

Compound	Peak	δ (ppm)
αCC	A	4.64
AP1	F	2.04
AP2	J	1.14
TP1	L	2.07

3. Evidence for reactive thiolate generation

Thiols are acidic compounds and primary amines are characterized by rather high basicity. Mixing the amine **A2** (yellow liquid) the thiol **T2** (colorless liquid) in DMF leads to a slow crystallization of a white solid. This solid salt can be isolated by filtration followed by washing with diethyl ether. The formation of this salt has already been reported in the literature[3].

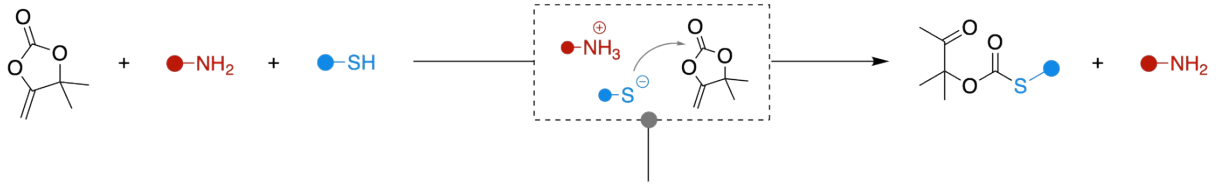

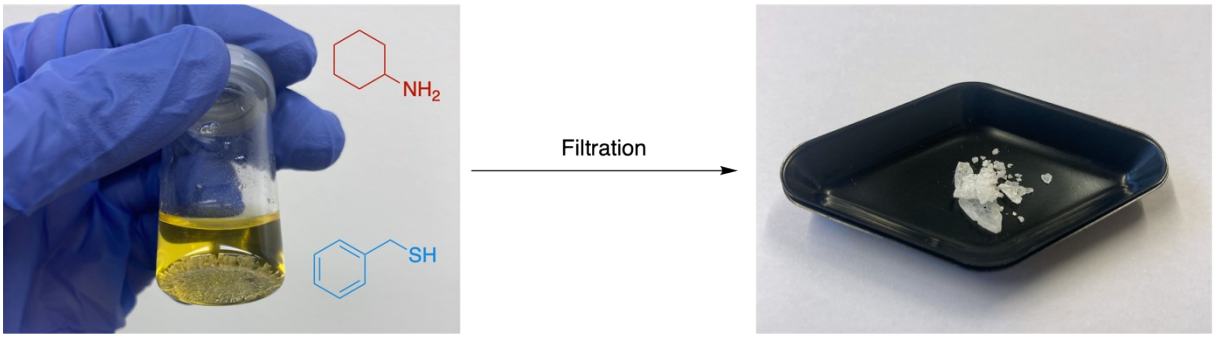

Scheme S2 – Catalytic role of the amine to generate thiolates species for the formation of the monothiocarbonate **TP1**. Mixing cyclohexylamine **A2** and benzyl mercaptan **T2** in DMF give rise to the formation of white crystals.

The formation of the salt is highlighted in both solid and dissolved forms. By ^{1}H-NMR spectroscopy in $CDCl_3$ as deuterated solvent (the salt has shown insolubility in DMSO-d_6), the formation of a salt is highlighted by a disappearance of the thiol hydrogen at 1.78 ppm (triplet) and the metamorphosis of the methylene at 3.76 ppm from a doublet to a singlet due to the absence of neighboring hydrogen (Figure S7). An ATR-IR spectrum has also been recorded and displays typical vibrations of primary amine salts[4,5], characterized by a wide absorbance in the region from 2800 to 2200 cm^{-1} and the presence of a lone band at 2110 cm^{-1} (Figure S8).

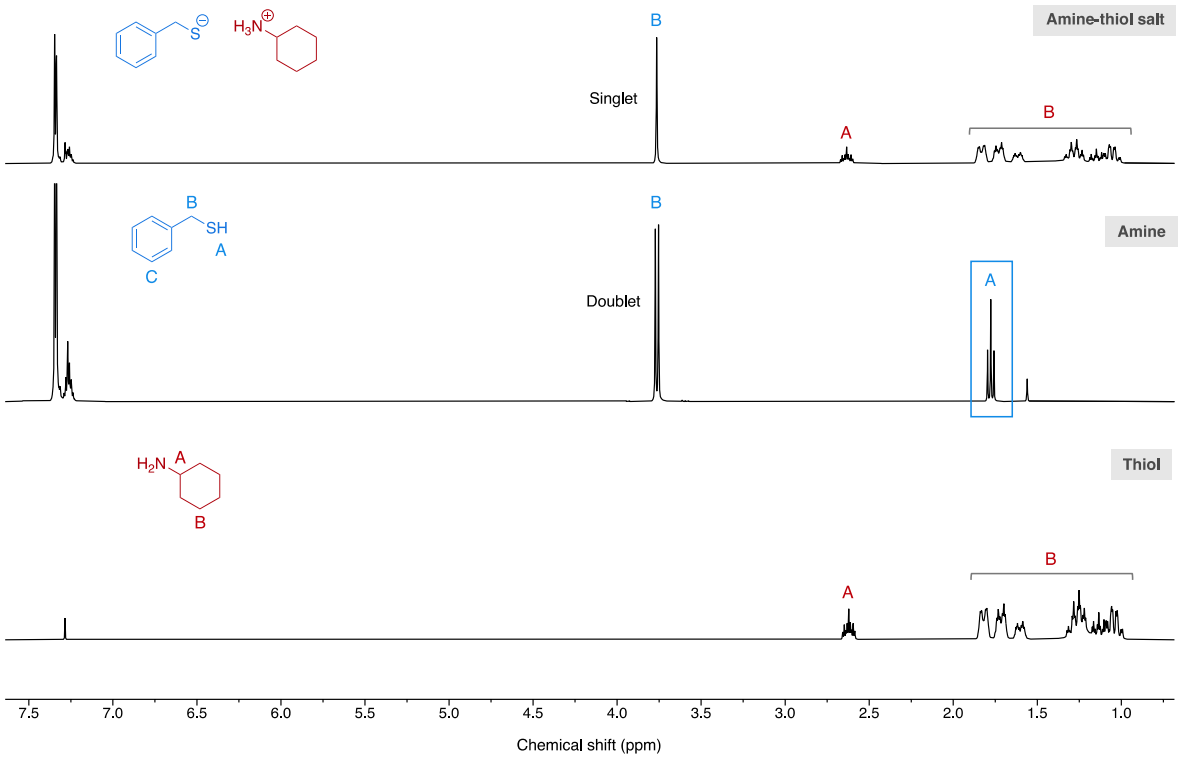

Figure S7 – ^{1}H-NMR spectra of the thiol, the amine, and the amine-thiol salt (400 MHz, DMSO-d_6).

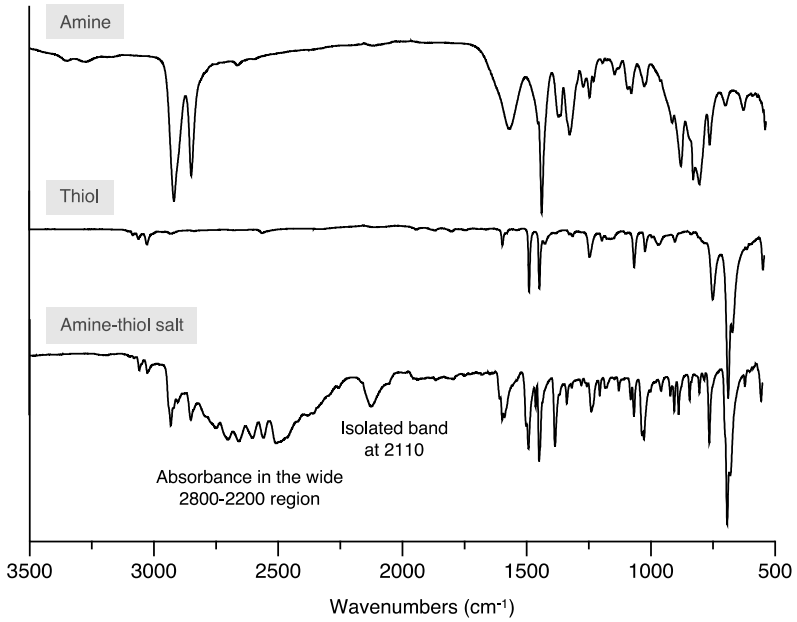

Figure S8 – ATR-IR spectra of the amine, the thiol, and the amine-thiol salt.

4. Solubility table of the synthesized polymers

Table S1 – Solubility of the pure polymers in different organic solvents at rt.

	DMSO	DMF	THF	Acetone	$CHCl_3$
P(A1T1)	✓	✓	✓	✓	✓
P(A1T1)C	✓	✓	✓	✓	✗
P(A1T2)	✓	✓	✓	✓	✗
P(A2T1)	✓	✓	✓	✓	✓
P(A2T1)C	✓	✓	✓	✓	✗
P(A2T2)	✓	✓	✓	✓	✓
P(A3T1)	✓	✓	✓	✓	✗
P(A3T1)C	✓	✓	✓	✓	✗
P(A3T2)	✓	✓	✓	✓	✗

5. NMR characterization of the pure polymers

P(A1T1)

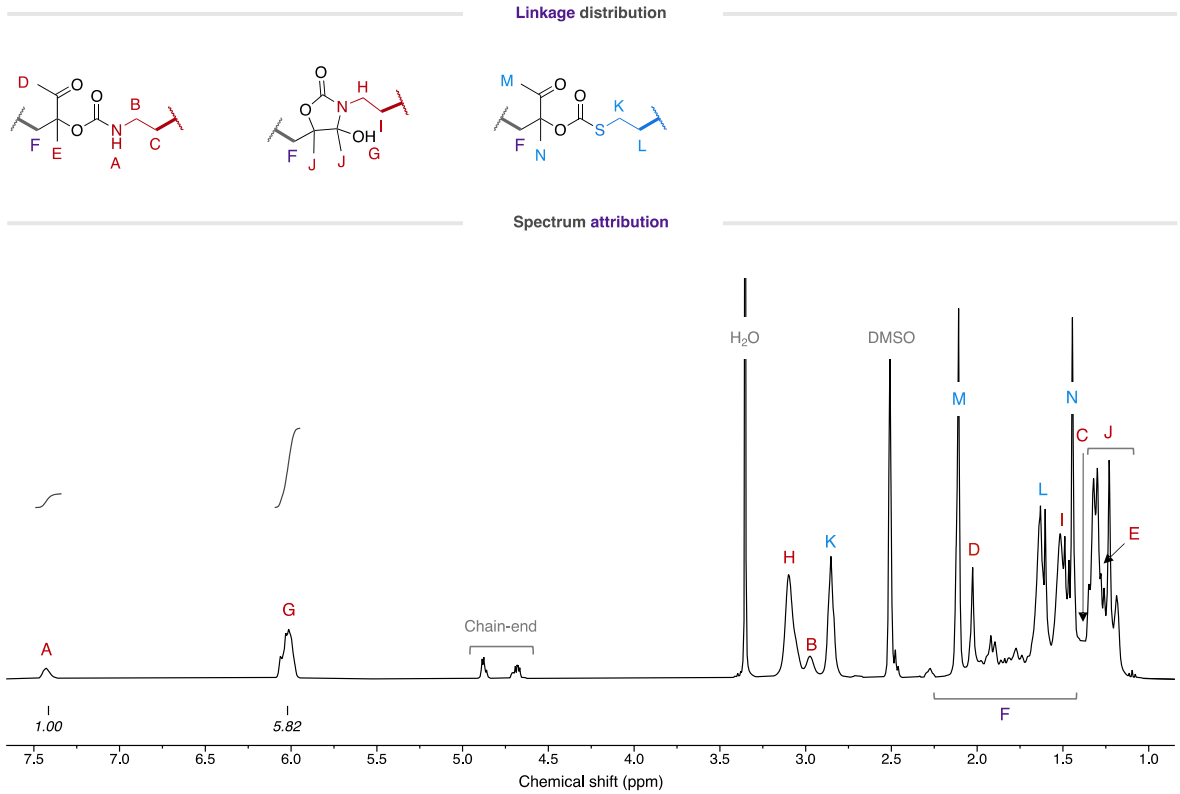

Figure S9 – ^{1}H-NMR spectrum of P(A1T1) (400 MHz, DMSO-d_6).

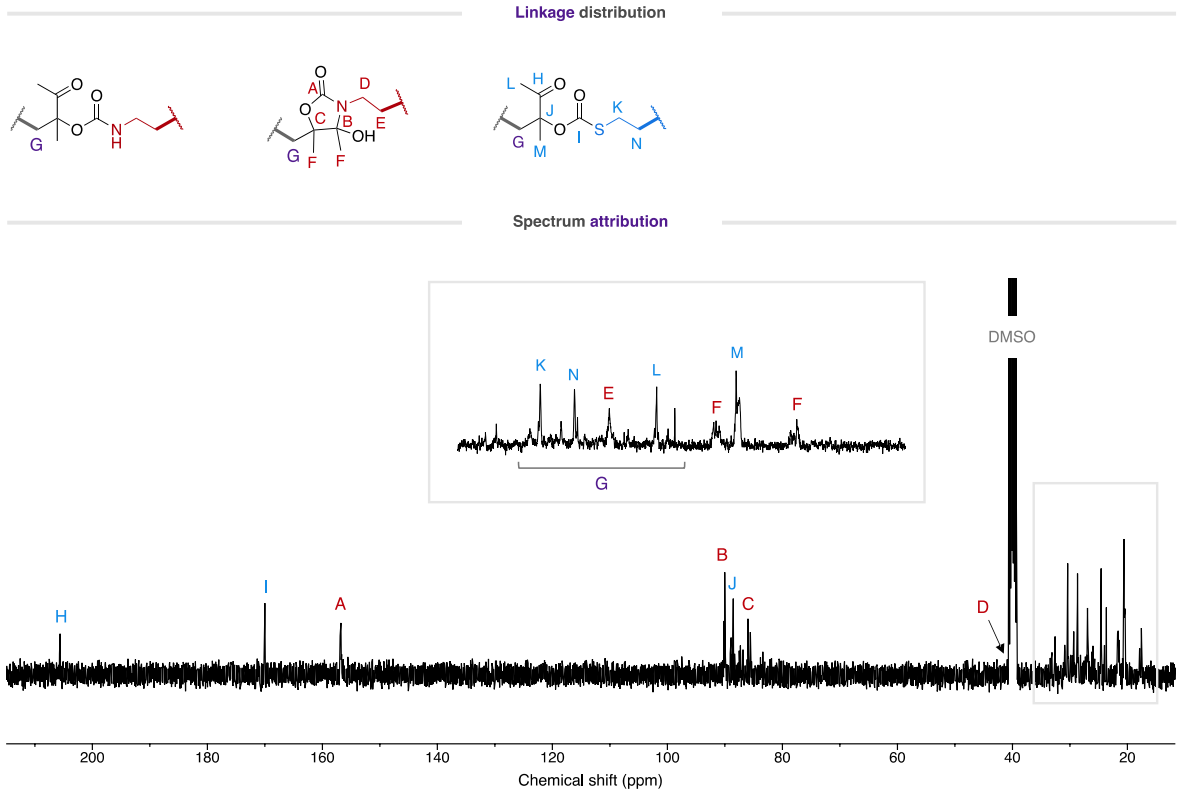

Figure S10 – ^{13}C-NMR spectrum of P(A1T1) (400 MHz, DMSO-d_6).

P(A1T1)C

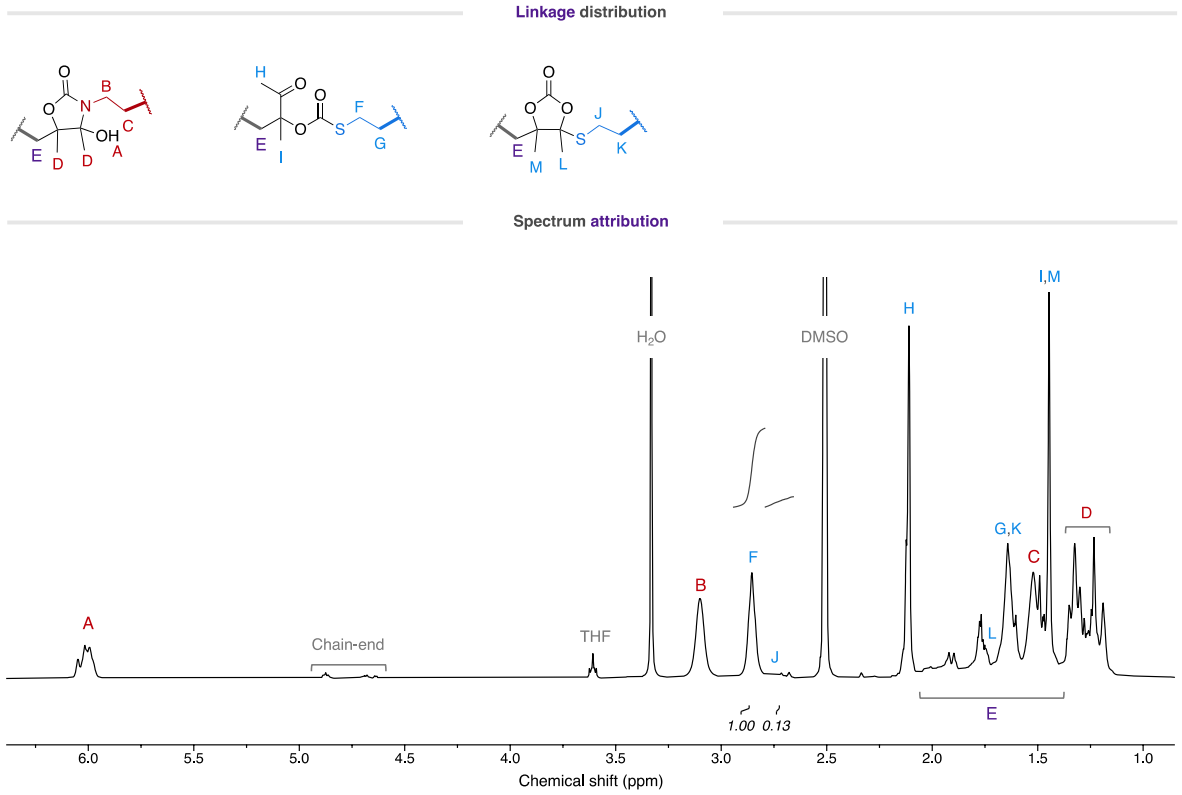

Figure S11 – ^{1}H-NMR spectrum of P(A1T1)C (400 MHz, DMSO-d_6).

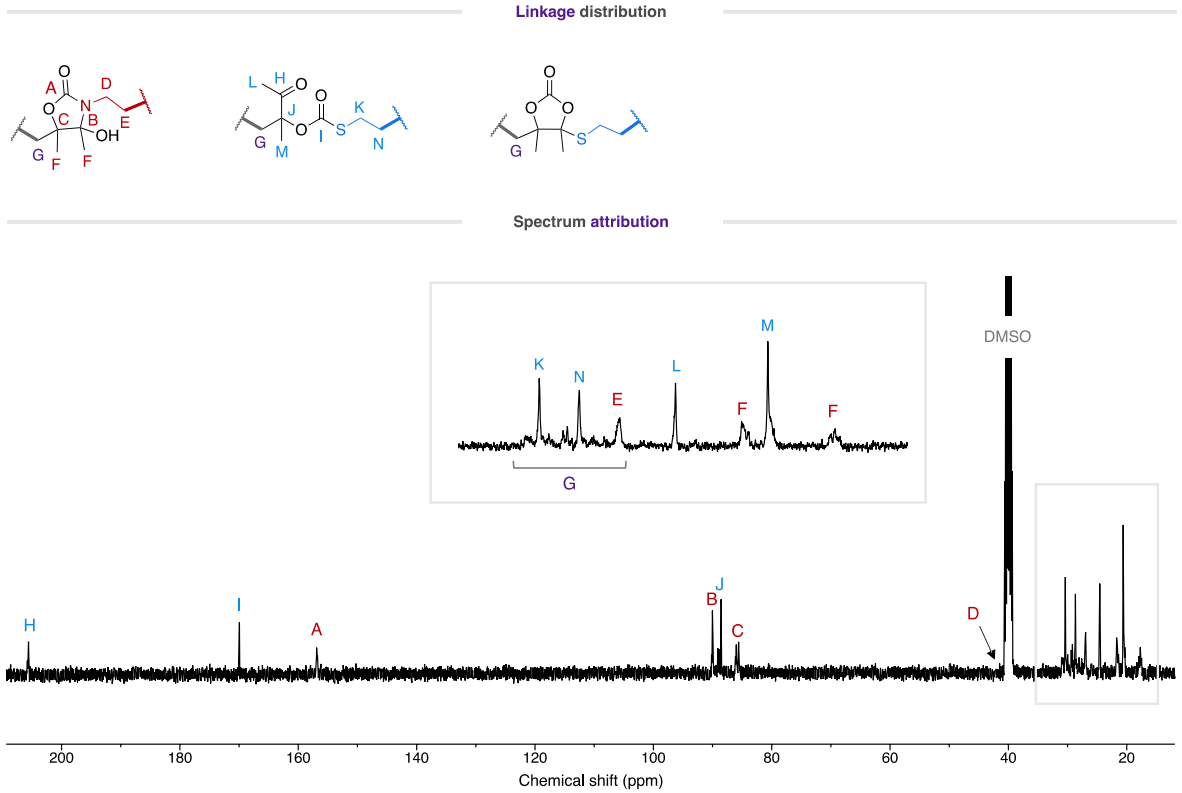

Figure S12 – ^{13}C-NMR spectrum of P(A1T1)C (400 MHz, DMSO-d_6).

P(A1T2)

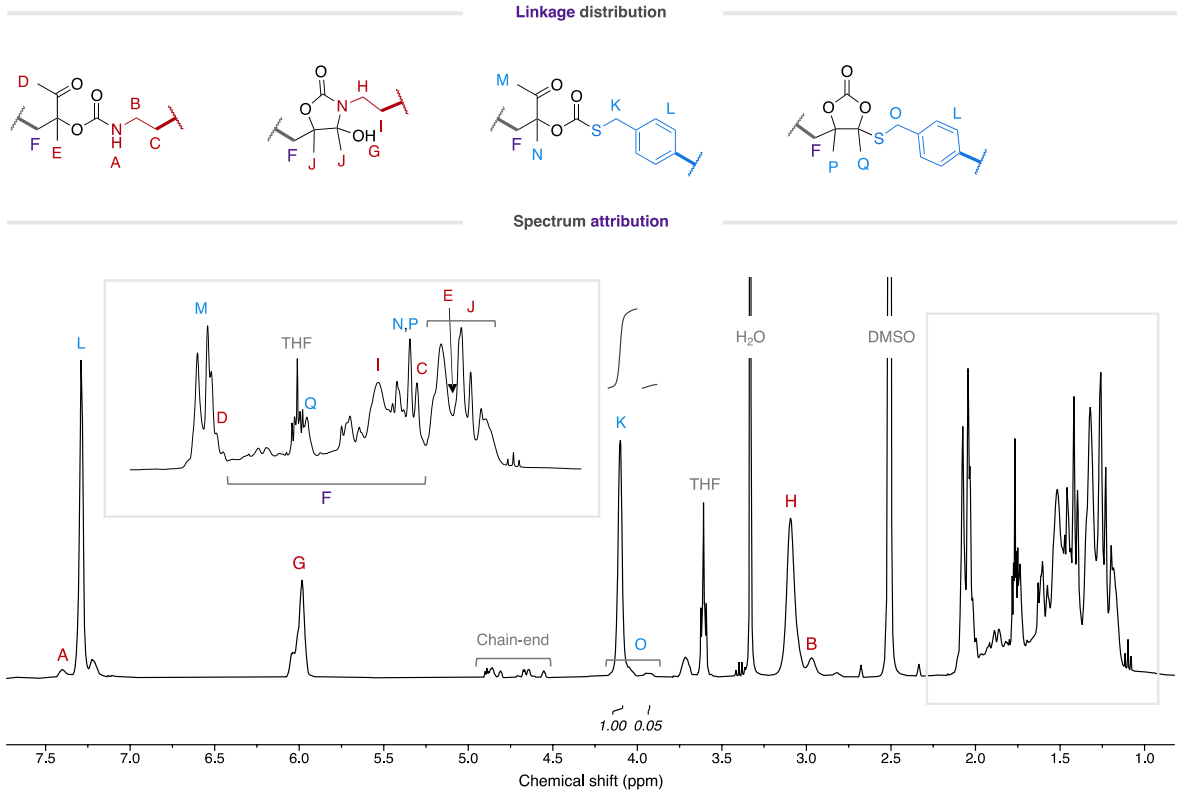

Figure S13 – ^{1}H-NMR spectrum of P(A1T2) (400 MHz, DMSO-d_6).

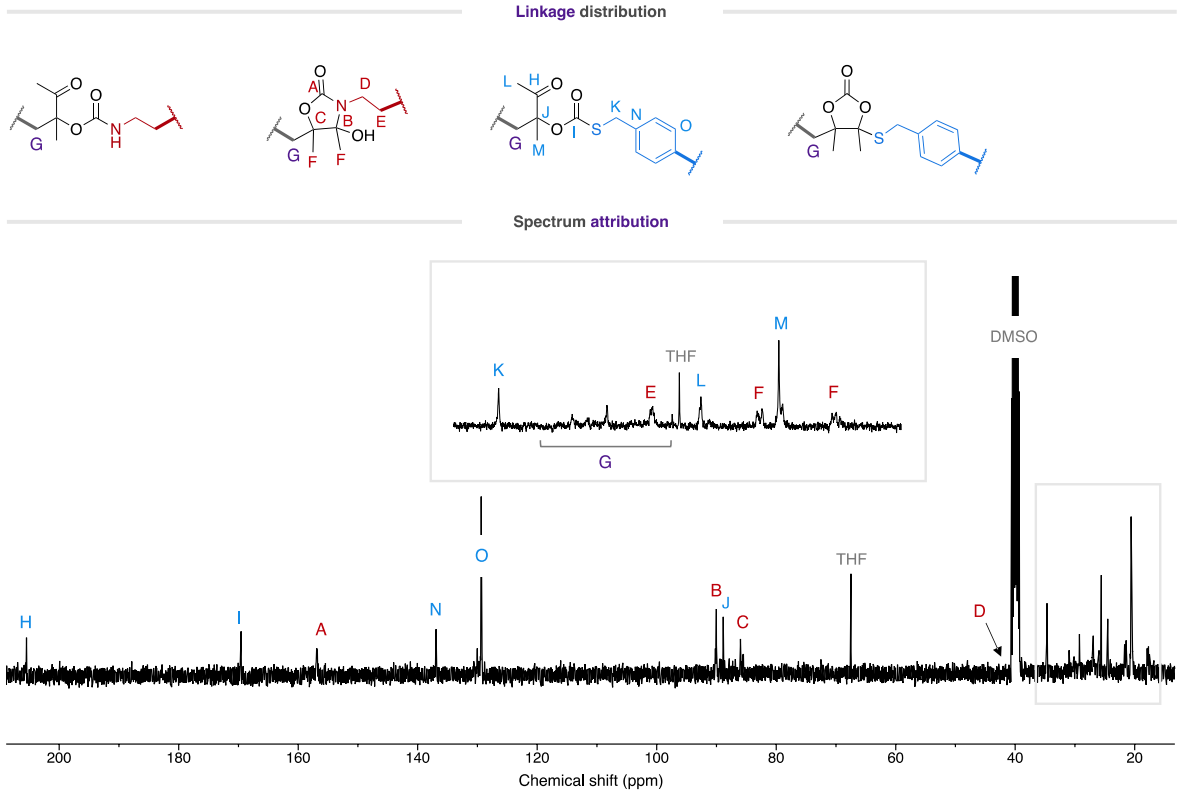

Figure S14 – ^{13}C-NMR spectrum of P(A1T2) (400 MHz, DMSO-d_6).

P(A2T1)

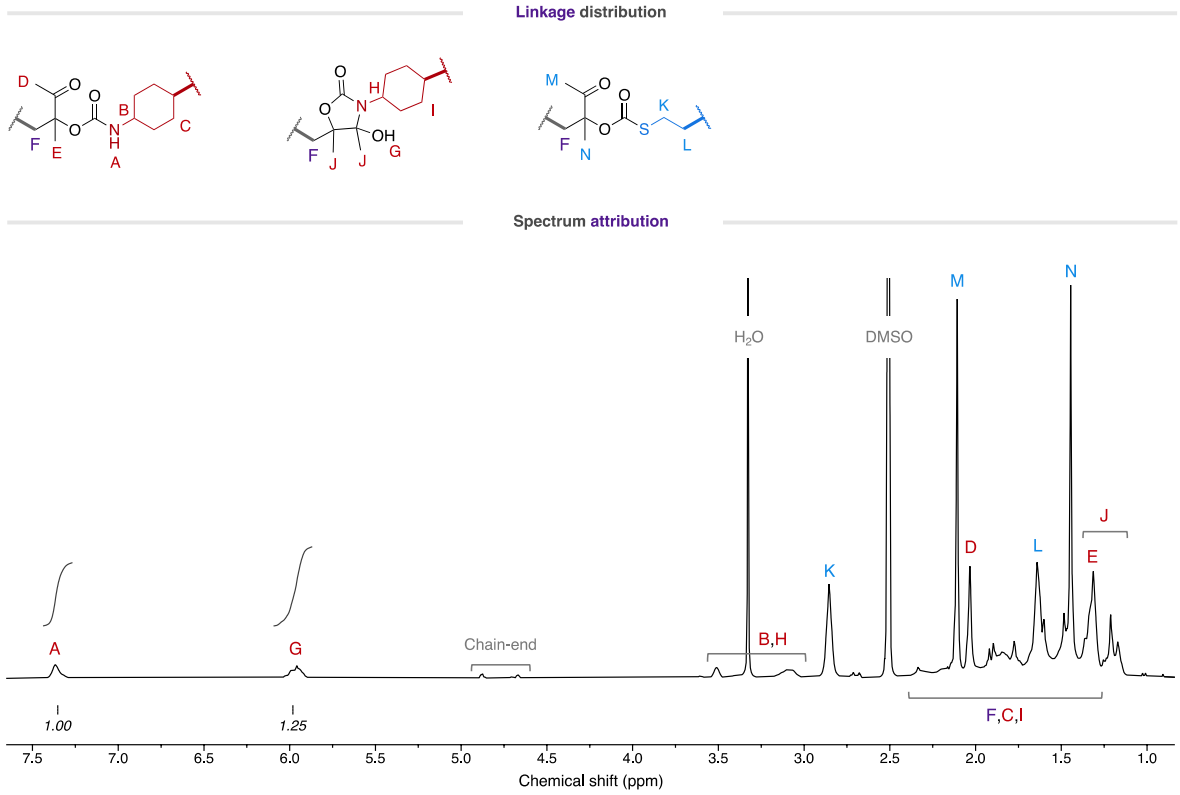

Figure S15 – ^{1}H-NMR spectrum of P(A2T1) (400 MHz, DMSO-d_6).

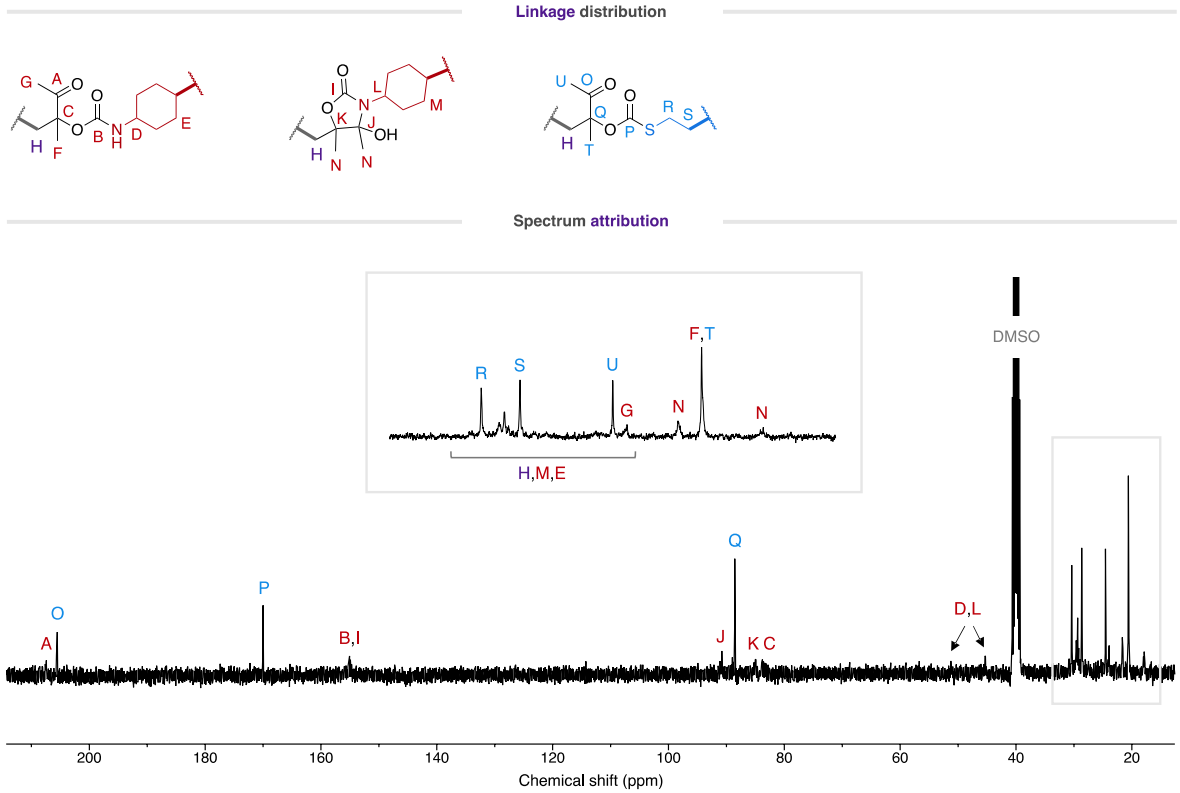

Figure S16 – ^{13}C-NMR spectrum of P(A2T1) (400 MHz, DMSO-d_6).

P(A2T1)C

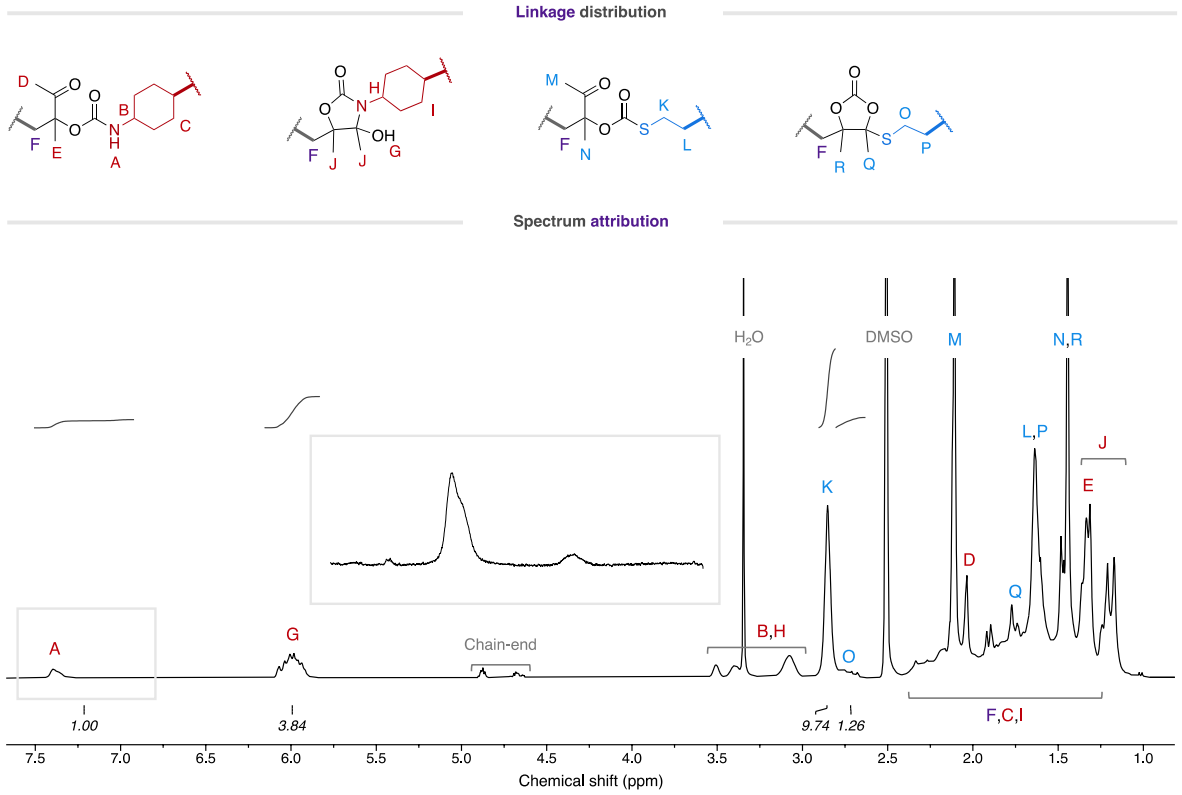

Figure S17 – ^{1}H-NMR spectrum of P(A2T1) (400 MHz, DMSO-d_6).

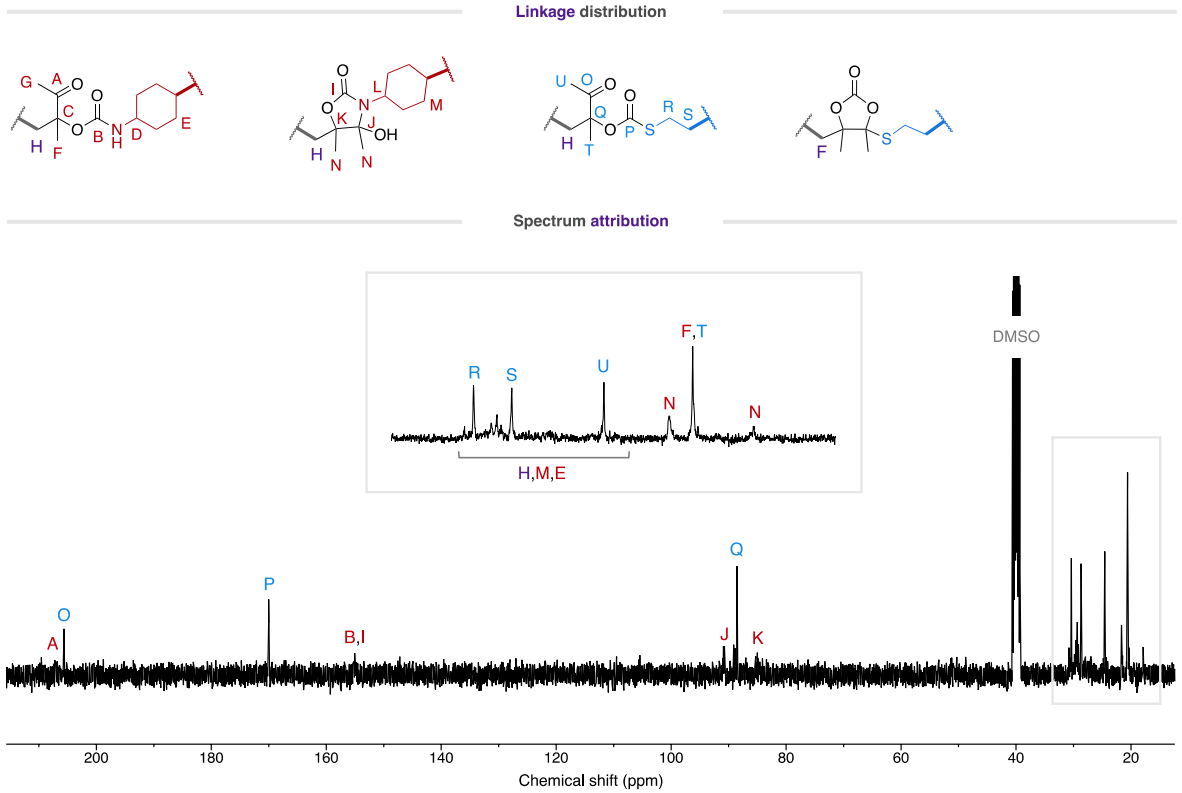

Figure S18 – ^{13}C-NMR spectrum of P(A2T1)C (400 MHz, DMSO-d_6).

P(A2T2)

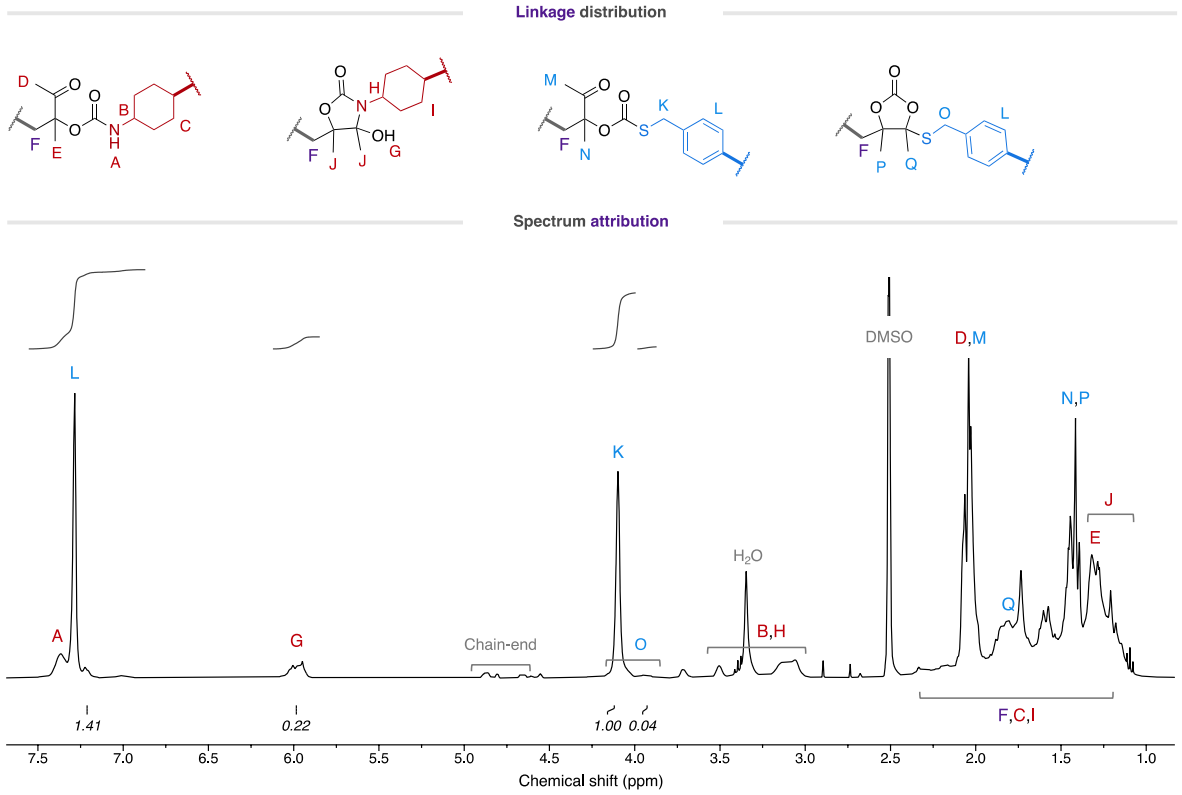

Figure S19 – ^{1}H-NMR spectrum of P(A2T2) (400 MHz, DMSO-d_6).

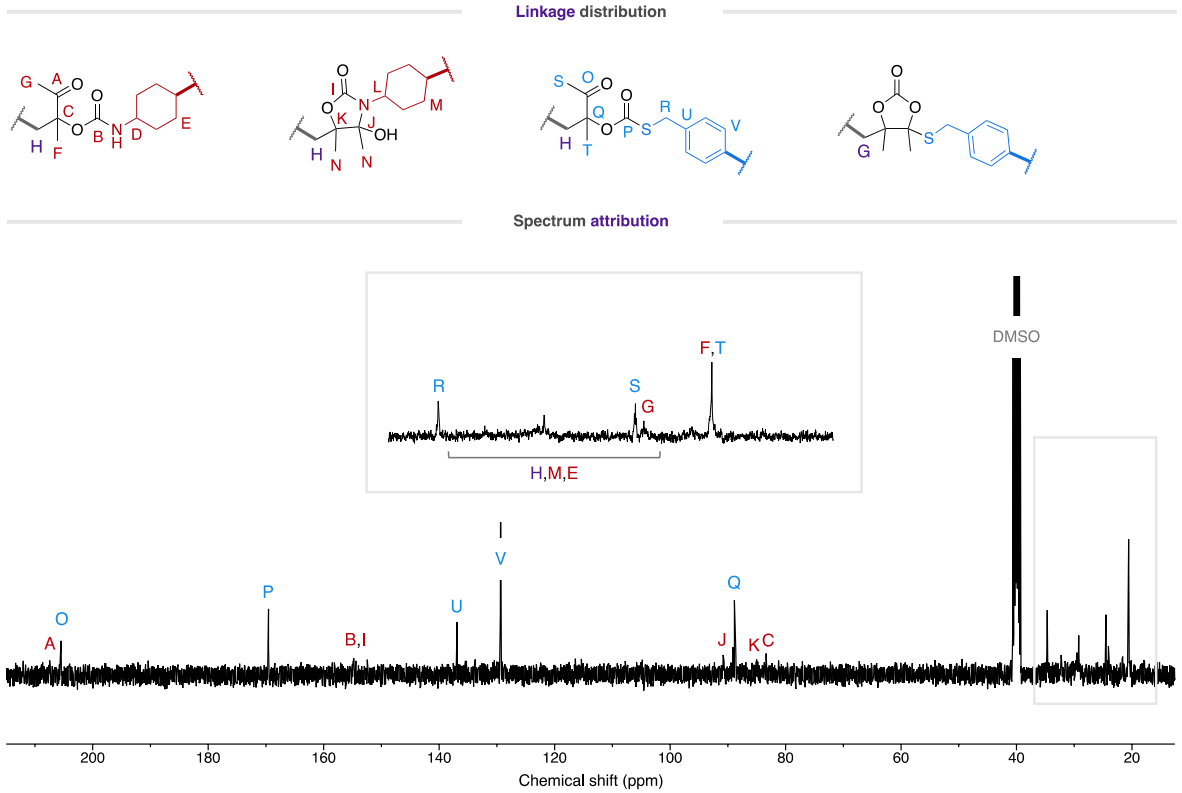

Figure S20 – ^{13}C-NMR spectrum of P(A2T2) (400 MHz, DMSO-d_6).

P(A3T1)

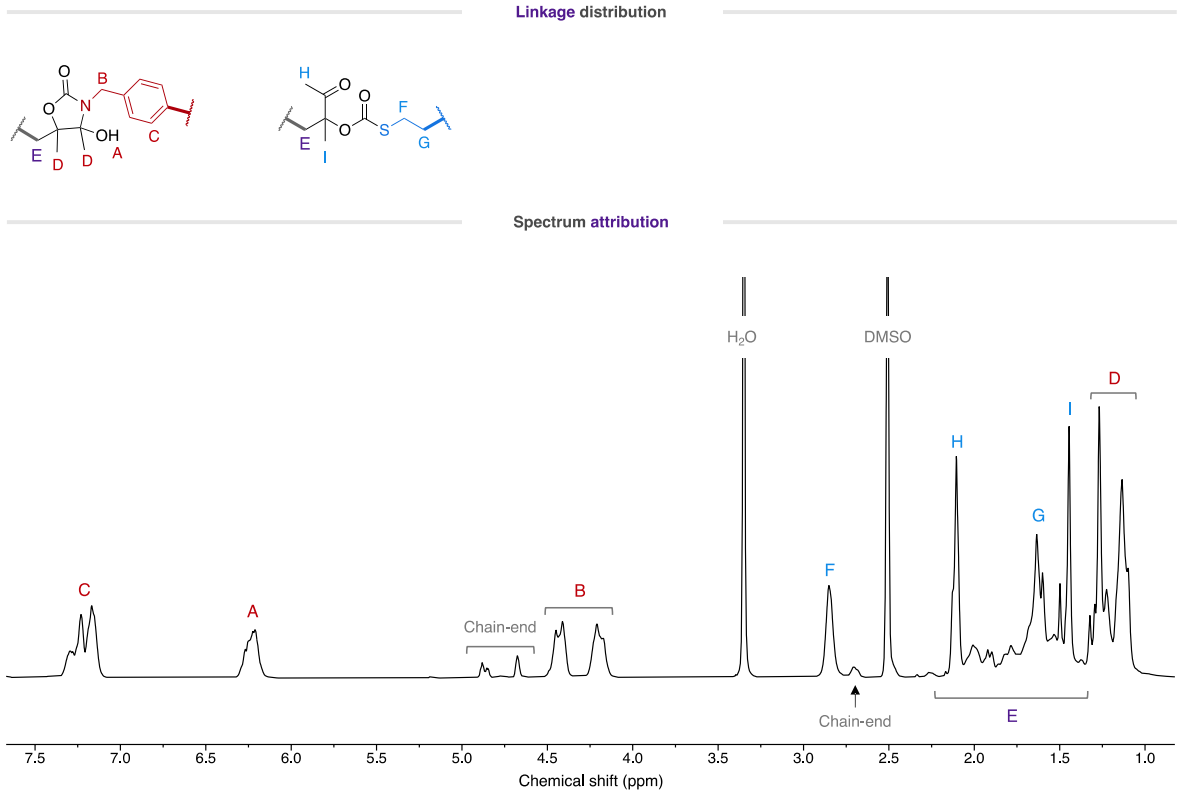

Figure S21 – ^{1}H-NMR spectrum of P(A3T1) (400 MHz, DMSO-d_6).

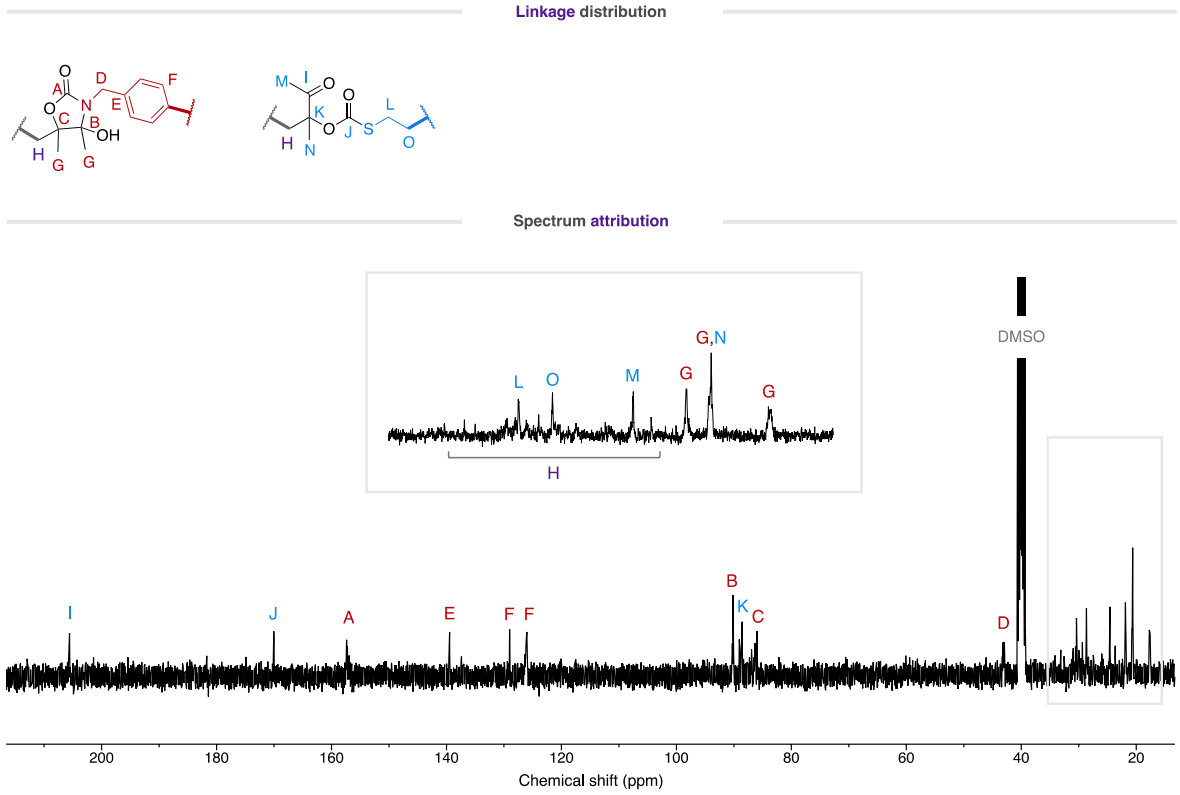

Figure S22 – ^{13}C-NMR spectrum of P(A3T1) (400 MHz, DMSO-d_6).

P(A3T1)C

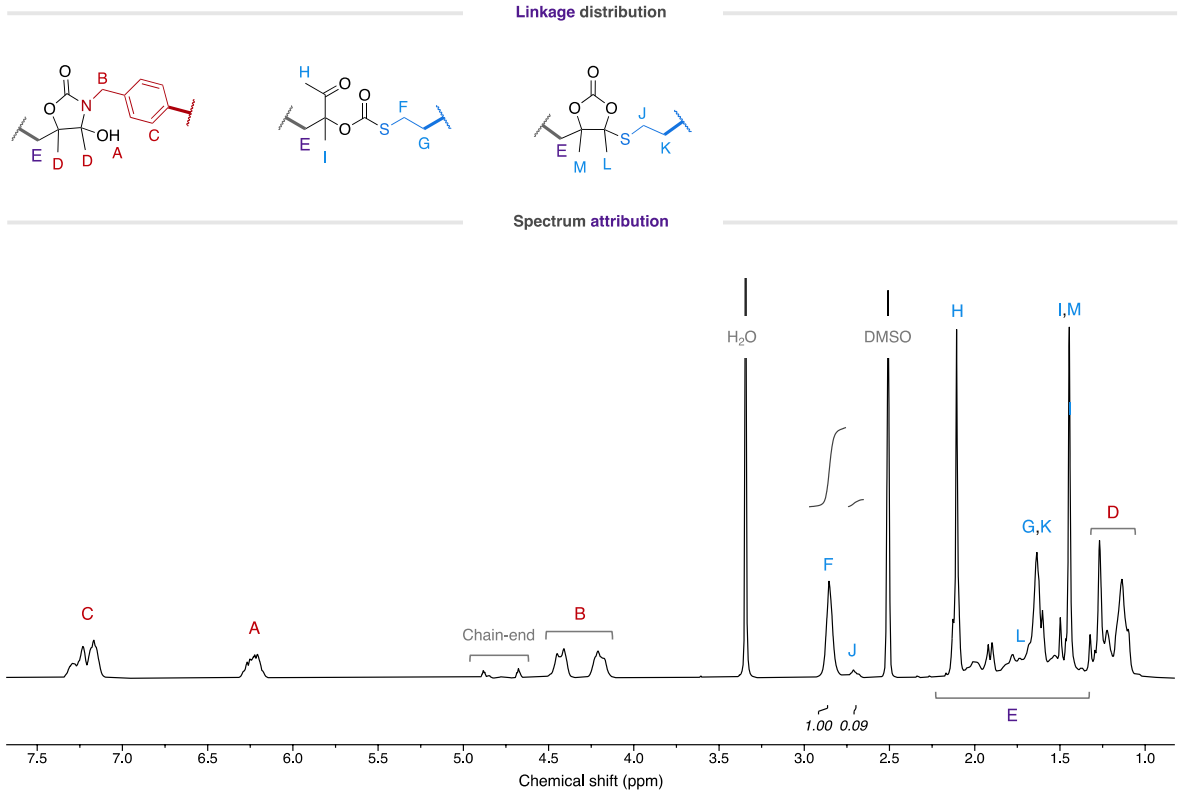

Figure S23 – ^{1}H-NMR spectrum of P(A3T1)C (400 MHz, DMSO-d_6).

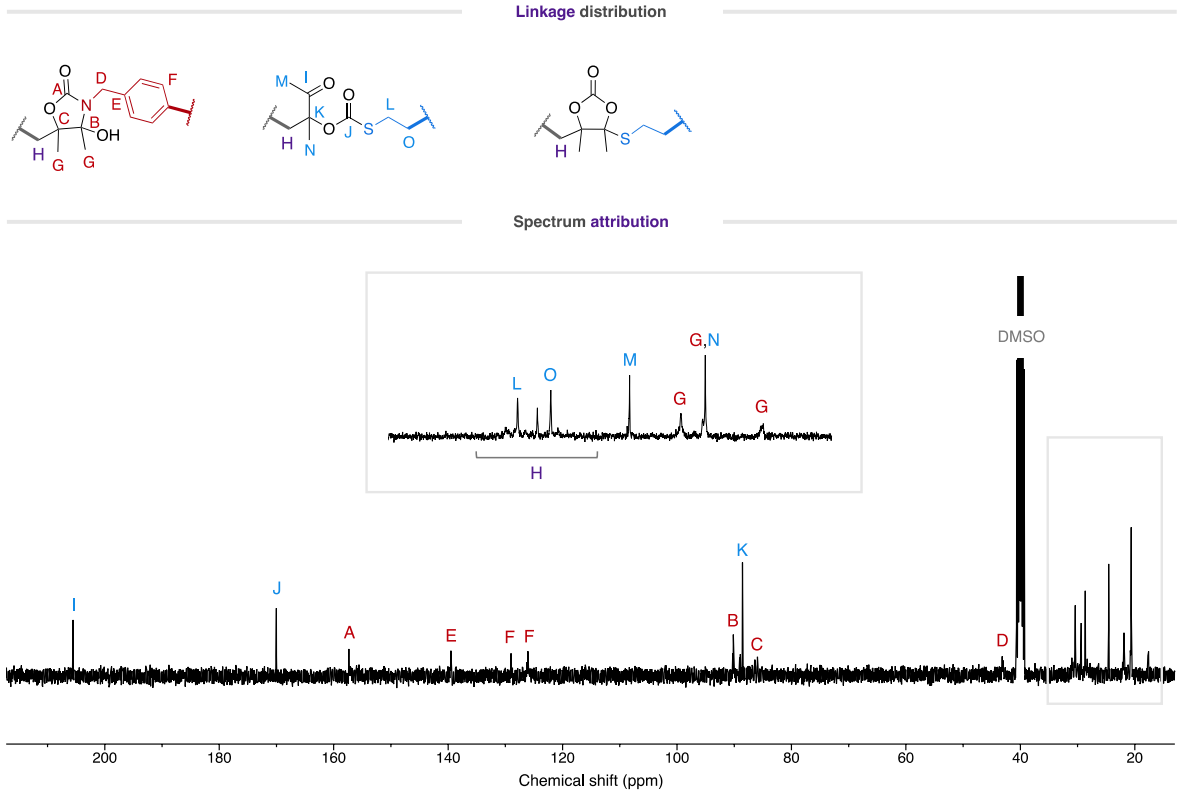

Figure S24 – ^{13}C-NMR spectrum of P(A3T1)C (400 MHz, DMSO-d_6).

P(A3T2)

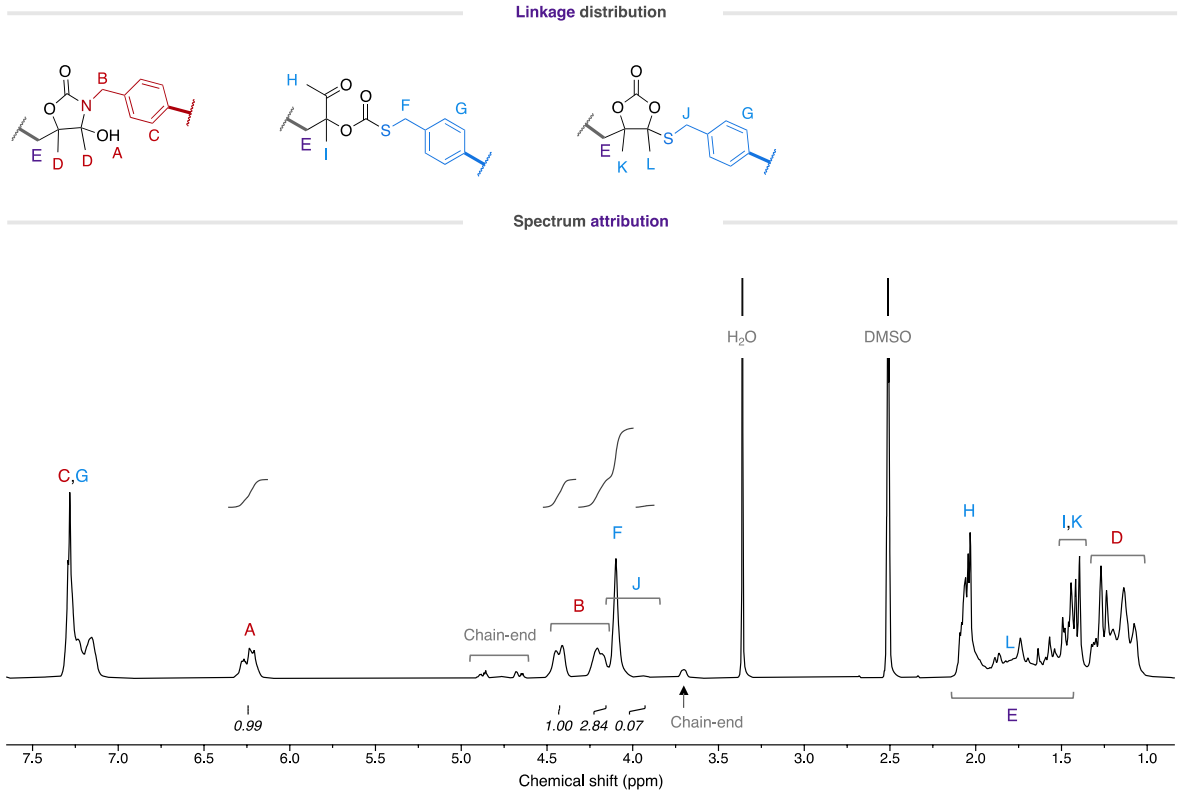

Figure S25 – ^{1}H-NMR spectrum of P(A3T2) (400 MHz, DMSO-d_6).

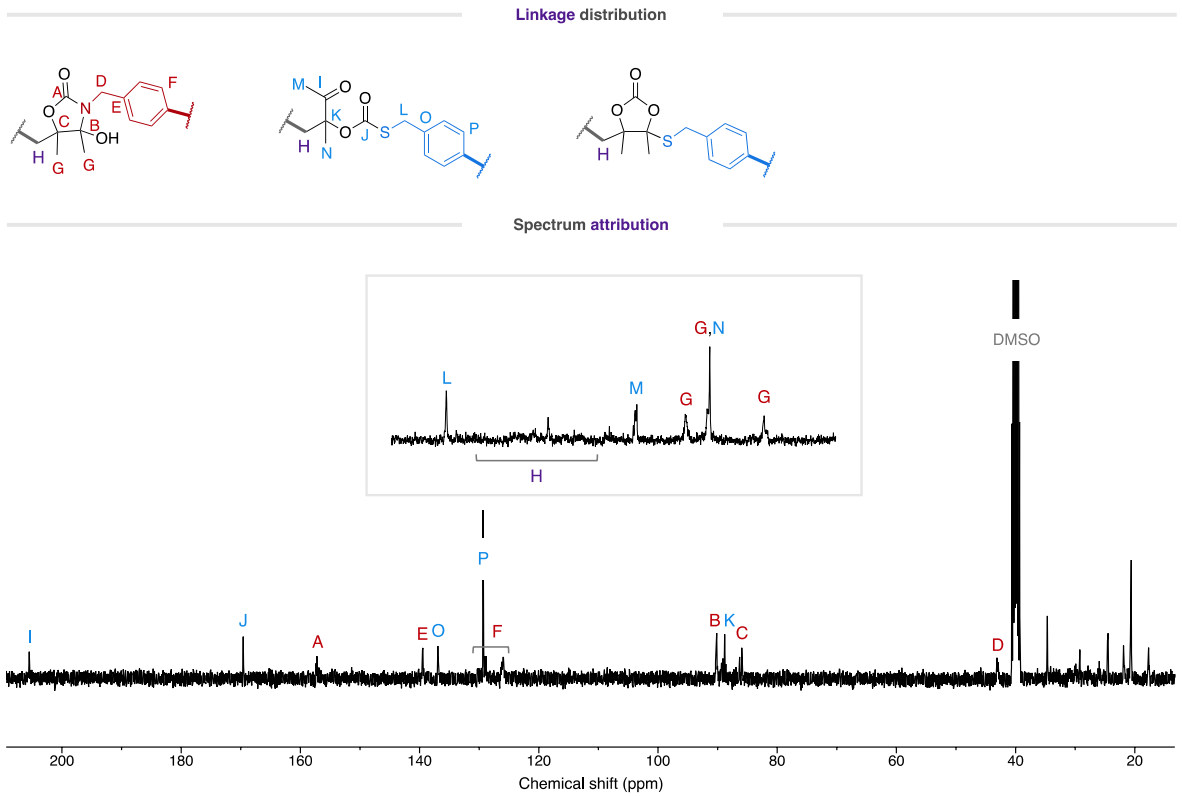

Figure S26 – ^{13}C-NMR spectrum of P(A3T2) (400 MHz, DMSO-d_6).

6. SEC chromatograms of crude reactions

Typical SEC chromatograms of crude reaction medium are shown below for polymers synthesized without catalyst and with 2 mol% of DBU.

P(A1T1)

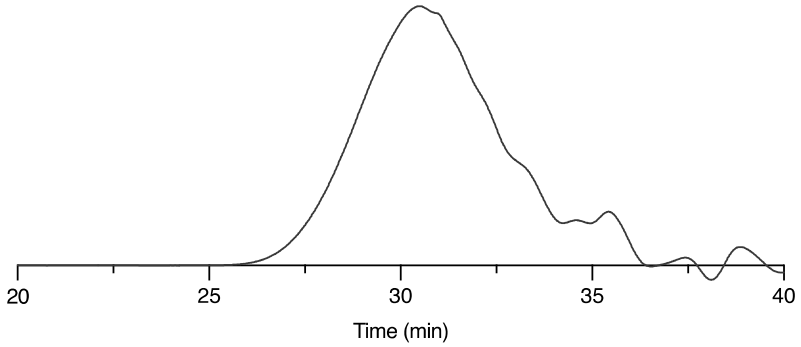

Figure S27 – SEC chromatogram (before purification) of P(A1T1).

P(A1T1)C

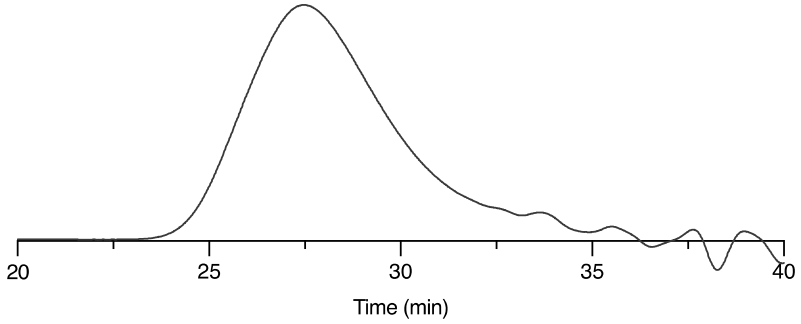

Figure S28 – SEC chromatogram (before purification) of P(A1T1)C.

P(A1T2)

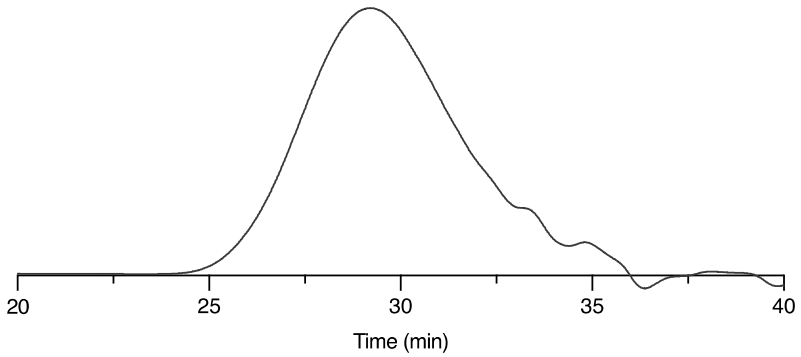

Figure S29 – SEC chromatogram (before purification) of P(A1T2).

P(A2T1)

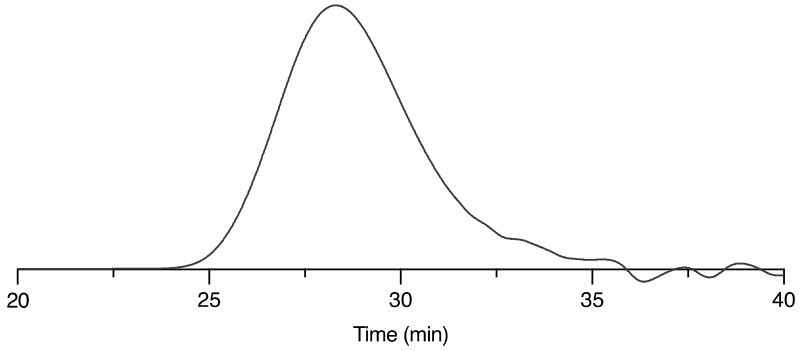

Figure S30 – SEC chromatogram (before purification) of P(A2T1).

P(A2T1)C

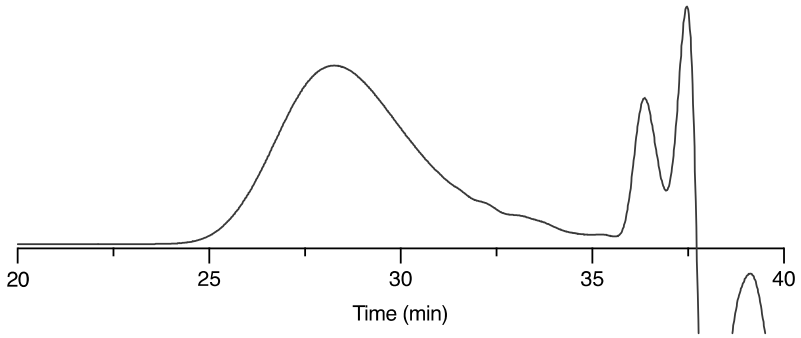

Figure S31 – SEC chromatogram (before purification) of P(A2T1)C.

P(A2T2)

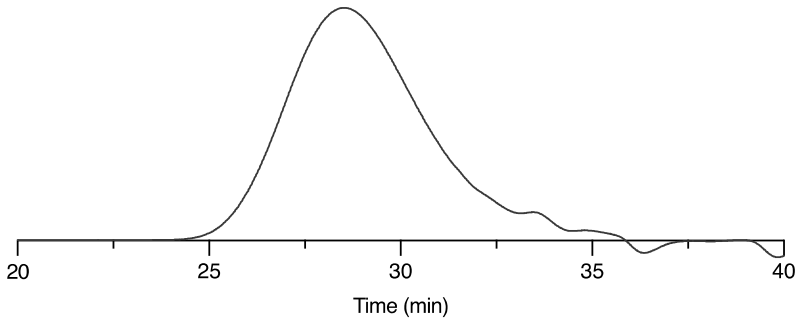

Figure S32 – SEC chromatogram (before purification) of P(A2T2).

P(A3T1)

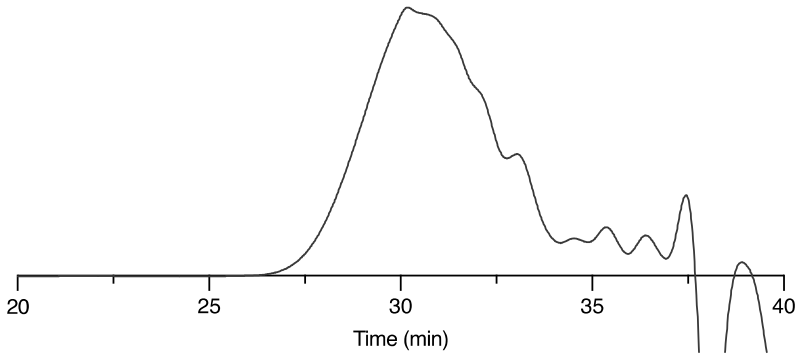

Figure S33 – SEC chromatogram (before purification) of P(A3T1).

P(A3T1)C

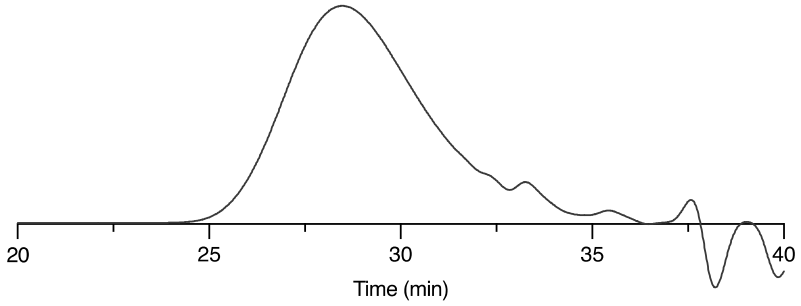

Figure S34 – SEC chromatogram (before purification) of P(A3T1)C.

P(A3T2)

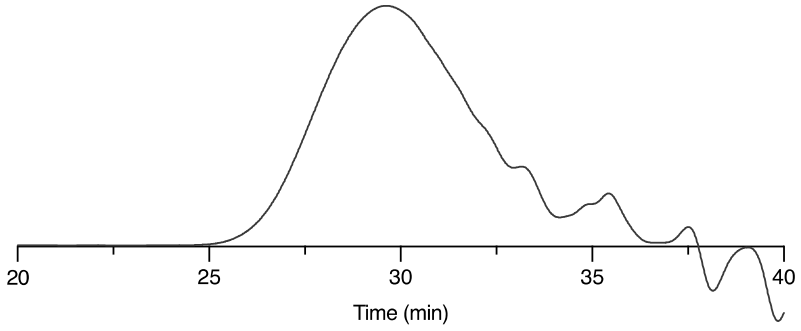

Figure S35 – SEC chromatogram (before purification) of P(A3T2).

7. TGA analyses of pure polymers

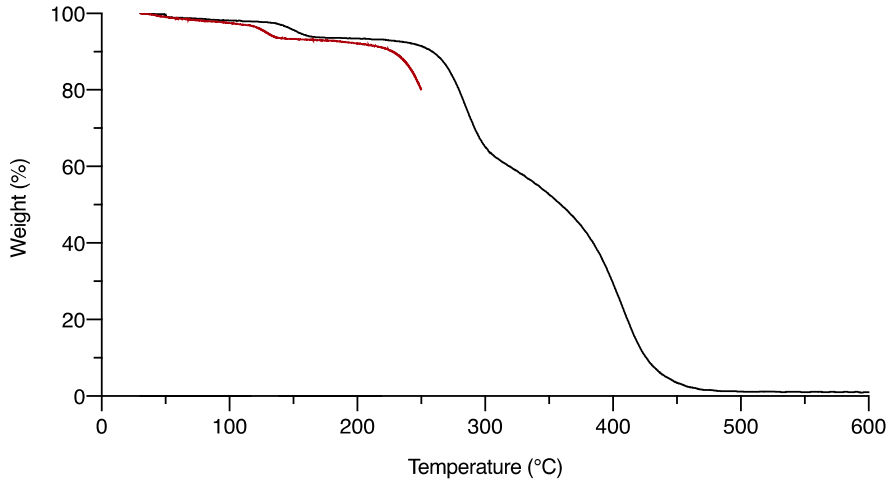

Figure S36 – TGA plot of P(A1T1) at a heating rate of 20 K/min (black) and 2 K/min (red).

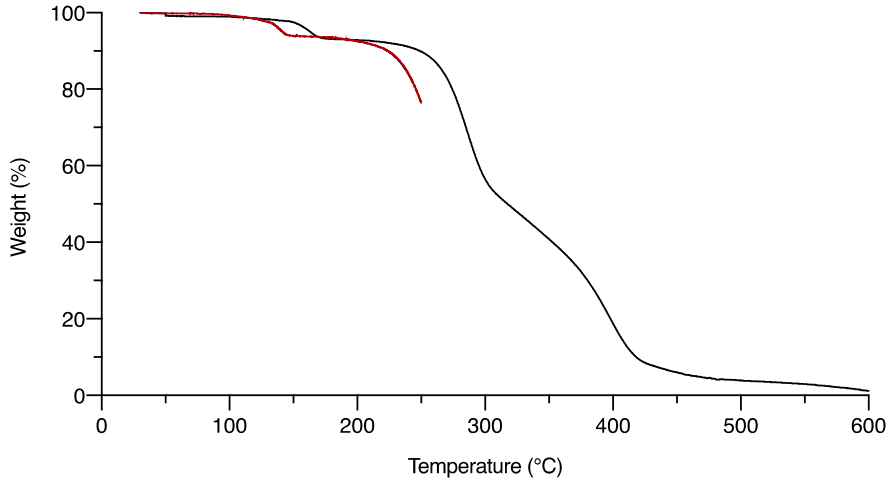

Figure S37 – TGA plot of P(A1T1)C at a heating rate of 20 K/min (black) and 2 K/min (red).

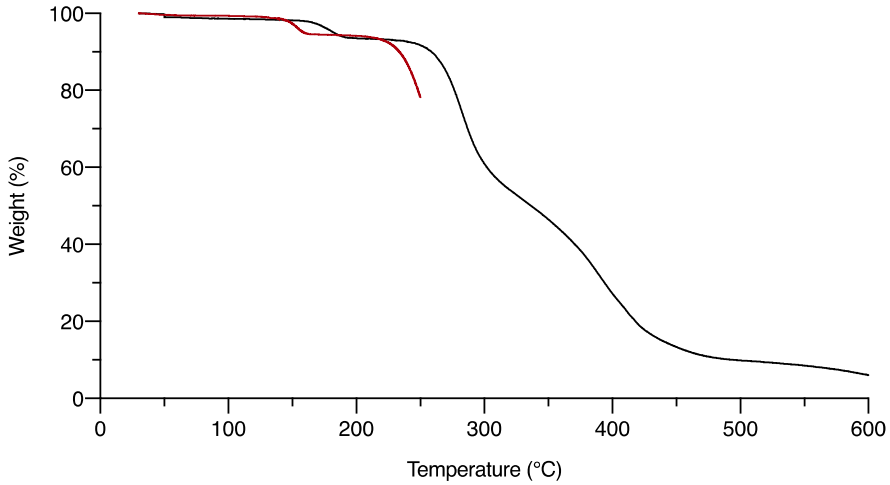

Figure S38 – TGA plot of P(A1T2) at a heating rate of 20 K/min (black) and 2 K/min (red).

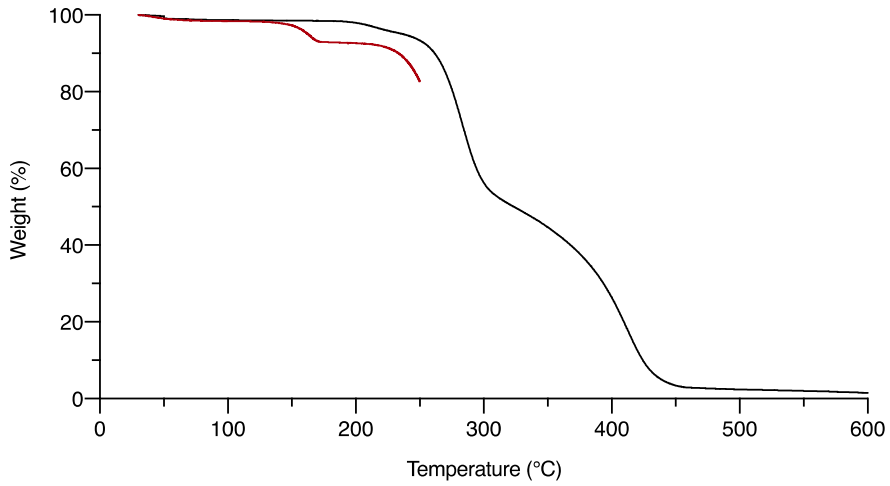

Figure S39 – TGA plot of P(A2T1) at a heating rate of 20 K/min (black) and 2 K/min (red).

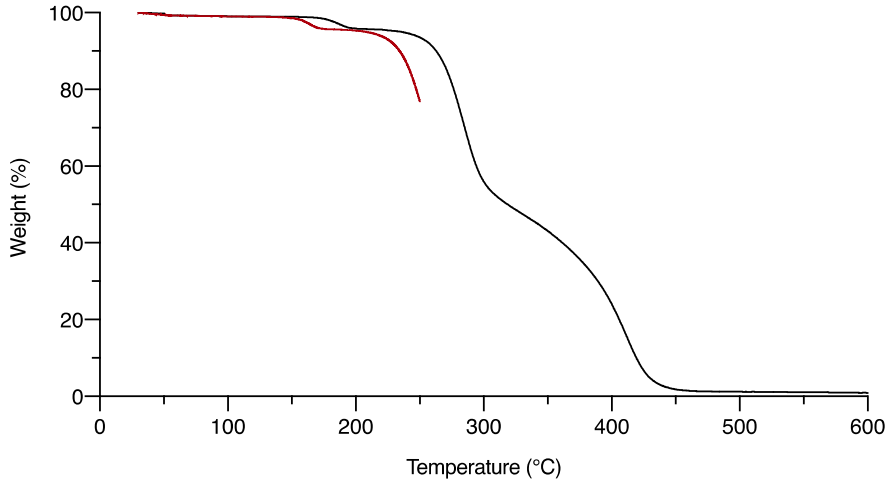

Figure S40 – TGA plot of P(A2T1)C at a heating rate of 20 K/min (black) and 2 K/min (red).

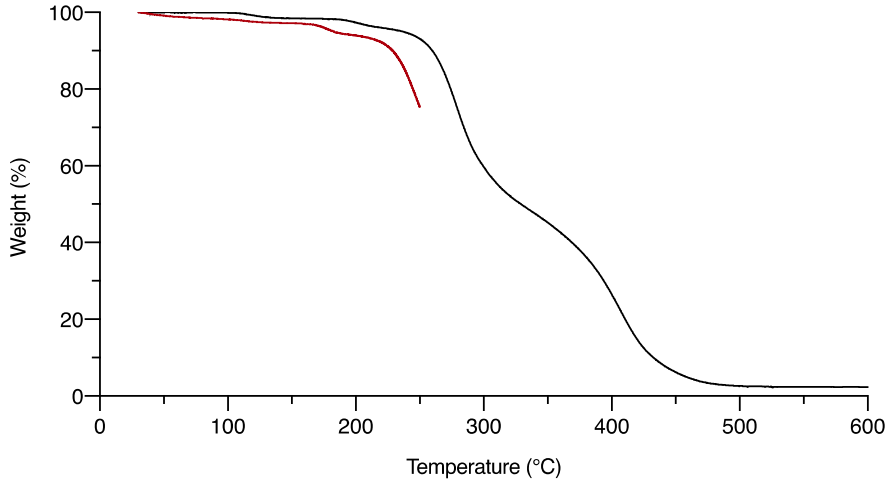

Figure S41 – TGA plot of P(A2T2) at a heating rate of 20 K/min (black) and 2 K/min (red).

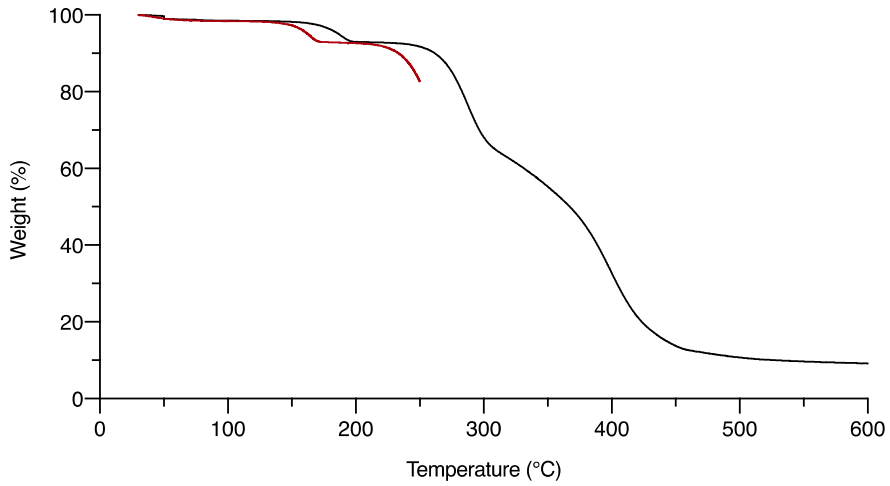

Figure S42 – TGA plot of P(A3T1) at a heating rate of 20 K/min (black) and 2 K/min (red).

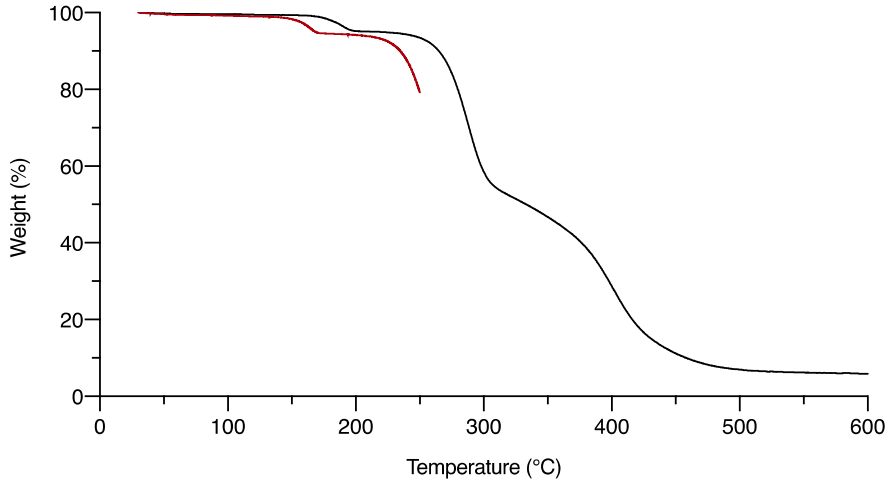

Figure S43 – TGA plot of P(A3T1)C at a heating rate of 20 K/min (black) and 2 K/min (red).

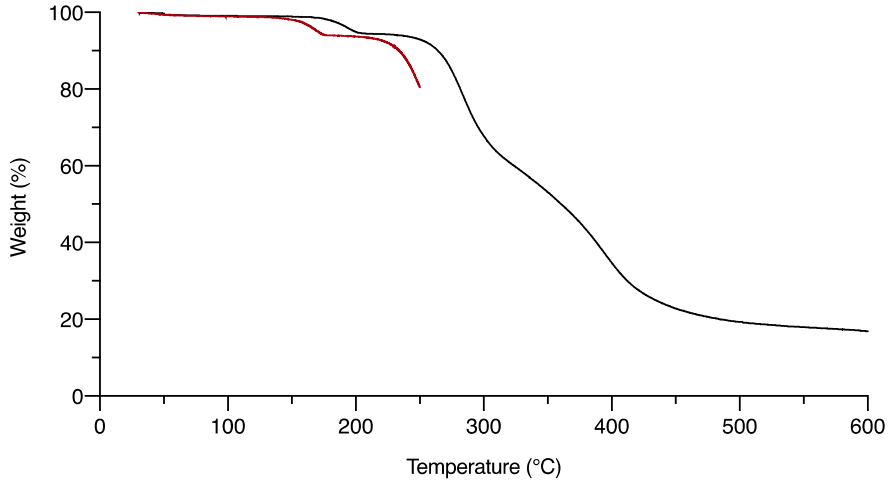

Figure S44 – TGA plot of P(A3T2) at a heating rate of 20 K/min (black) and 2 K/min (red).

8. DSC analyses of pure polymers

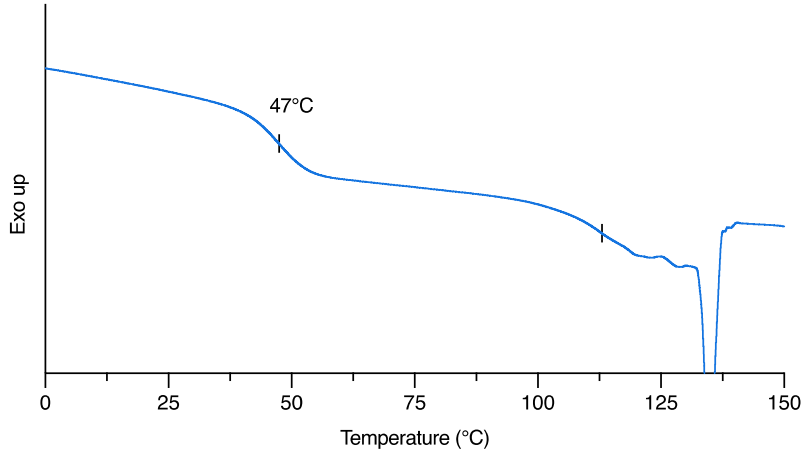

Figure S45 – Reversing heat flow by modulated DSC of P(A1T1).

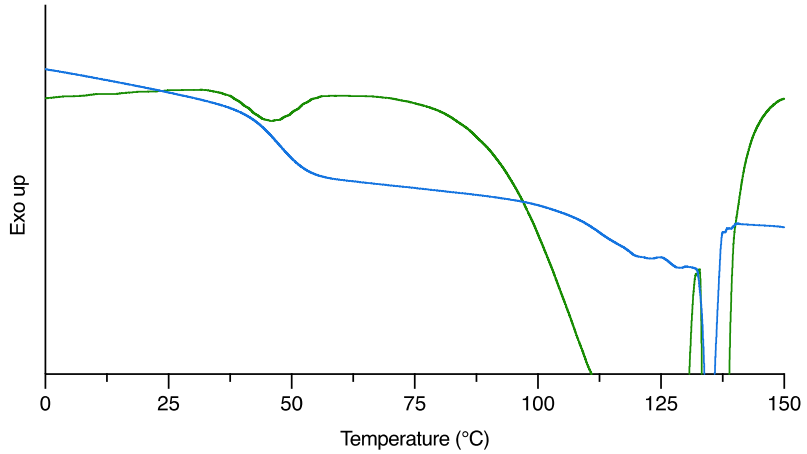

Figure S46 – Reversing heat flow (blue) and non-reversing heat flow (green) by modulated DSC of P(A1T1). The non-reversing curve displays a strong peak due to dehydration overlapping with the potential second T_g region.

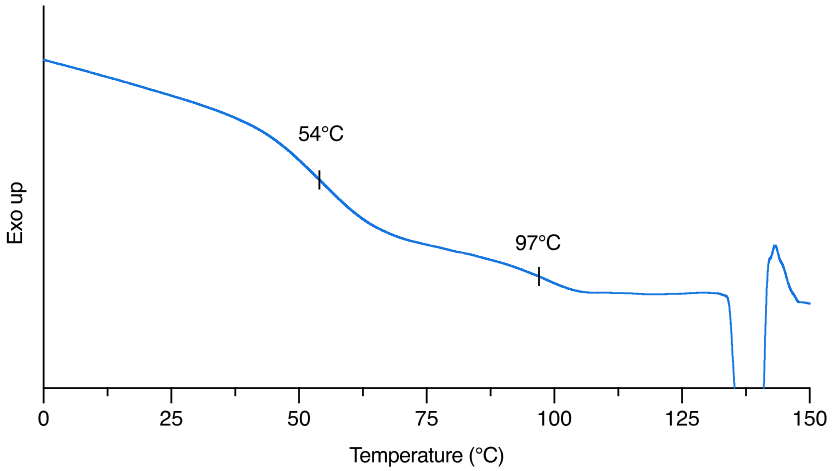

Figure S47 – Reversing heat flow by modulated DSC of P(A1T1)C.

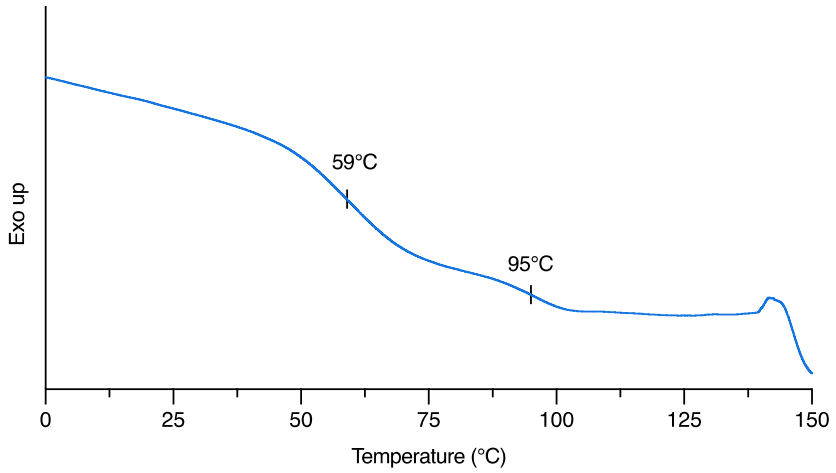

Figure S48 – Reversing heat flow by modulated DSC of P(A1T2).

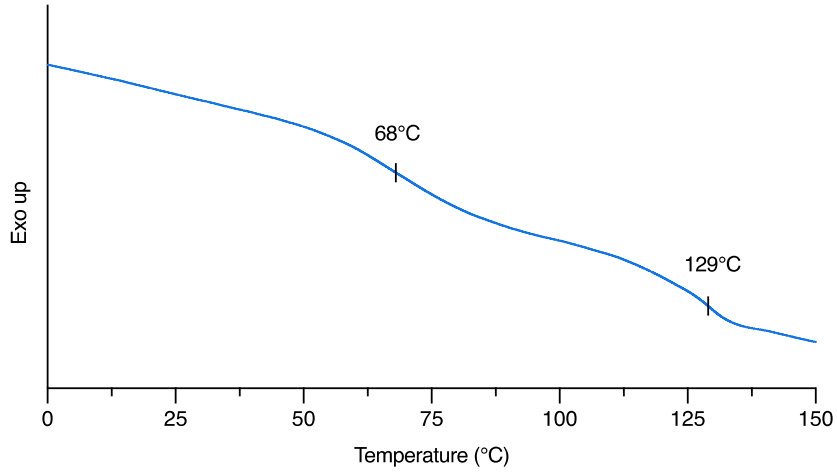

Figure S49 – Reversing heat flow by modulated DSC of P(A2T1).

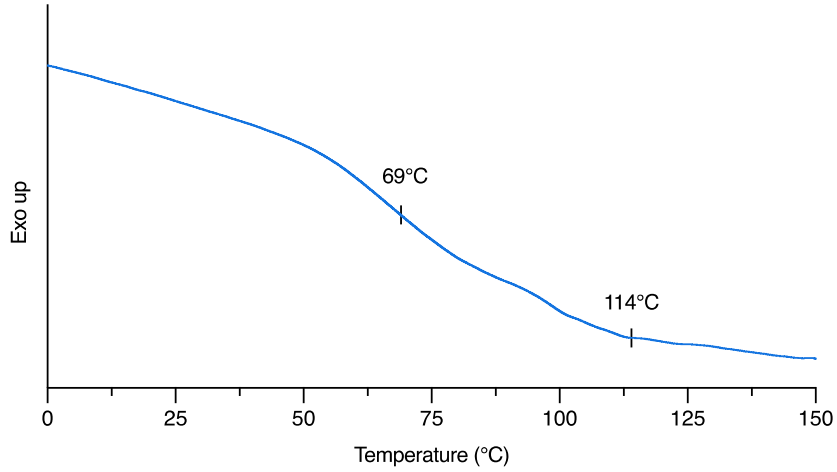

Figure S50 – Reversing heat flow by modulated DSC of P(A2T1)C.

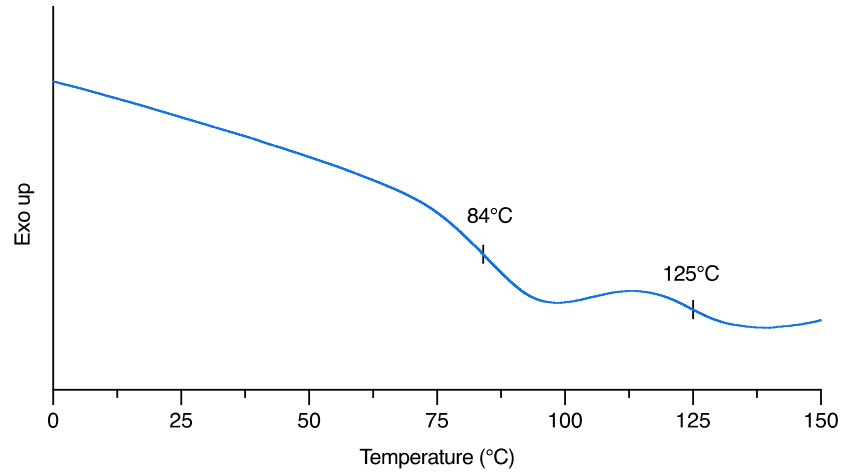

Figure S51 – Reversing heat flow by modulated DSC of P(A2T2).

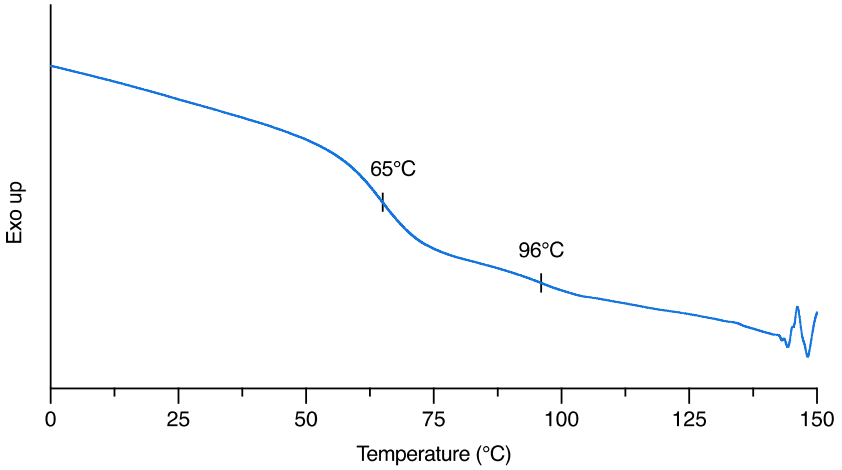

Figure S52 – Reversing heat flow by modulated DSC of P(A3T1).

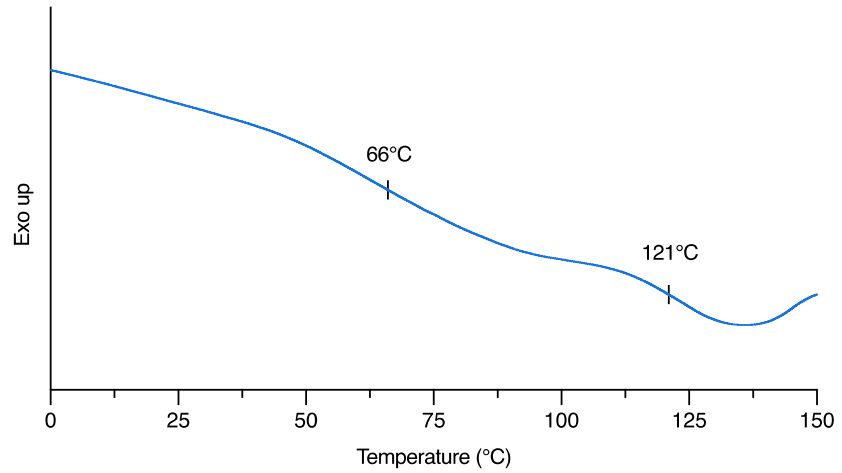

Figure S53 – Reversing heat flow by modulated DSC of P(A3T1)C.

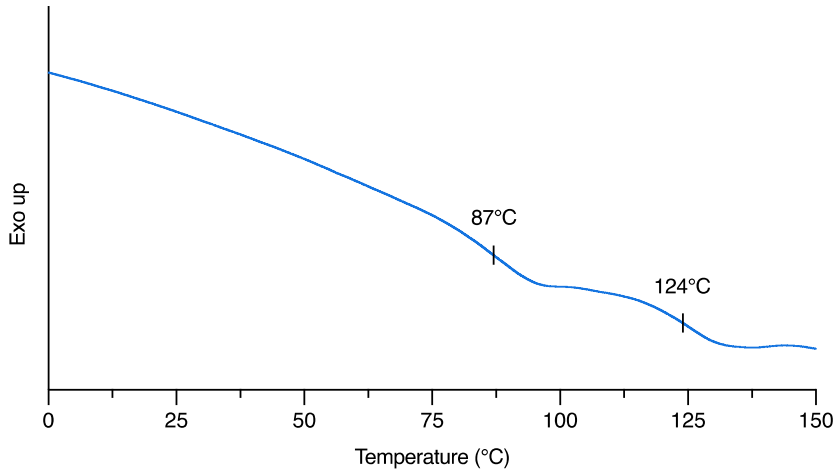

Figure S54 – Reversing heat flow by modulated DSC of P(A3T2).

9. Modulated DSC experiments

Conventional DSC experiments didn't lead to any exploitable results. However, the modulated DSC technique is characterized by a higher sensitivity which has lead to the observation to 2 weak and broad T_gs for all copolymers. In order to shed light on this unusual feature, several experiments were achieved on the polymer P(A1T2), chosen for an optimal temperature window between the second transition and the dehydration reaction at higher temperature which can be observed on the non-reversing heat flow curve. For most polymers, the dehydration peak start was close to the second transition. After selection of the polymer, the herein described experiments were conducted:

General procedure:

- Heating from 25 to 90 °C (10 °C/min)
- Cooling to -40 °C (10 °C/min)
- *Modulation of temperature (amplitude 2°C; period 60 s)*
- Heating to 200 °C (2 °C/min)

This procedure leads to the observation of two weak and broad T_g.

Annealing above the second T_g:

- Heating from 25 to 90 °C (10 °C/min)
- Cooling to -40 °C (10 °C/min)
- *Modulation of temperature (amplitude 2°C; period 60 s)*
- Heating to 110 °C (2 °C/min) [Annealing of polymer]
- Cooling to -40 °C (10 °C/min)
- Heating to 130 °C (2 °C/min)

With this procedure, the first part of the experiment stays the same except that the sample is heated up to 110 °C. The second T_g of the polymer, determined in the first curve, is observed at 95°C. On the next cycle (after annealing without isothermal), only the first T_g is observed.

As dehydrated polymers are characterized by a single T_g similar to the first T_g of the hydroxy-polymers, a new experiment was achieved with post-experience polymer chemical structure analysis.

Annealing above the second T_g with post-experiment characterization:

- Heating from 25 to 90 °C (10 °C/min)
- Cooling to -40 °C (10 °C/min)
- *Modulation of temperature (amplitude 2°C; period 60 s)*
- Heating to 110 °C (2 °C/min) [Annealing of polymer]

As this experiment stops just after polymer annealing, the sample was subsequently taken out of the pan and analyzed by ^{1}H-NMR analysis. No trace of dehydration was observed and the chemical structure of the polymer was intact. Then, these experiments indicate that the second transition may be an irreversible event which disappears after fast annealing.

Other experiments were conducted:

- Slow cooling (rate of 2 °C/min) after annealing
- Isothermal of 30 minutes at 85°C (between the two transitions) on cooling
- Fast cooling (rate of 150 °C/min) after annealing

However, these supplementary experiments didn't affect the curves.

10. Polymerizations with various DBU loadings

The polymerization of **bisαCC** was considered with **AA1** and **TT1** using different loadings of DBU. The linkage ratio **TL1** / **TL2** was determined by integration of characteristic peaks for each functionality (peak F for **TL1**; peak J for **TL2**). As the residual DMF peaks were overlapping with the 2 signals of interest, the lone peak of DMF at 7.95 ppm was simply integrated and used to subtract the theorical DMF integration from the F and J signals (Figure S56).

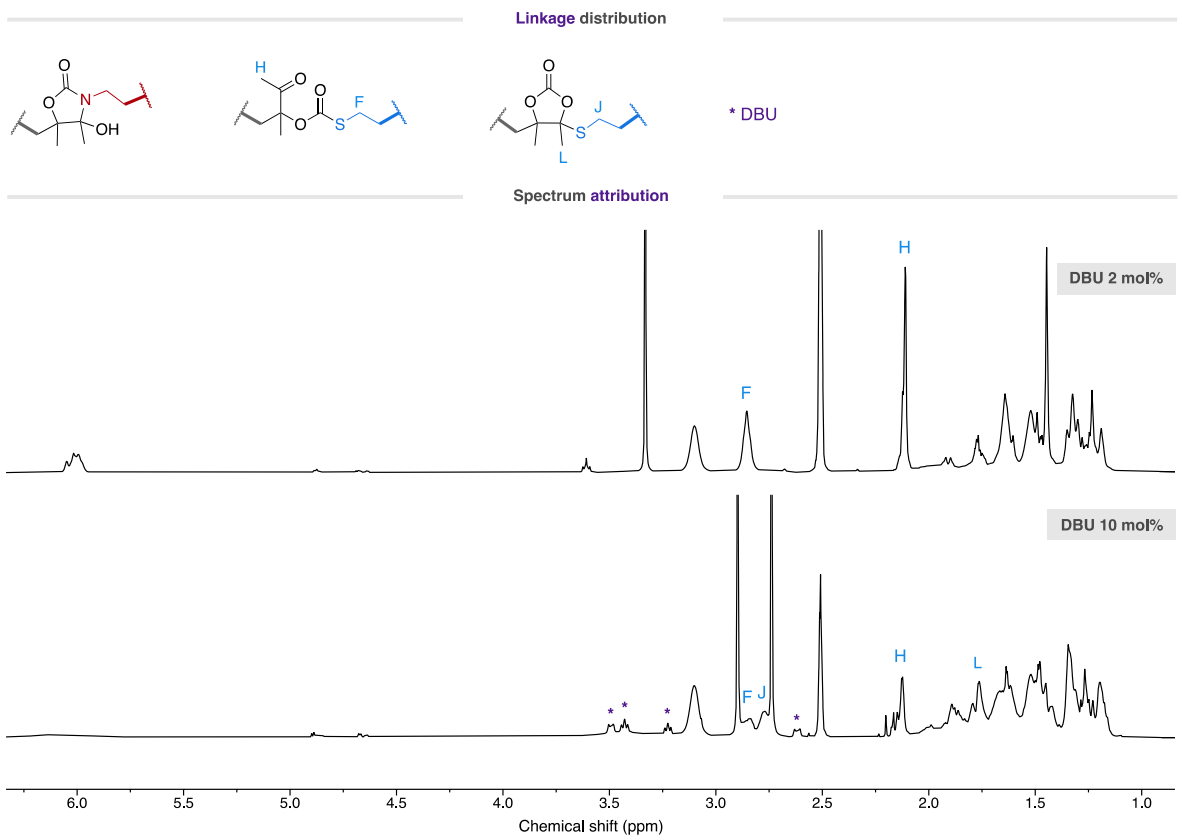

Figure S55 – ^{1}H-NMR spectrum of polymers made from **AA1** and **TT1** with 2 mol% and 10 mol% of DBU (400 MHz, DMSO-d_6). The polymer made from 2 mol% of DBU is pure (P(A1T1)C) and the polymer made from 10 mol% of DBU was analyzed after one precipitation in diethyl ether.

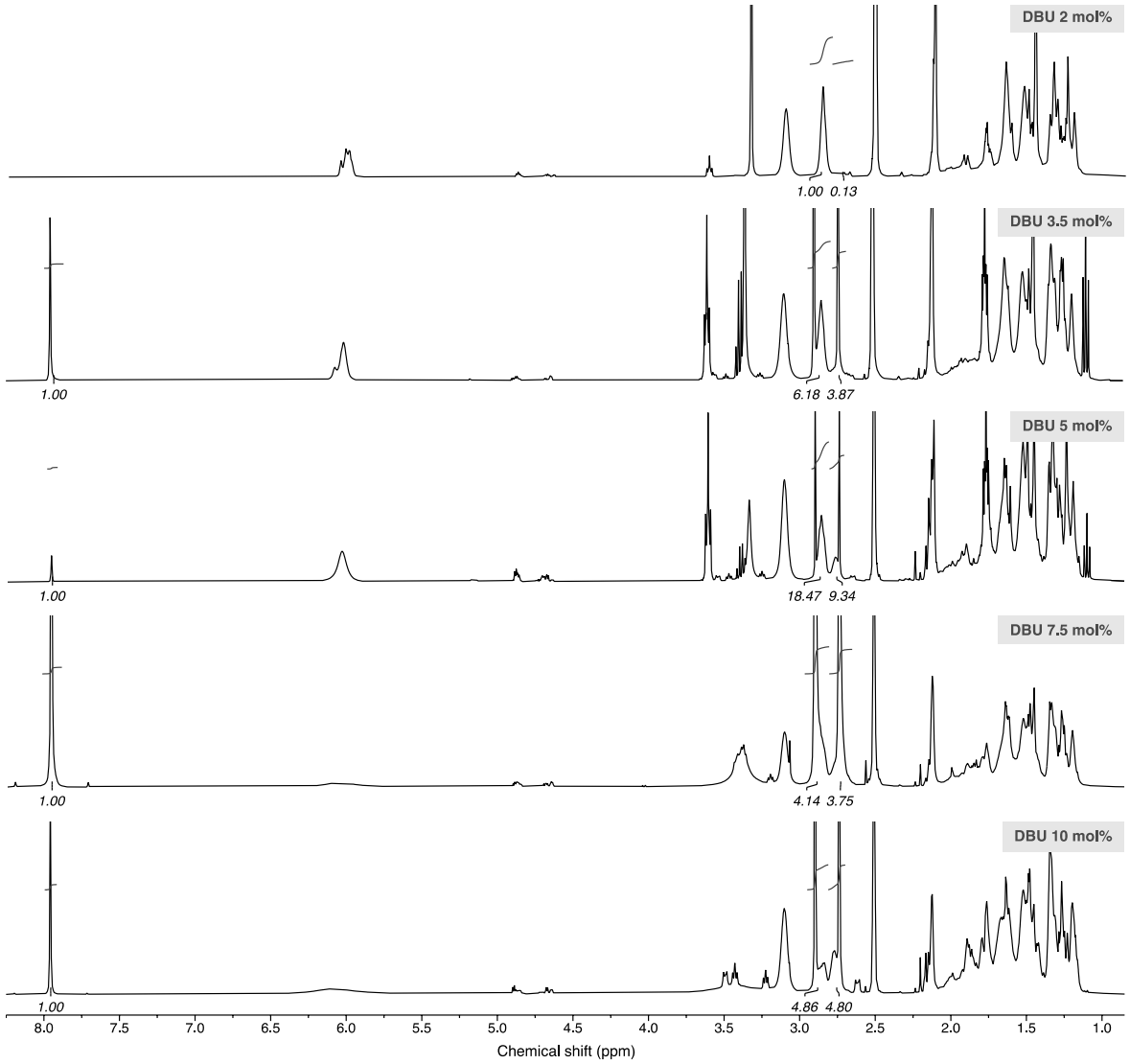

Figure S56 – ^{1}H-NMR spectrum of polymers made from **AA1** and **TT1** with 2 mol% to 10 mol% of DBU (400 MHz, DMSO-d_6). The polymer made from 2 mol% of DBU is pure (P(A1T1)C) and the other polymers were analyzed after one precipitation in diethyl ether.

Table S2 - Molecular characteristics and linkages selectivity for the polymerization of BisαCC with **AA1** and **TT1** after 24h of reaction with different DBU loadings. Polymerizations were carried out at 25 °C in DMF.

Entry	Diamine	Dithiol	DBU loading (mol%)	M_n (g/mol)[a]	M_w (g/mol)[a]	D[a]	Ratio AL1/AL2	Ratio TL1/TL2
1	AA1	TT1	--	3500	6100	1.76	16 / 84	100 / 0
2			2	12900	24500	1.89	0 / 100	88 / 12
3			3.5	11400	20600	1.80	0 / 100	79 / 21
4			5	9800	16800	1.72	0 / 100	72 / 28
5			7.5	8900	15000	1.70	0 / 100	62 / 38
6			10	11100	19600	1.78	0 / 100	51 / 49

[a]Determined in the crude product by SEC in DMF/LiBr by using a PS calibration

11. NMR characterization of dehydrated polymers

P(A1T1) dehydrated

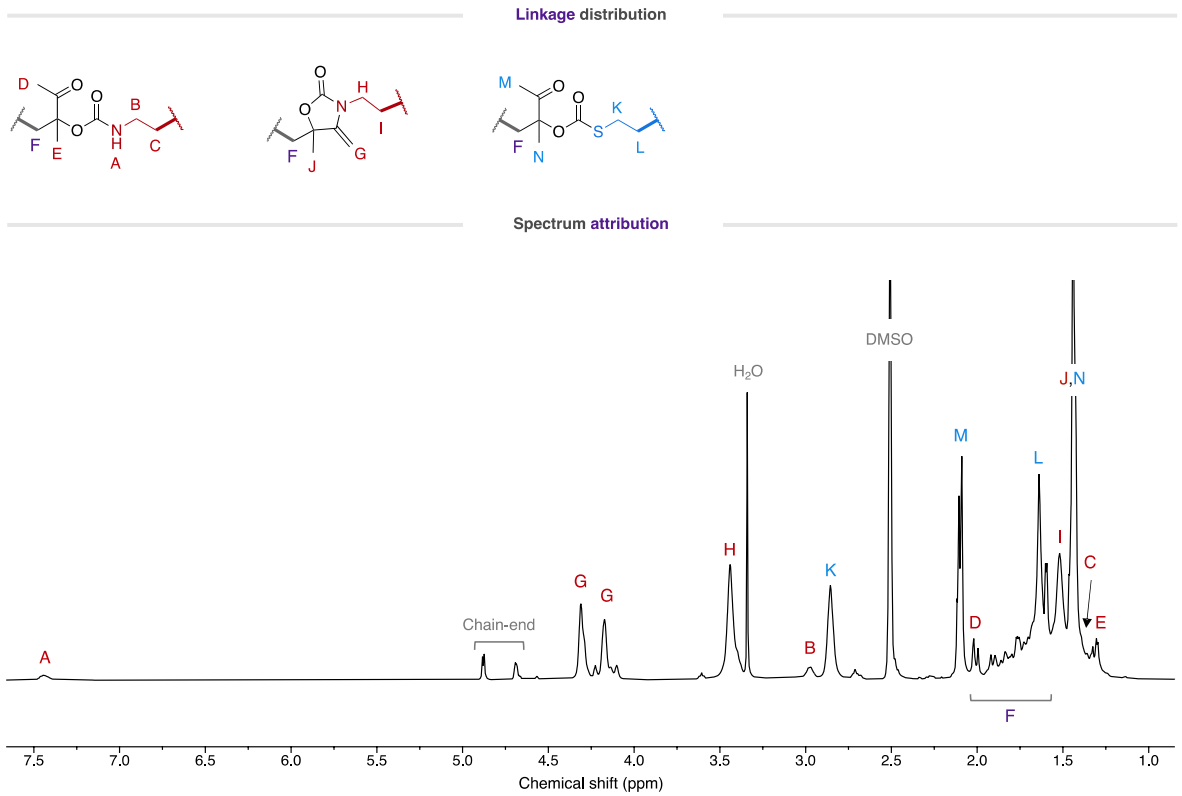

Figure S57 – ^{1}H-NMR spectrum of dehydrated P(A1T1) (400 MHz, DMSO-d_6).

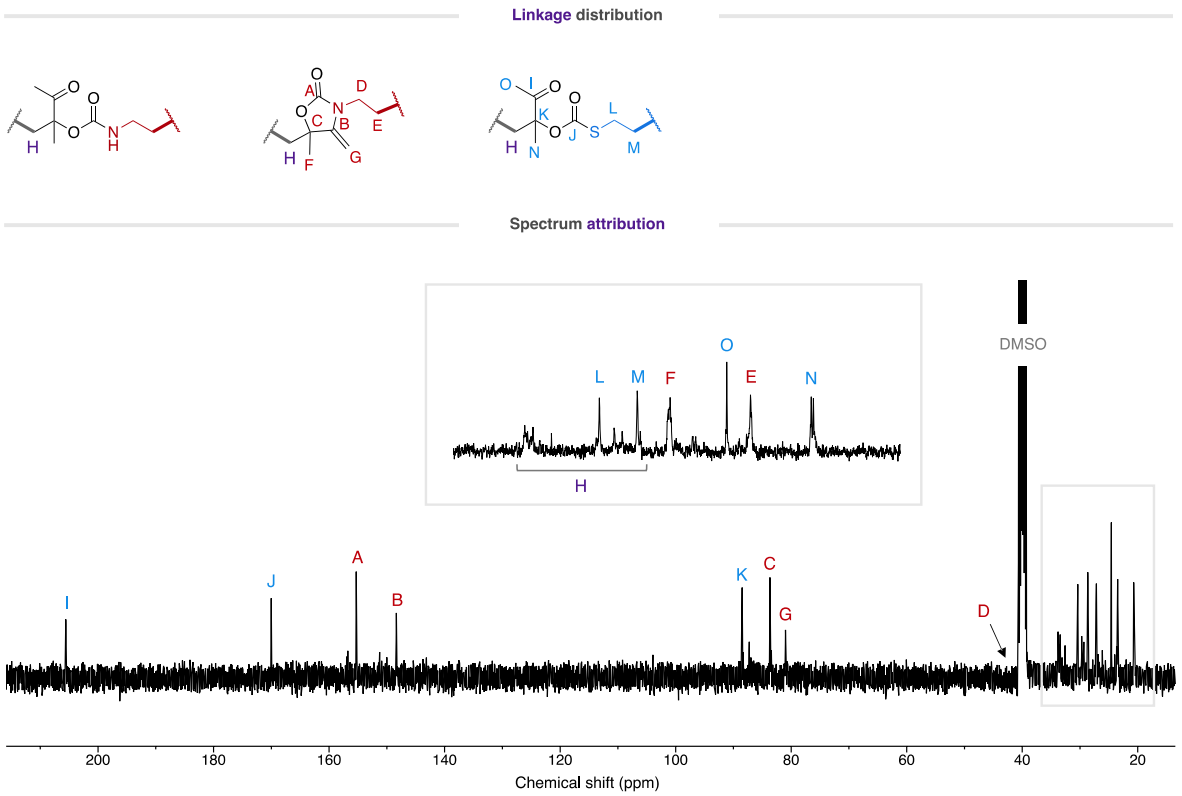

Figure S58 – ^{13}C-NMR spectrum of dehydrated P(A1T1) (400 MHz, DMSO-d_6).

P(A1T1)C dehydrated

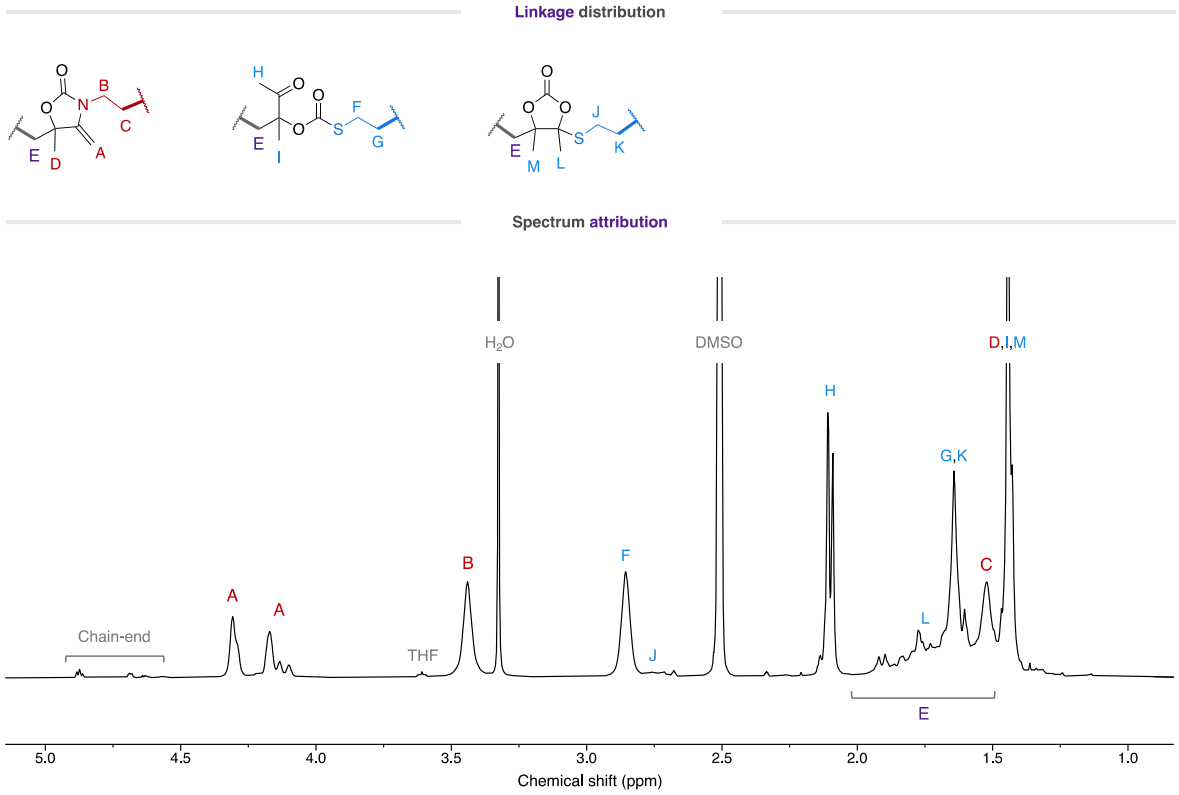

Figure S59 – ^{1}H-NMR spectrum of dehydrated P(A1T1)C (400 MHz, DMSO-d_6).

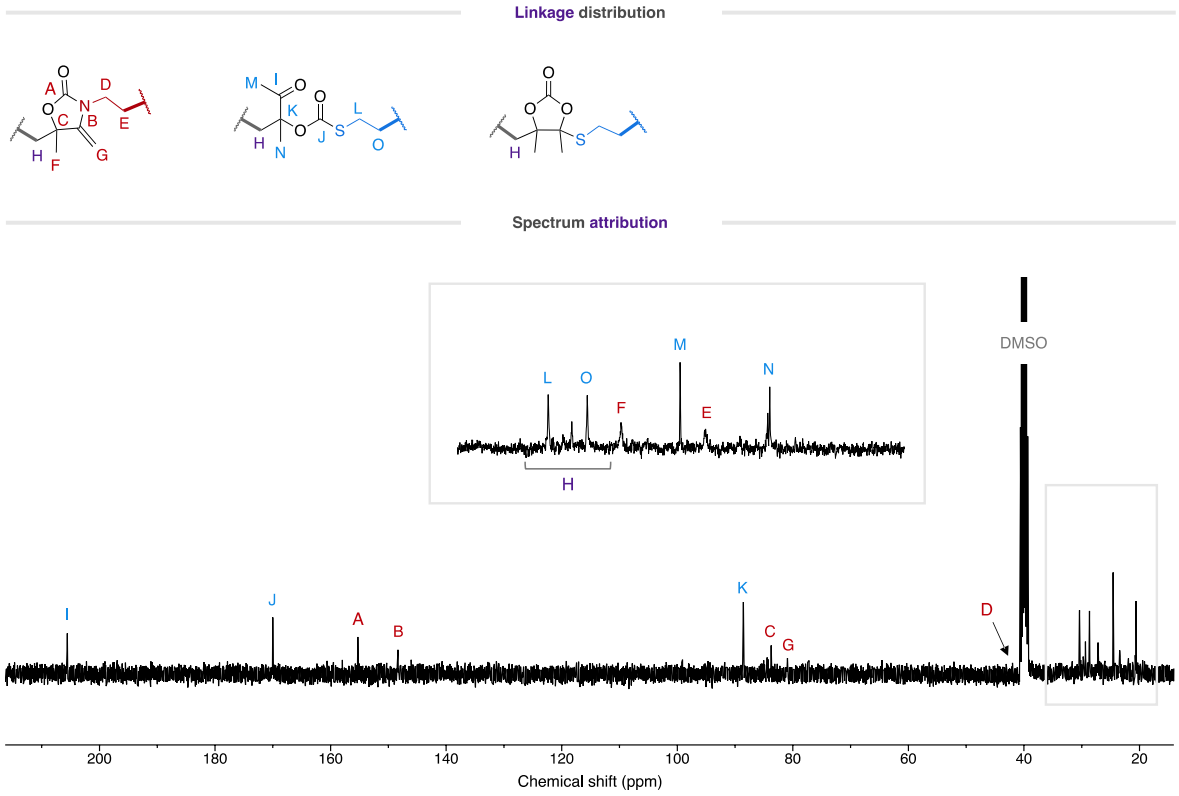

Figure S60 – ^{13}C-NMR spectrum of dehydrated P(A1T1)C (400 MHz, DMSO-d_6).

P(A1T2) dehydrated

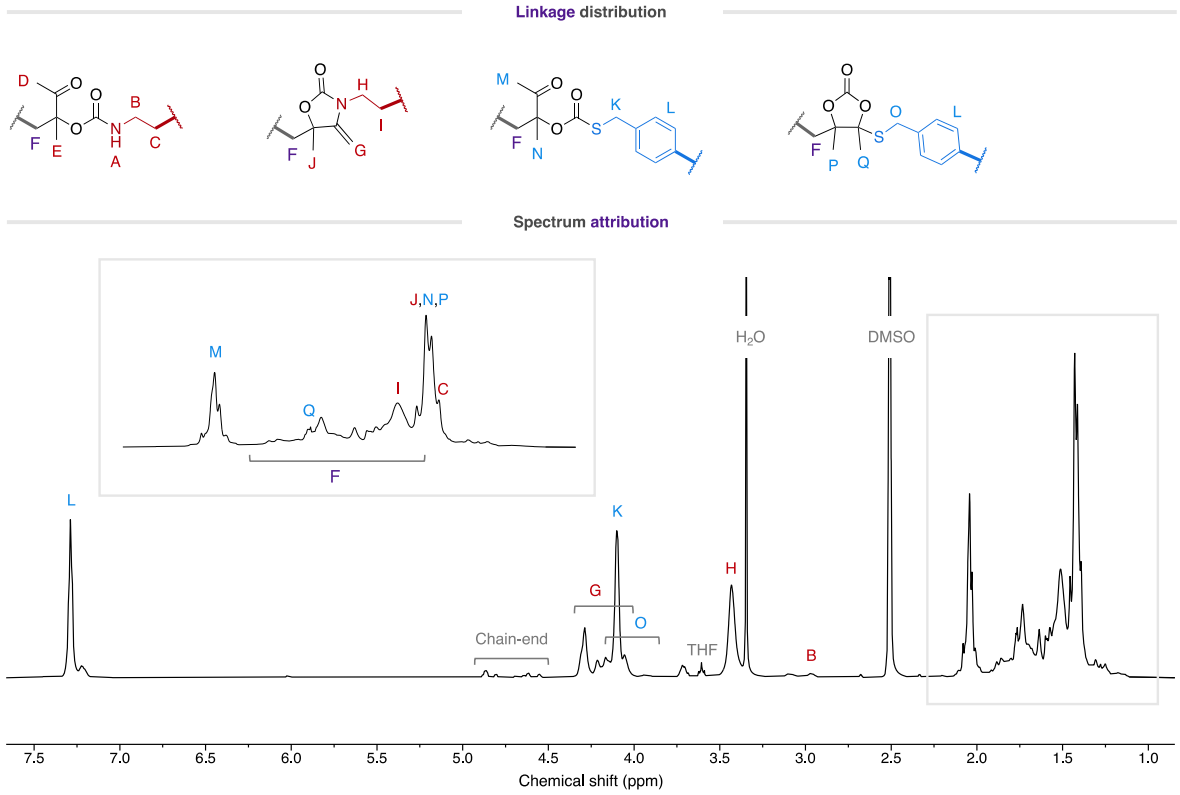

Figure S61 – ^{1}H-NMR spectrum of dehydrated P(A1T2) (400 MHz, DMSO-d_6).

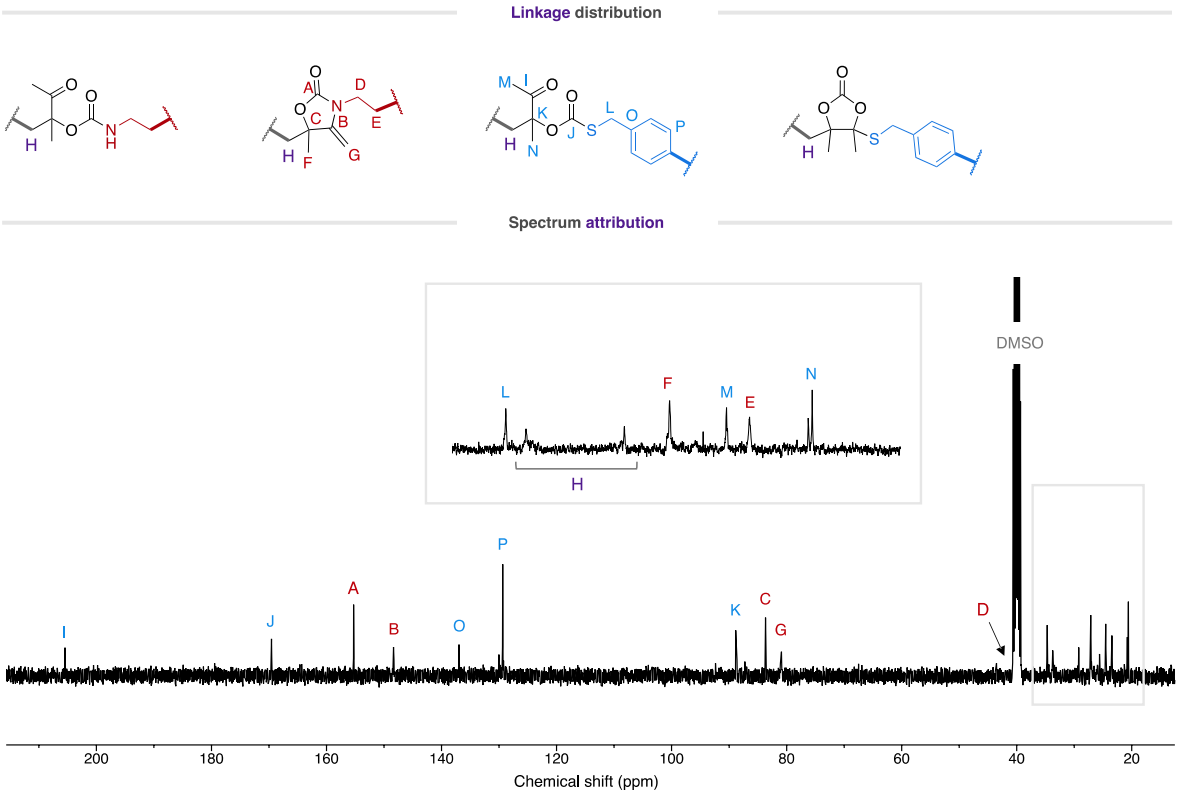

Figure S62 – ^{13}C-NMR spectrum dehydrated of P(A1T2) (400 MHz, DMSO-d_6).

P(A2T1) dehydrated

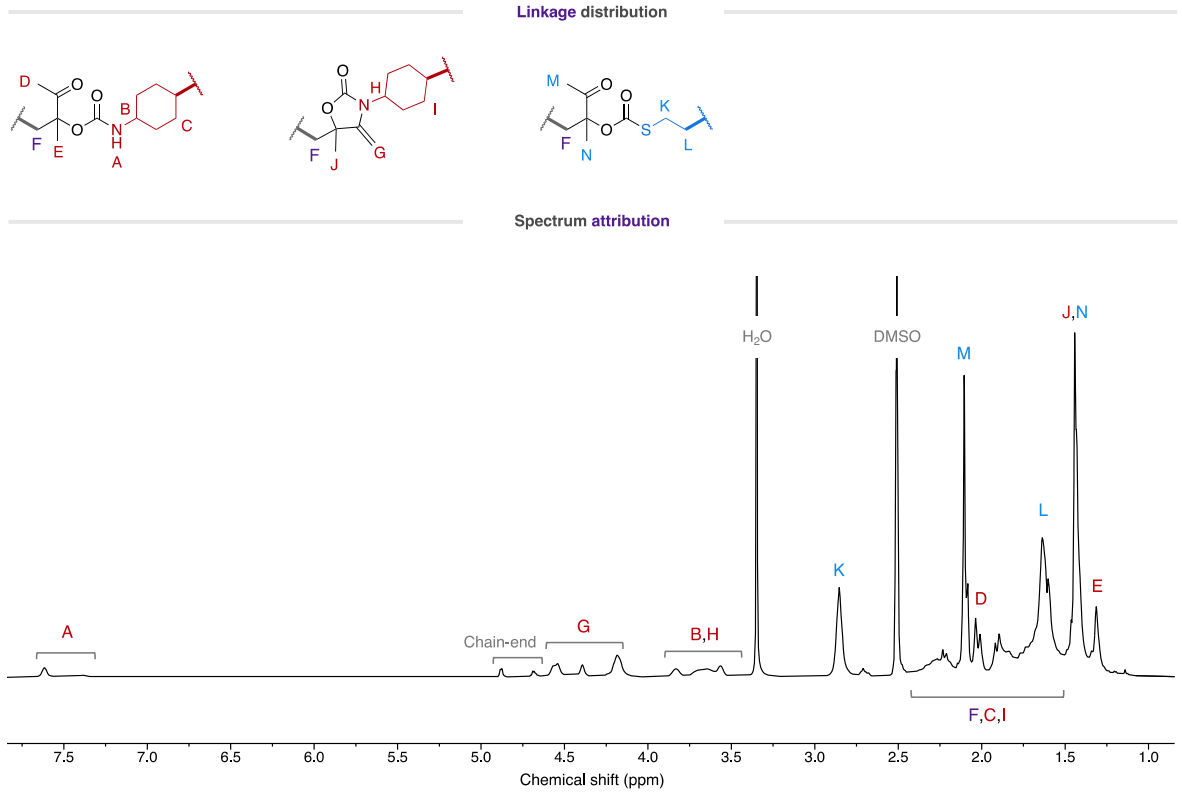

Figure S63 – ^{1}H-NMR spectrum of dehydrated P(A2T1) (400 MHz, DMSO-d_6).

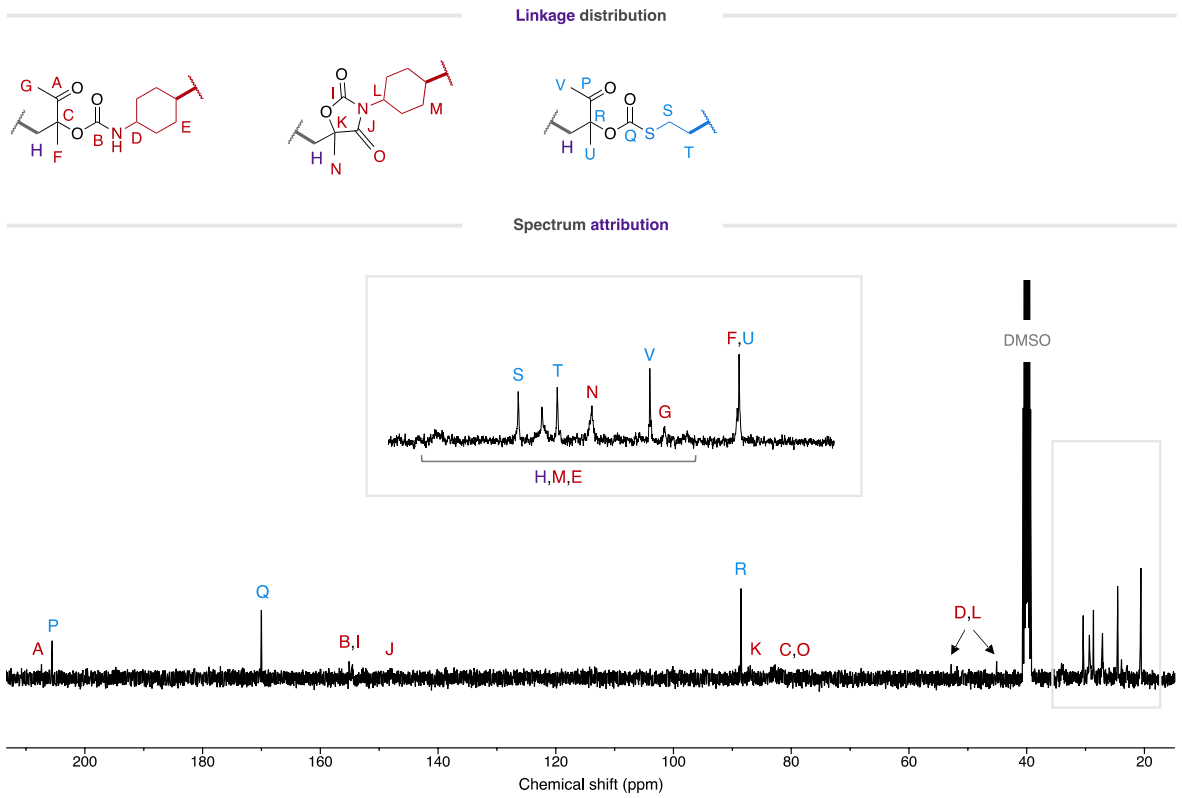

Figure S64 – ^{13}C-NMR spectrum of dehydrated P(A2T1) (400 MHz, DMSO-d_6).

P(A2T1)C dehydrated

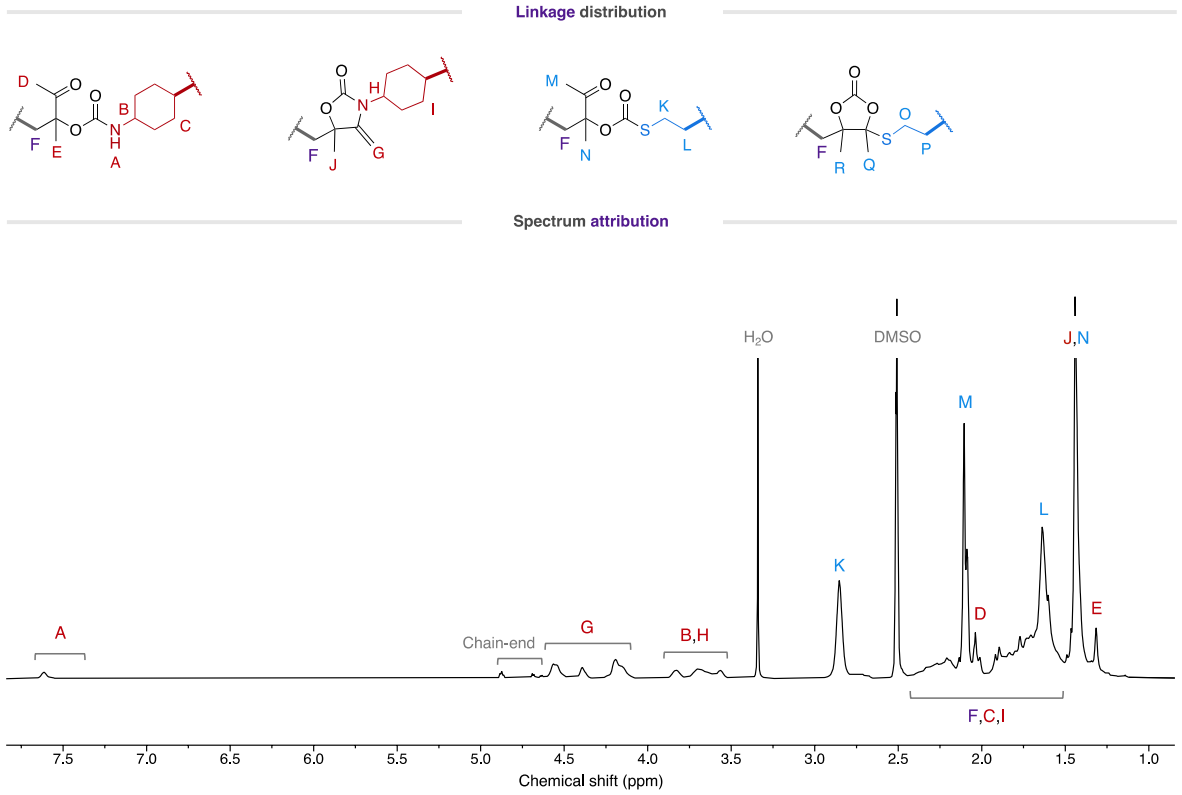

Figure S65 – ^{1}H-NMR spectrum of dehydrated P(A2T1)C (400 MHz, DMSO-d_6).

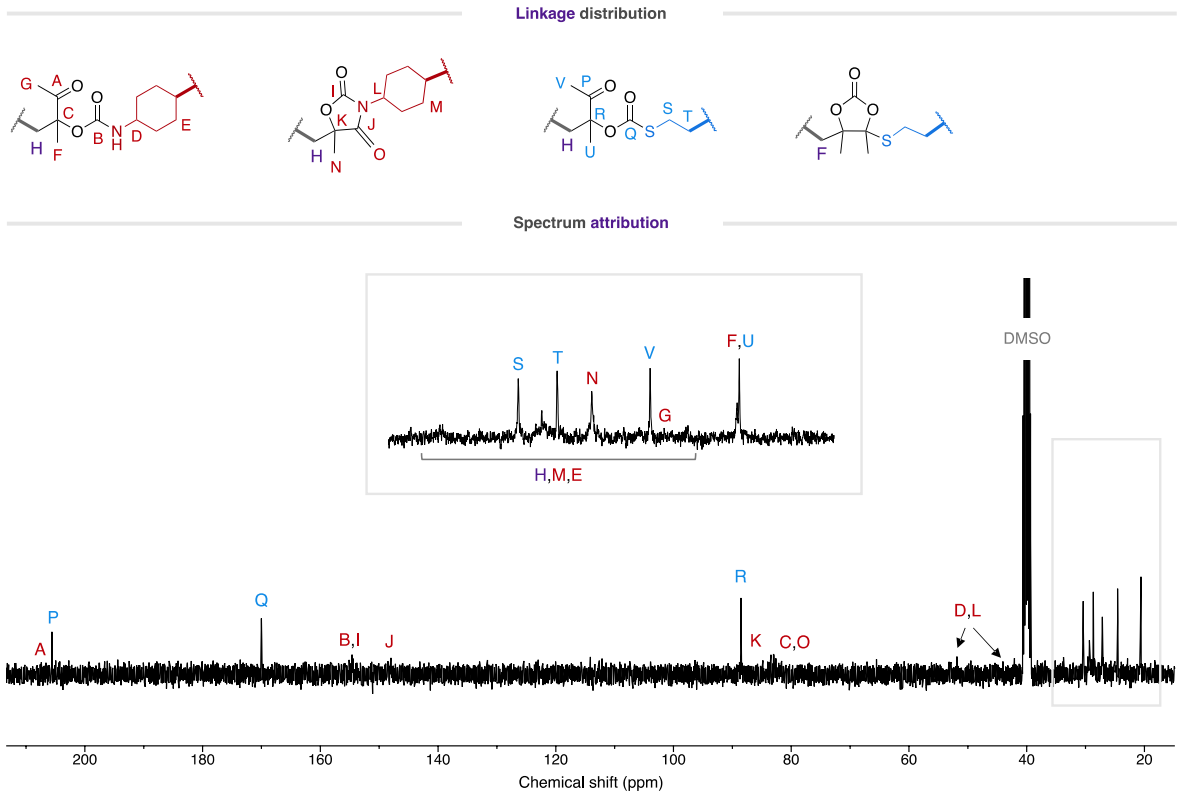

Figure S66 – ^{13}C-NMR spectrum of dehydrated P(A2T1)C (400 MHz, DMSO-d_6).

P(A2T2) dehydrated

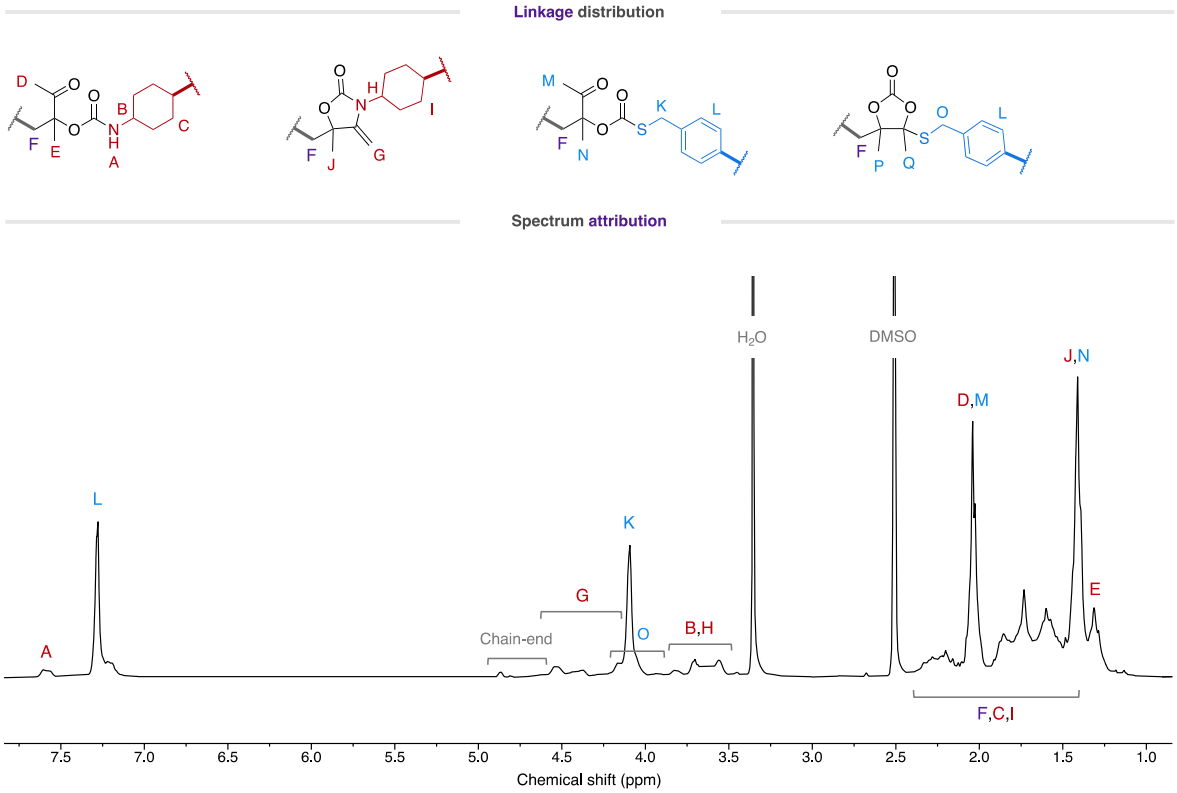

Figure S67 – ^{1}H-NMR spectrum of dehydrated P(A2T2) (400 MHz, DMSO-d_6).

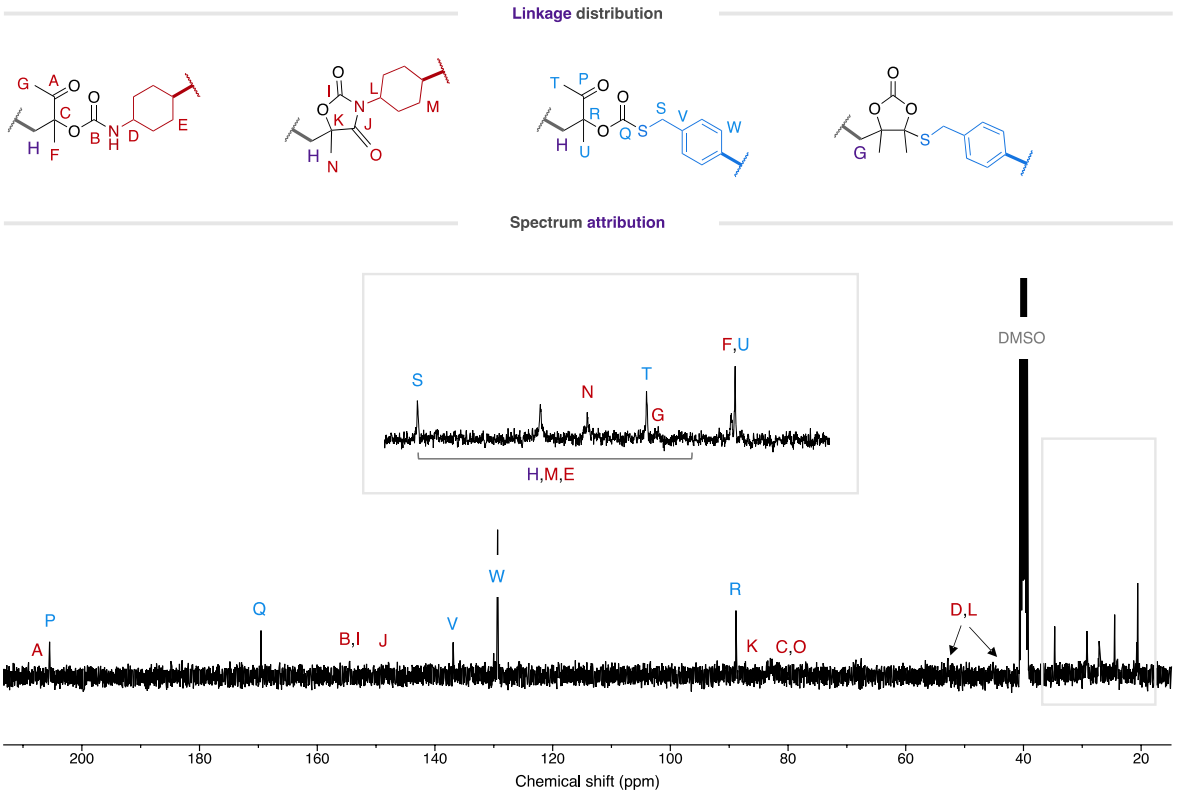

Figure S68 – ^{13}C-NMR spectrum dehydrated of P(A2T2) (400 MHz, DMSO-d_6).

P(A3T1) dehydrated

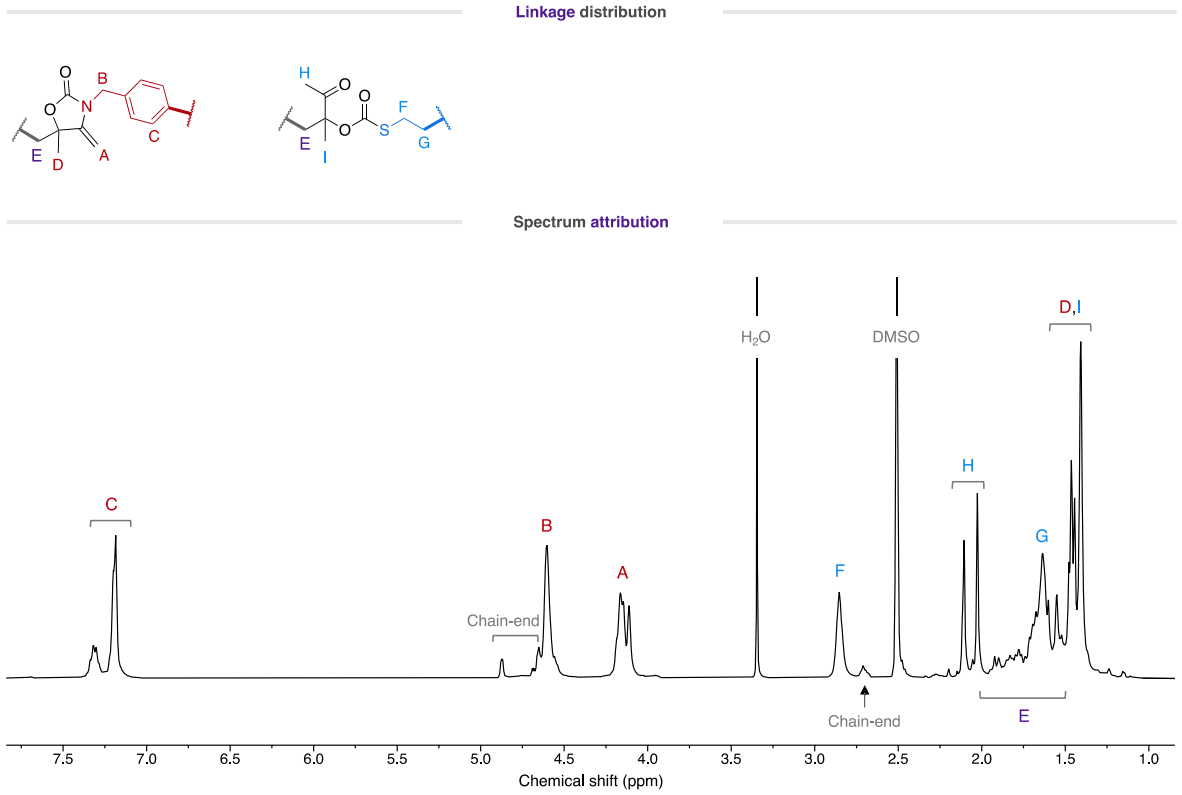

Figure S69 – ^{1}H-NMR spectrum dehydrated of P(A3T1) (400 MHz, DMSO-d_6).

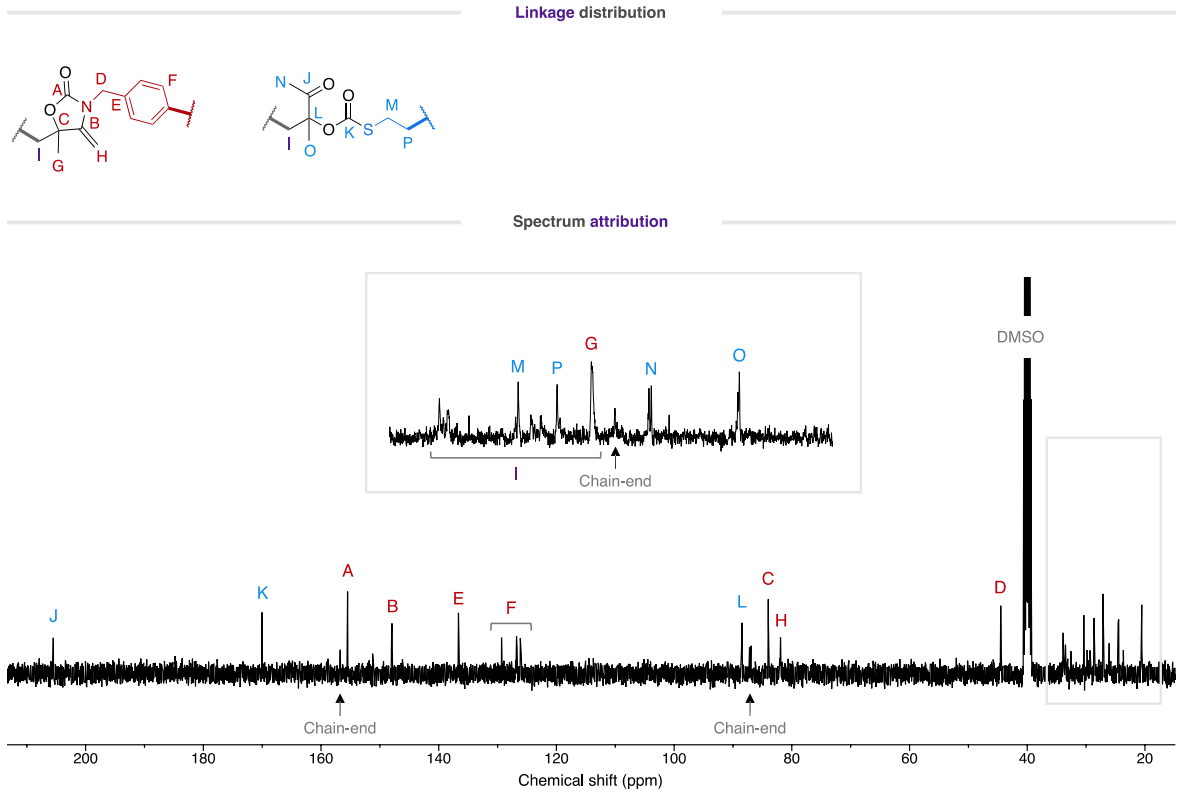

Figure S70 – ^{13}C-NMR spectrum of dehydrated P(A3T1) (400 MHz, DMSO-d_6).

P(A3T1)C dehydrated

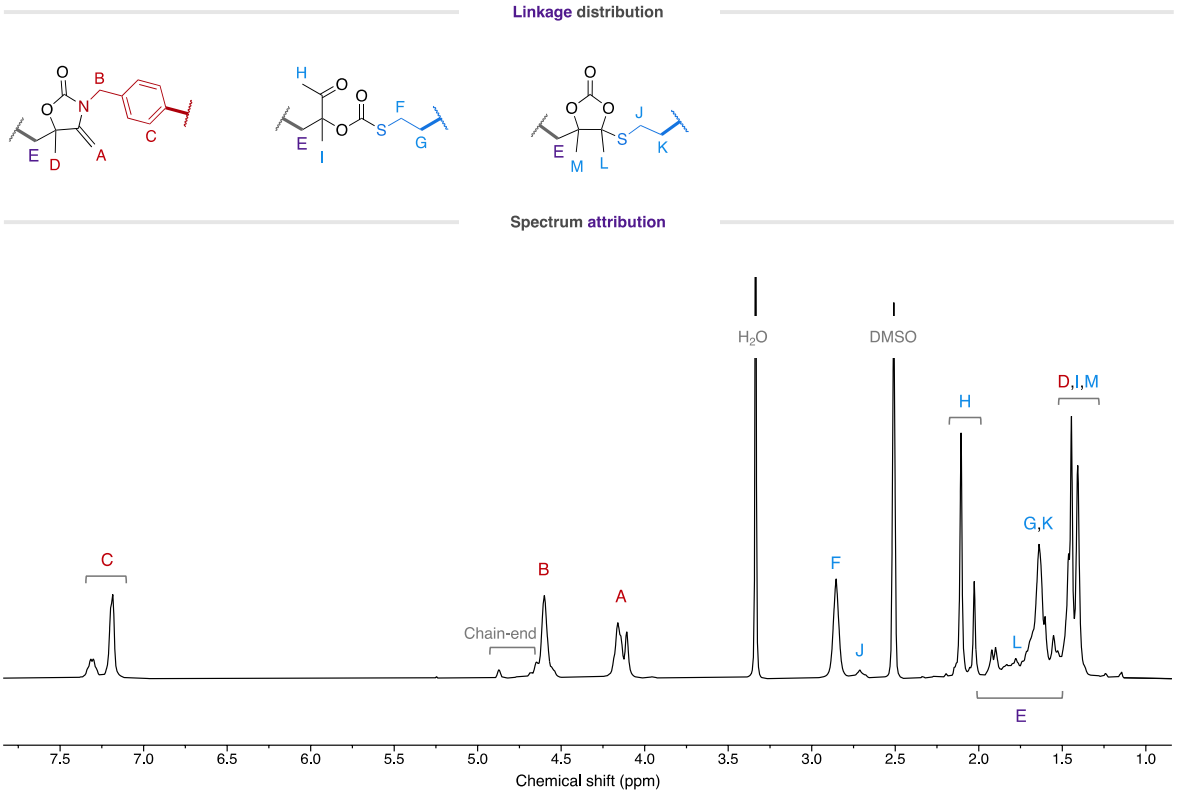

Figure S71 – ^{1}H-NMR spectrum of dehydrated P(A3T1)C (400 MHz, DMSO-d_6).

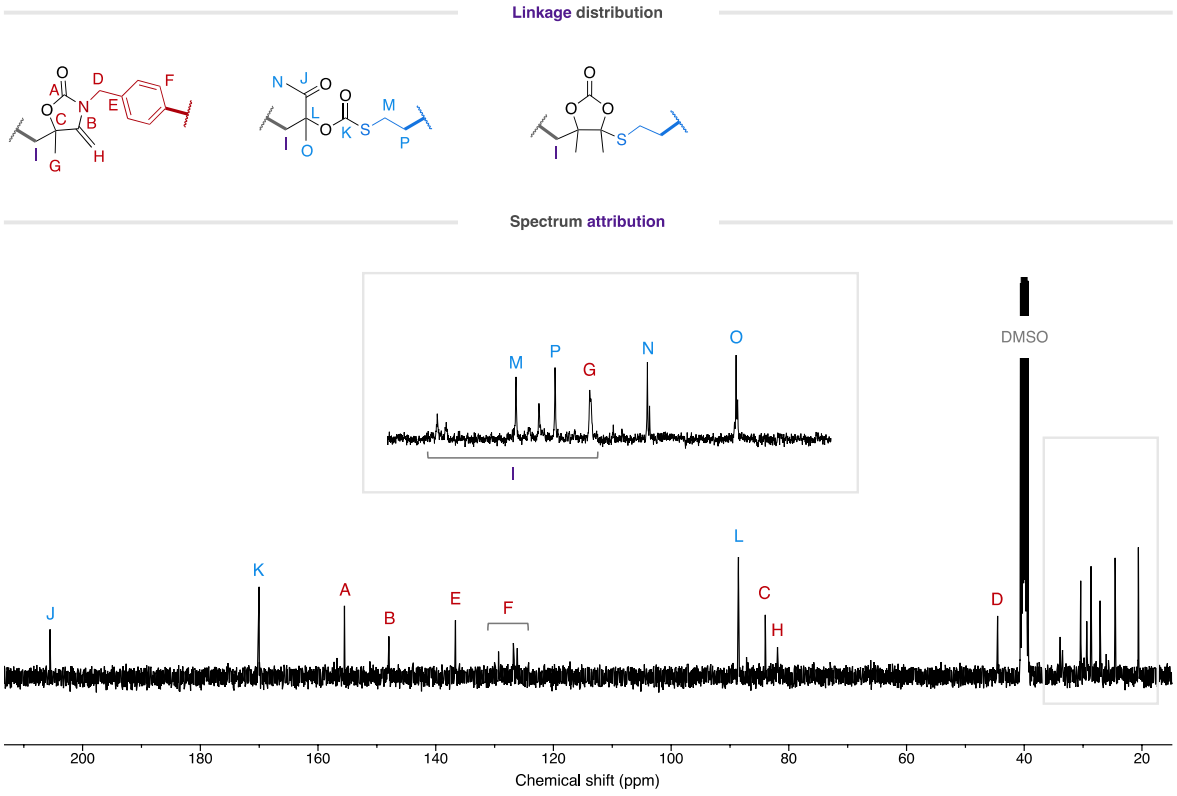

Figure S72 – ^{13}C-NMR spectrum of dehydrated P(A3T1)C (400 MHz, DMSO-d_6).

P(A3T2) dehydrated

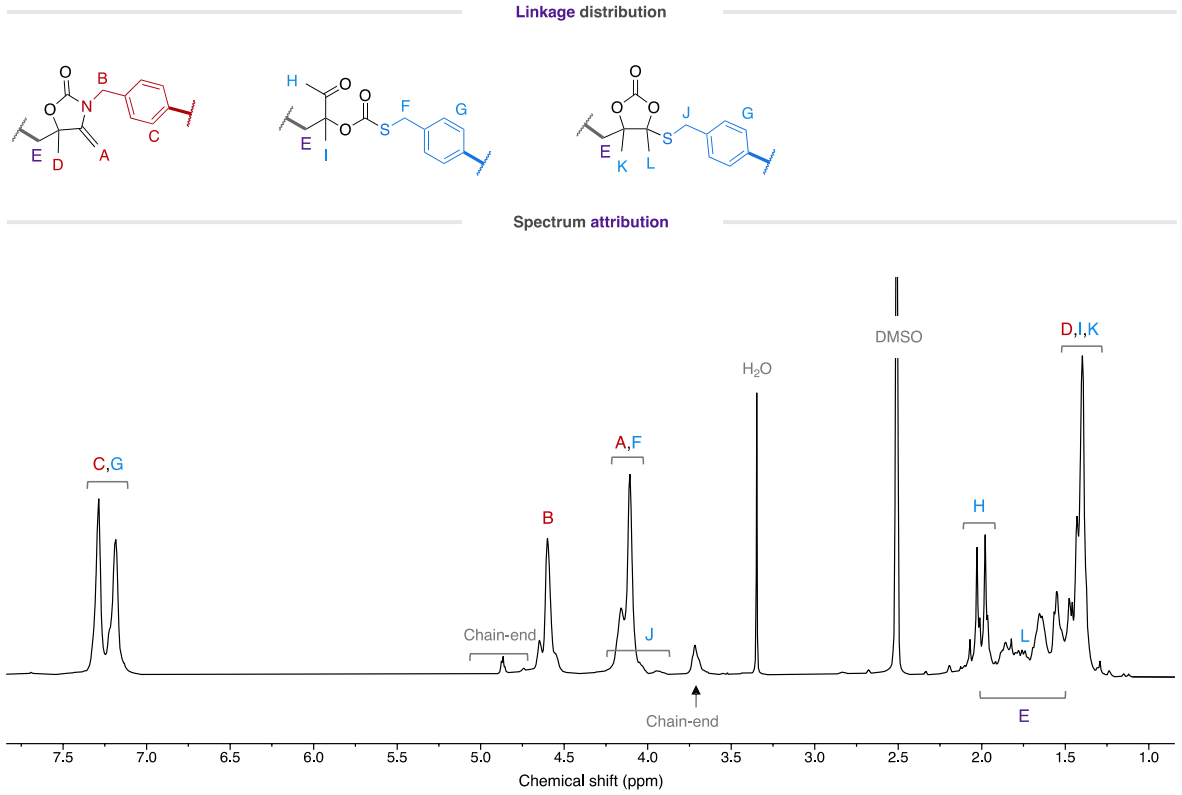

Figure S73 – ^{1}H-NMR spectrum of dehydrated P(A3T2) (400 MHz, DMSO-d_6).

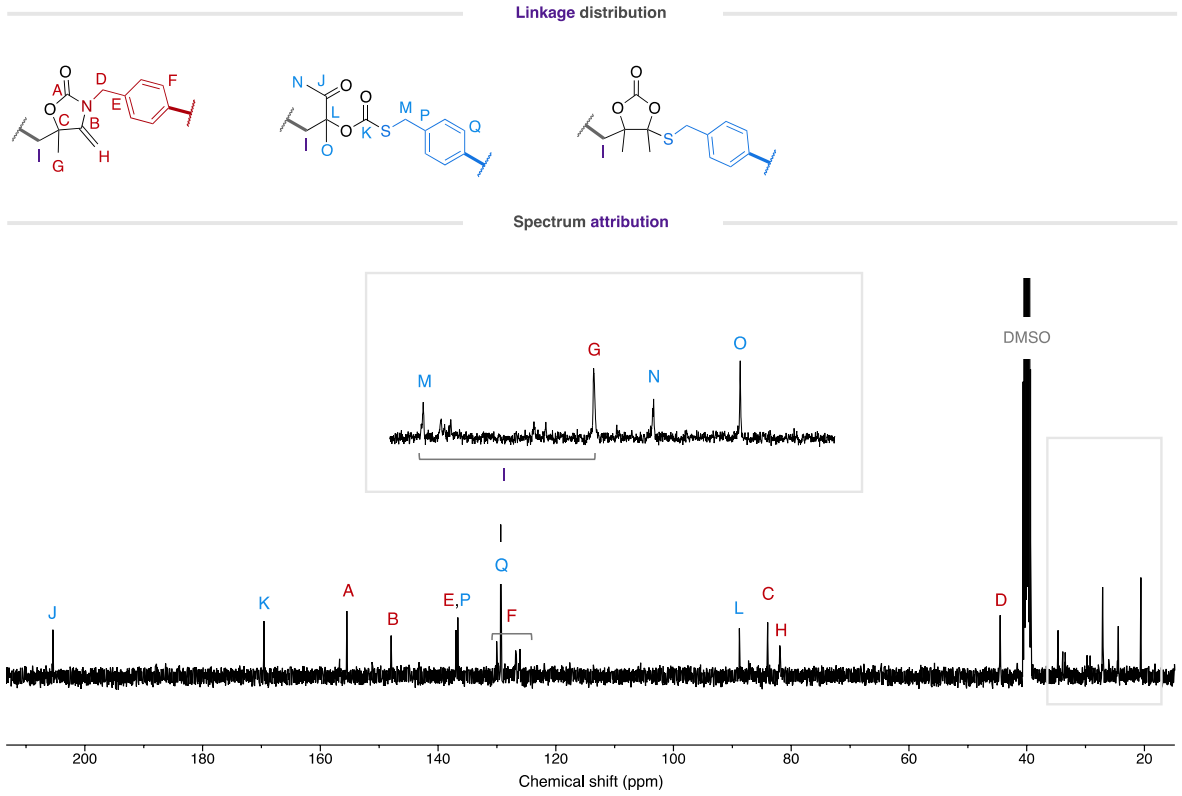

Figure S74 – ^{13}C-NMR spectrum of dehydrated P(A3T2) (400 MHz, DMSO-d_6).

12. SEC chromatograms of dehydrated polymers

Typical SEC chromatograms of pure hydroxyoxazolidone copolymers (dotted) and dehydrated α-alkylidene oxazolidone polymers (line) are shown below.

P(A1T1)

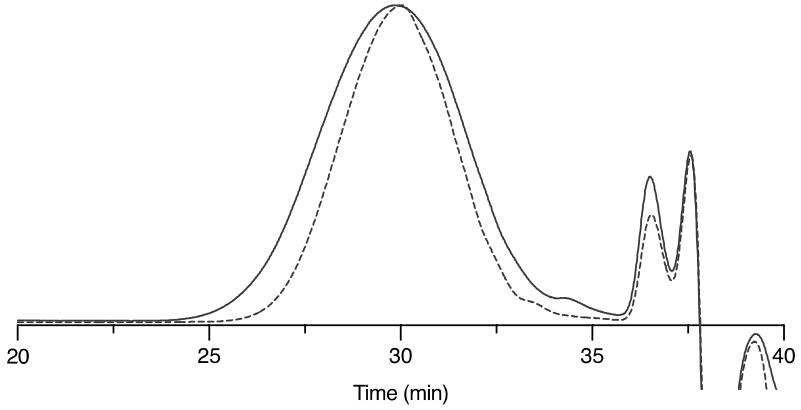

Figure S75. SEC chromatograms of P(A1T1) after purification (dotted) and after dehydration (line).

P(A1T1)C

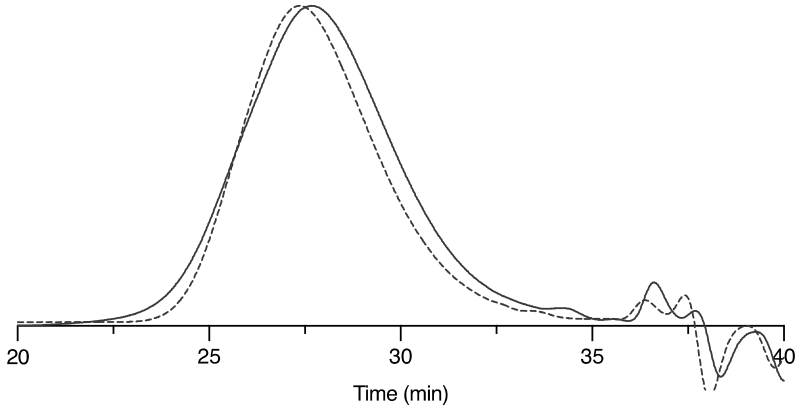

Figure S76. SEC chromatograms of P(A1T1)C after purification (dotted) and after dehydration (line).

P(A1T2)

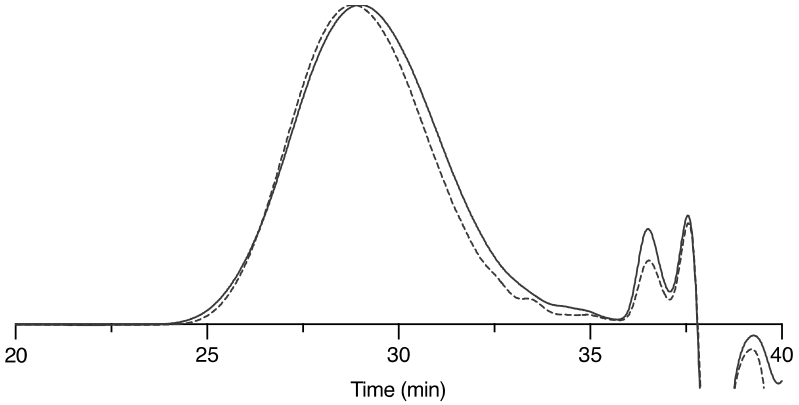

Figure S77. SEC chromatograms of P(A1T2) after purification (dotted) and after dehydration (line).

P(A2T1)

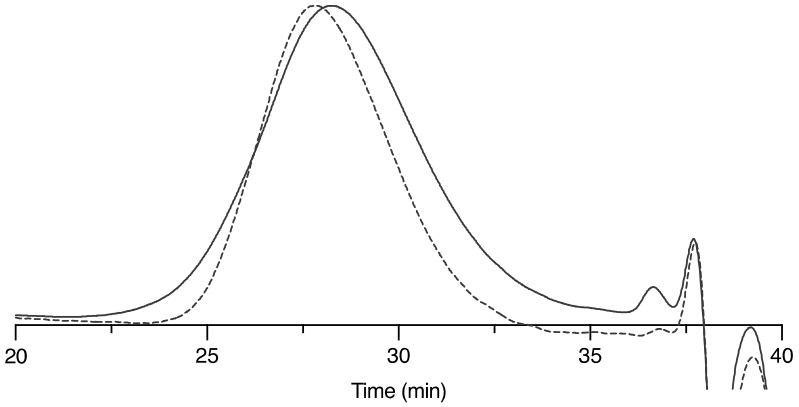

Figure S78. SEC chromatograms of P(A2T1) after purification (dotted) and after dehydration (line).

P(A2T1)C

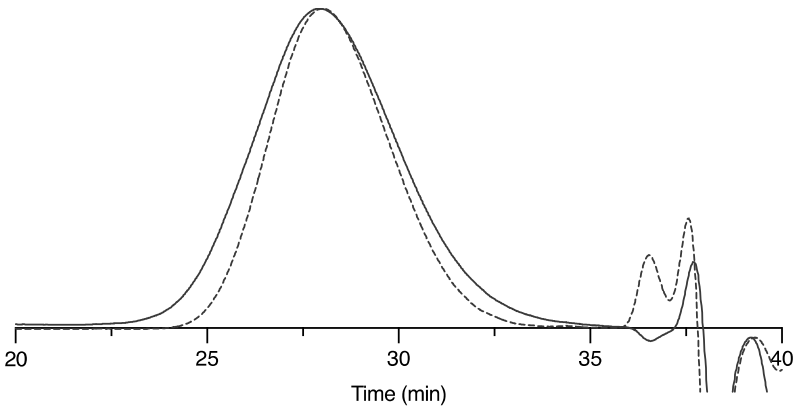

Figure S79. SEC chromatograms of P(A2T1)C after purification (dotted) and after dehydration (line).

P(A2T2)

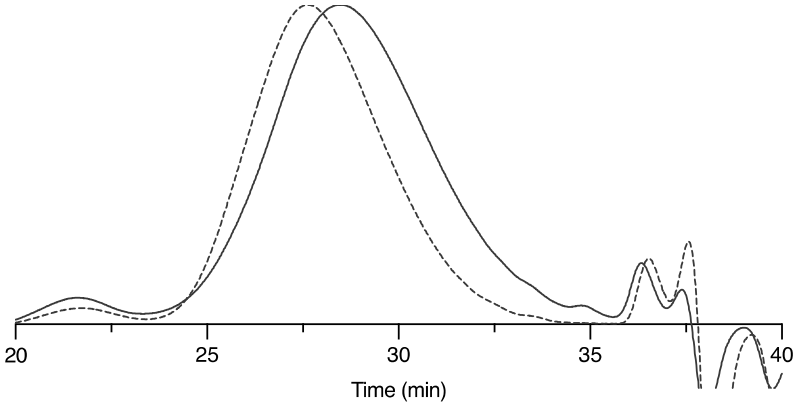

Figure S80. SEC chromatograms of P(A2T2) after purification (dotted) and after dehydration (line).

P(A3T1)

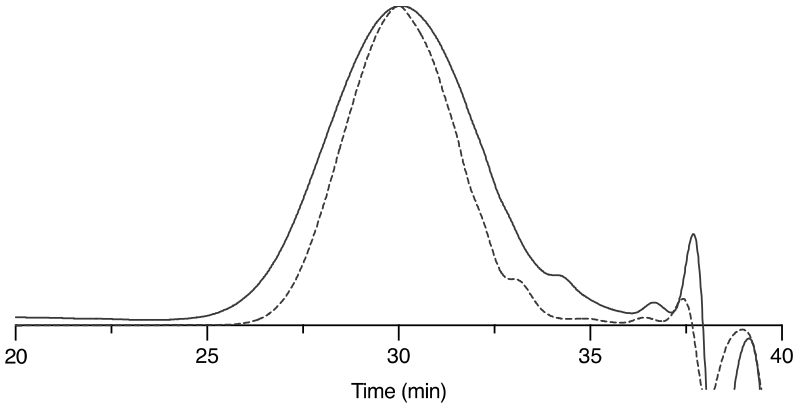

Figure S81. SEC chromatograms of P(A3T1) after purification (dotted) and after dehydration (line).

P(A3T1)C

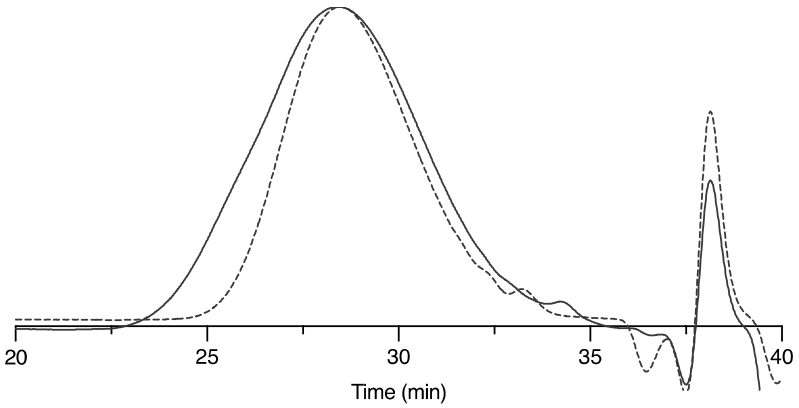

Figure S82. SEC chromatograms of P(A3T1)C after purification (dotted) and after dehydration (line).

P(A3T2)

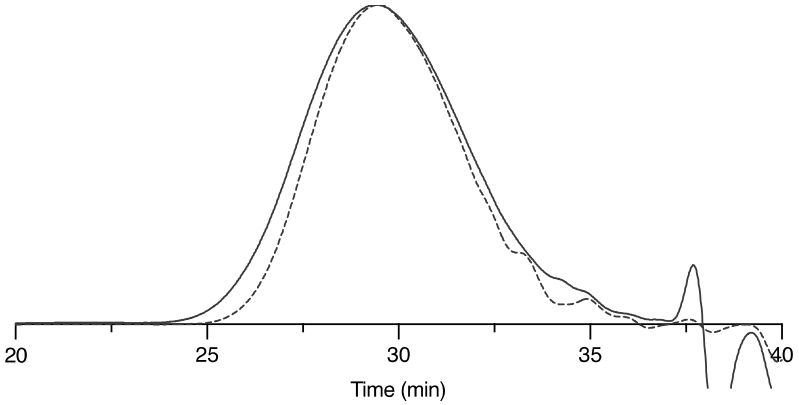

Figure S83. SEC chromatograms of P(A3T2) after purification (dotted) and after dehydration (line).

13. TGA analyses of dehydrated polymers

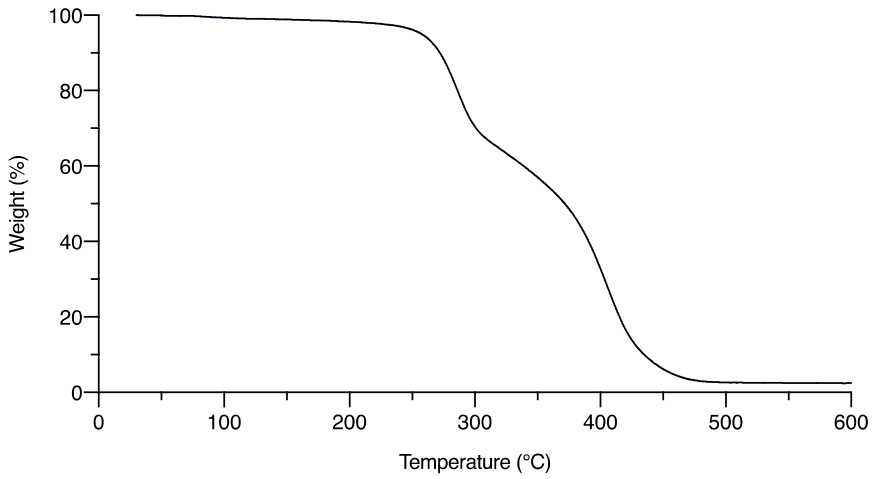

Figure S84 – TGA plot of dehydrated P(A1T1).

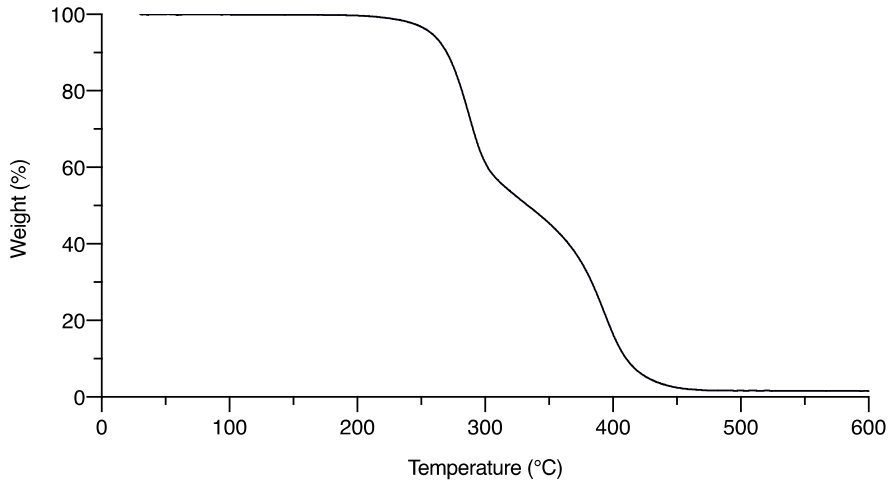

Figure S85 – TGA plot of dehydrated P(A1T1)C.

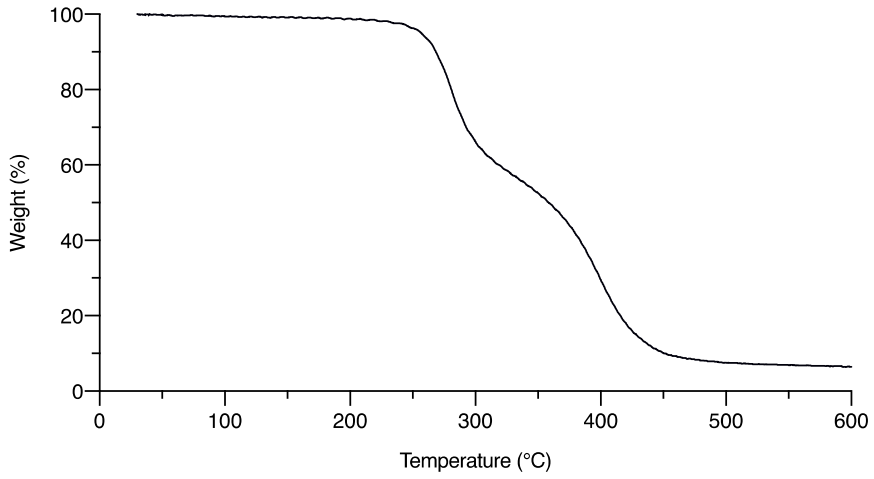

Figure S86 – TGA plot of dehydrated P(A1T2).

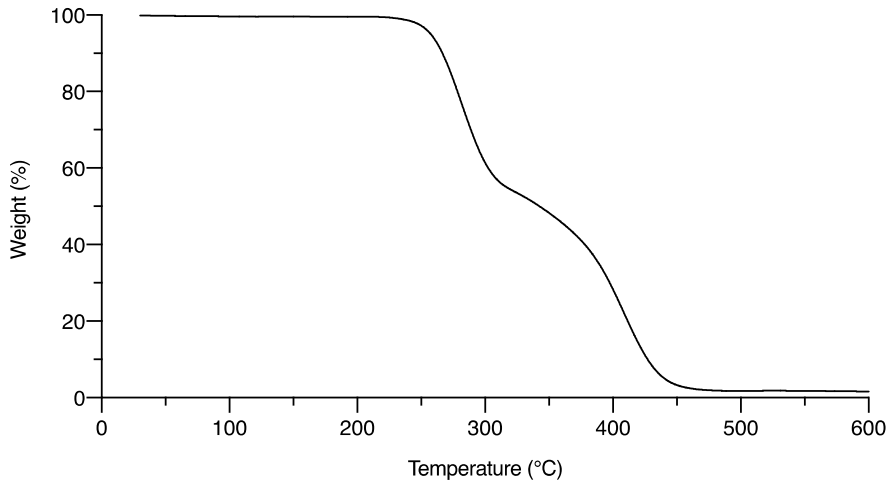

Figure S87 – TGA plot of dehydrated P(A2T1).

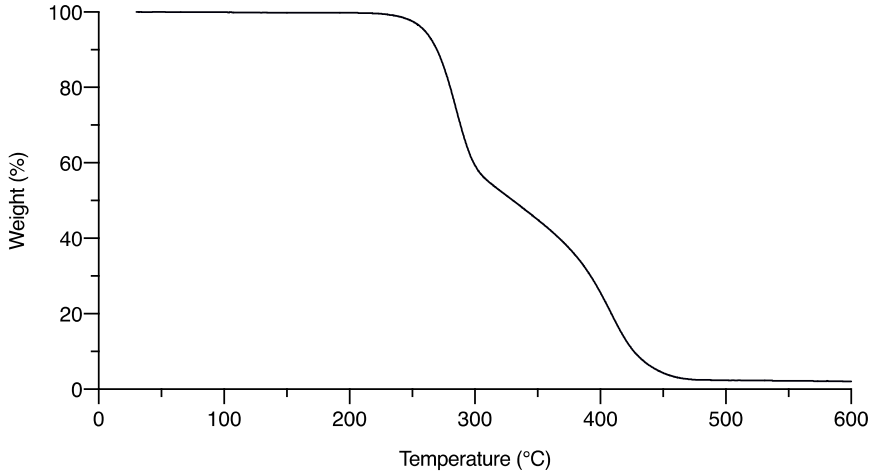

Figure S88 – TGA plot of dehydrated P(A2T1)C.

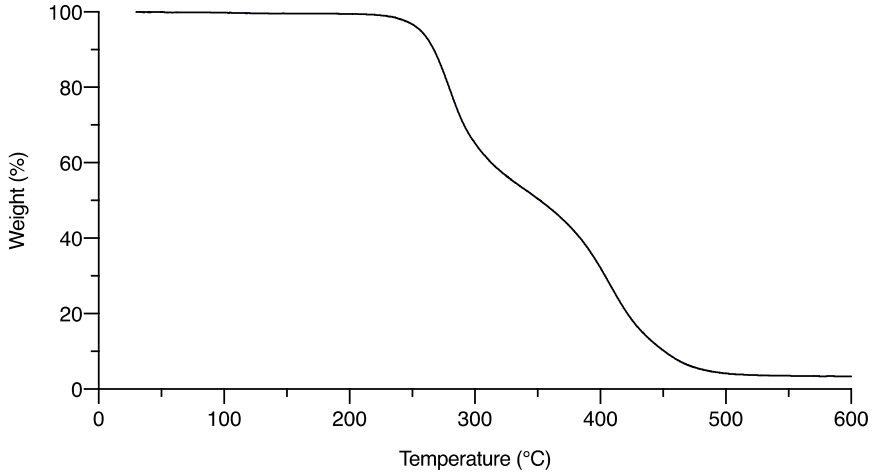

Figure S89 – TGA plot of dehydrated P(A2T2).

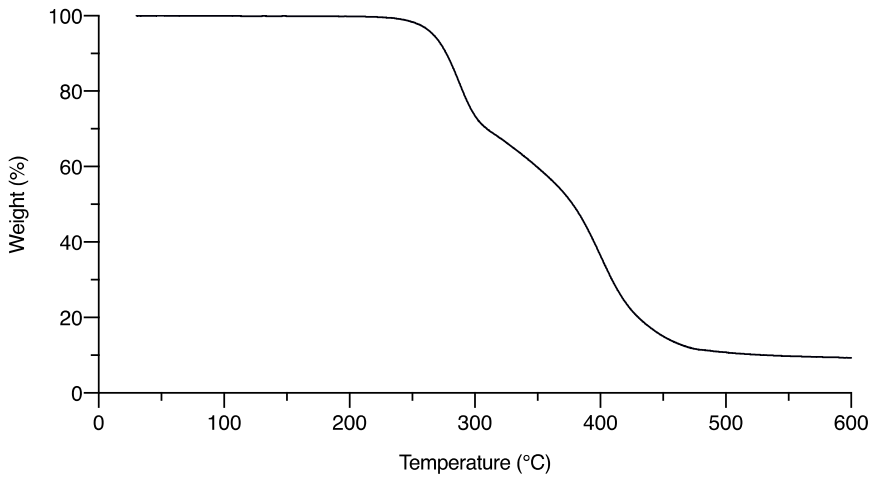

Figure S90 – TGA plot of dehydrated P(A3T1).

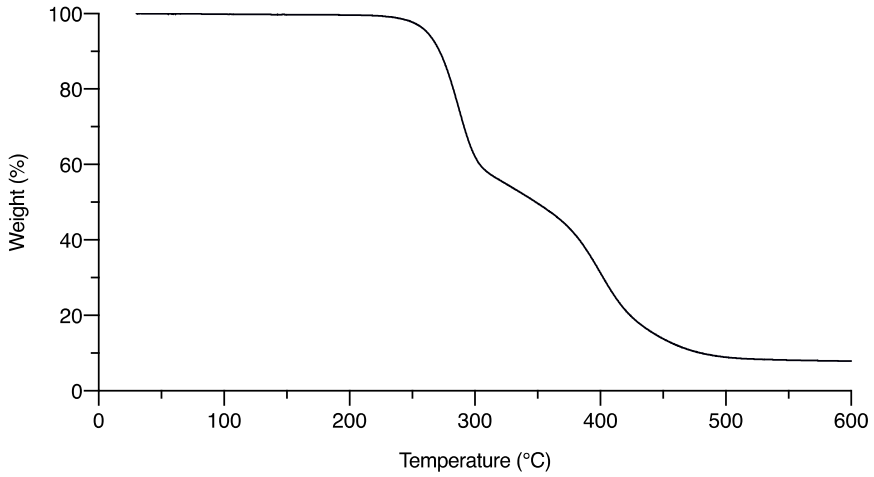

Figure S91 – TGA plot of dehydrated P(A3T1)C.

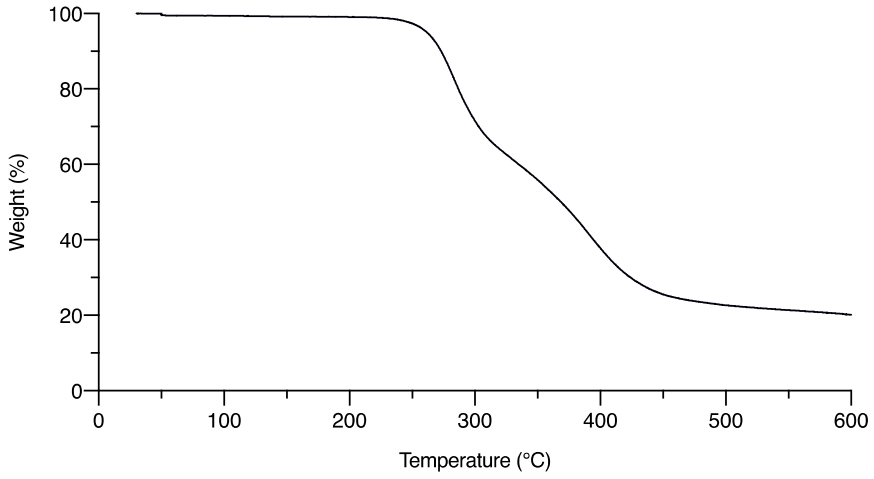

Figure S92 – TGA plot of dehydrated P(A3T2).

14. DSC analyses of dehydrated polymers

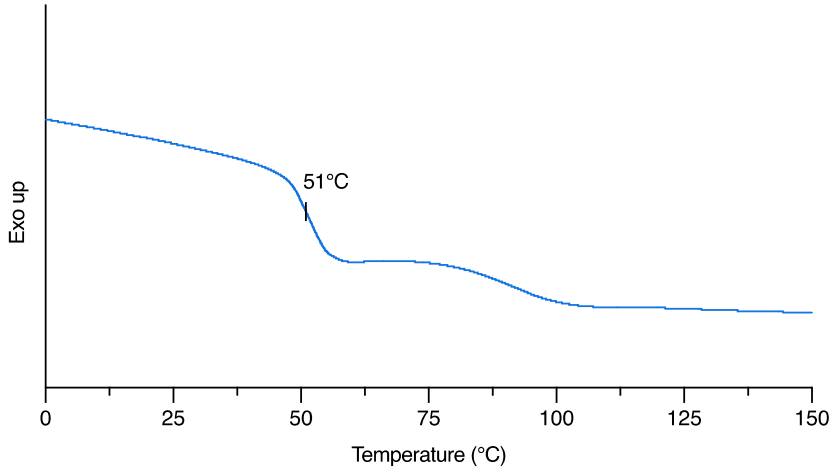

Figure S93 – DSC plot of dehydrated P(A1T1).

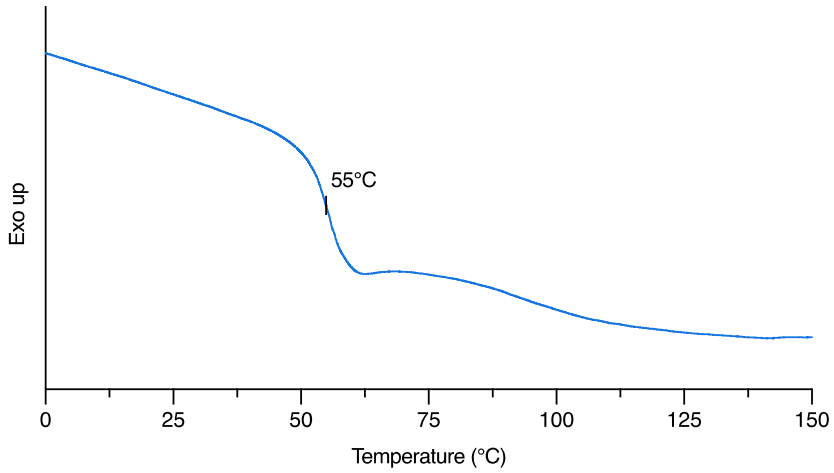

Figure S94 – DSC plot of dehydrated P(A1T1)C.

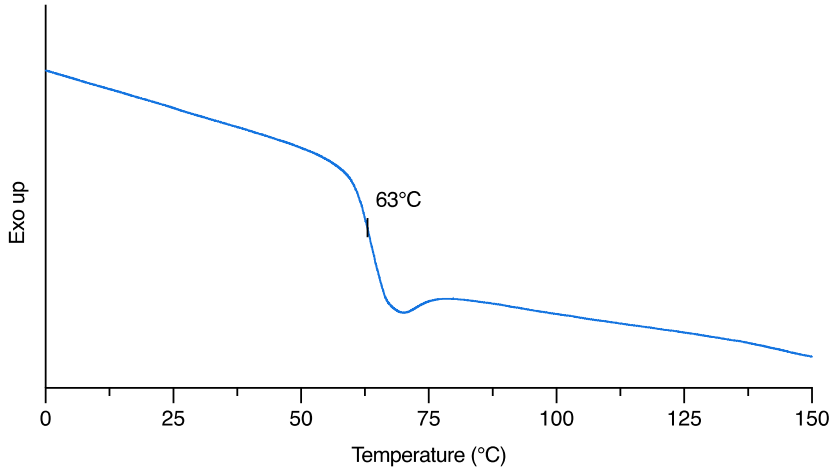

Figure S95 – DSC plot of dehydrated P(A1T2).

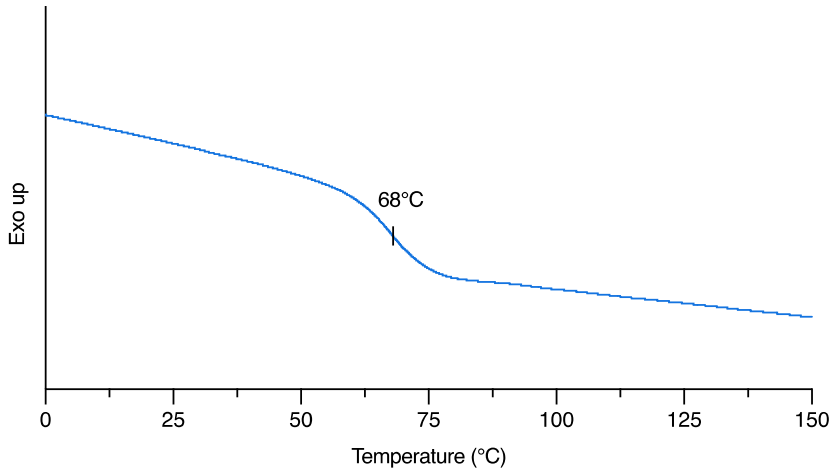

Figure S96 – DSC plot of dehydrated P(A2T1).

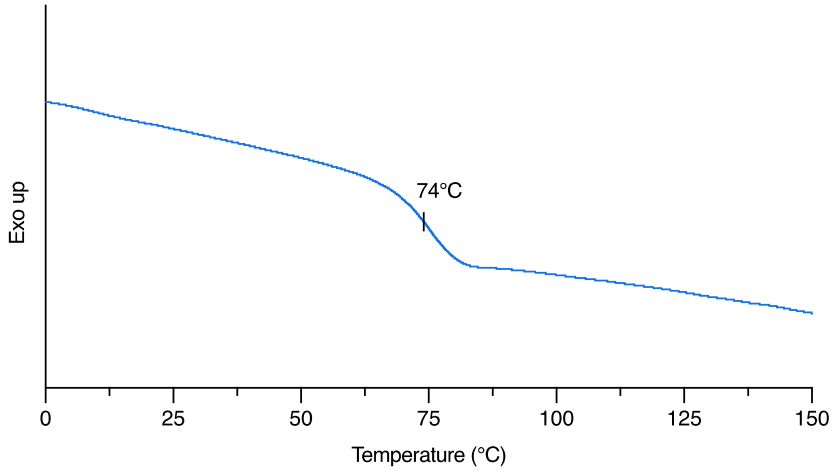

Figure S97 – DSC plot of dehydrated P(A2T1)C.

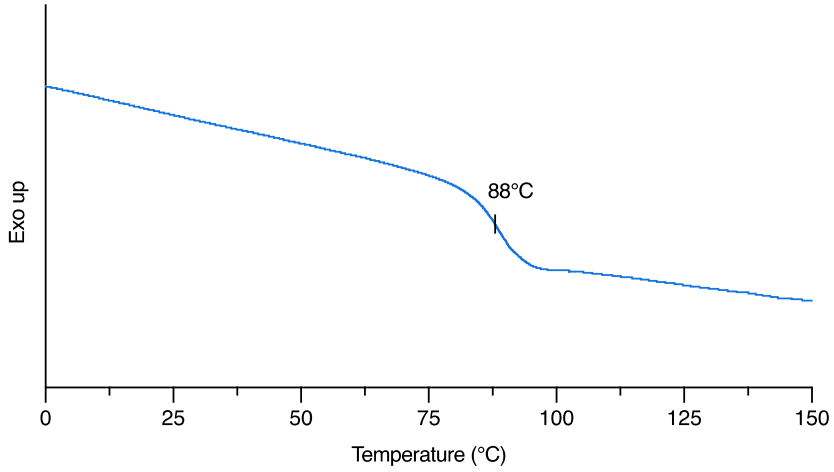

Figure S98 – DSC plot of dehydrated P(A2T2).

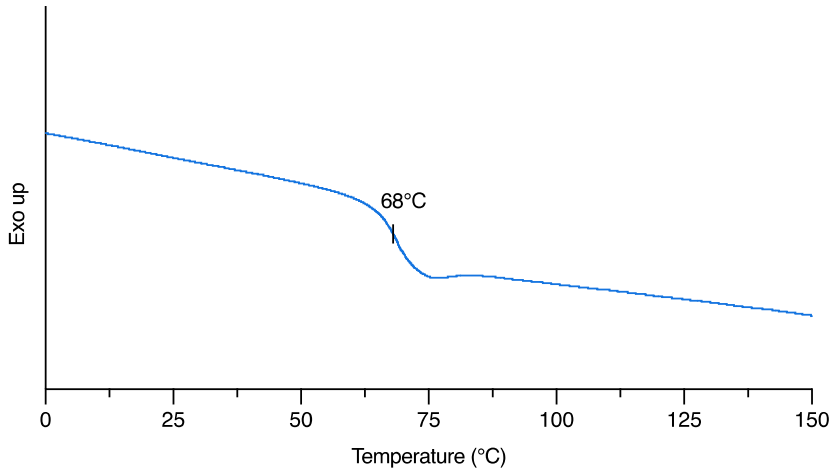

Figure S99 – DSC plot of dehydrated P(A3T1).

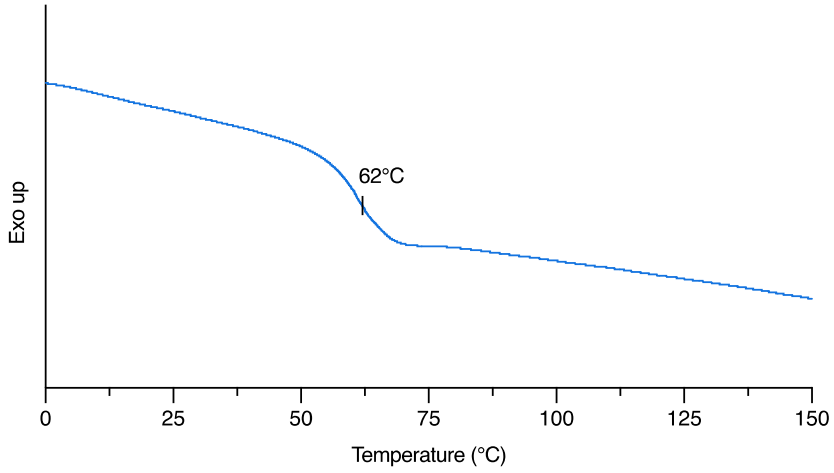

Figure S100 – DSC plot of dehydrated P(A3T1)C.

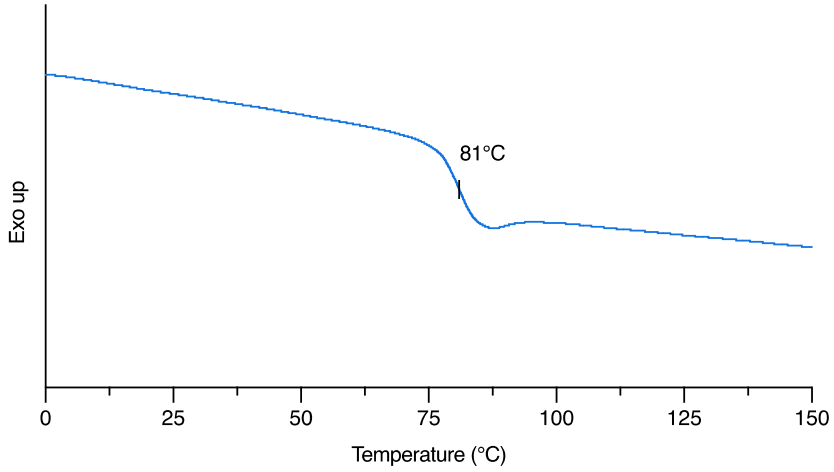

Figure S101 – DSC plot of dehydrated P(A3T2).

15. NMR characterization of functionalized polymers

P(A3T1)C dehydrated functionalized with benzyl mercaptan

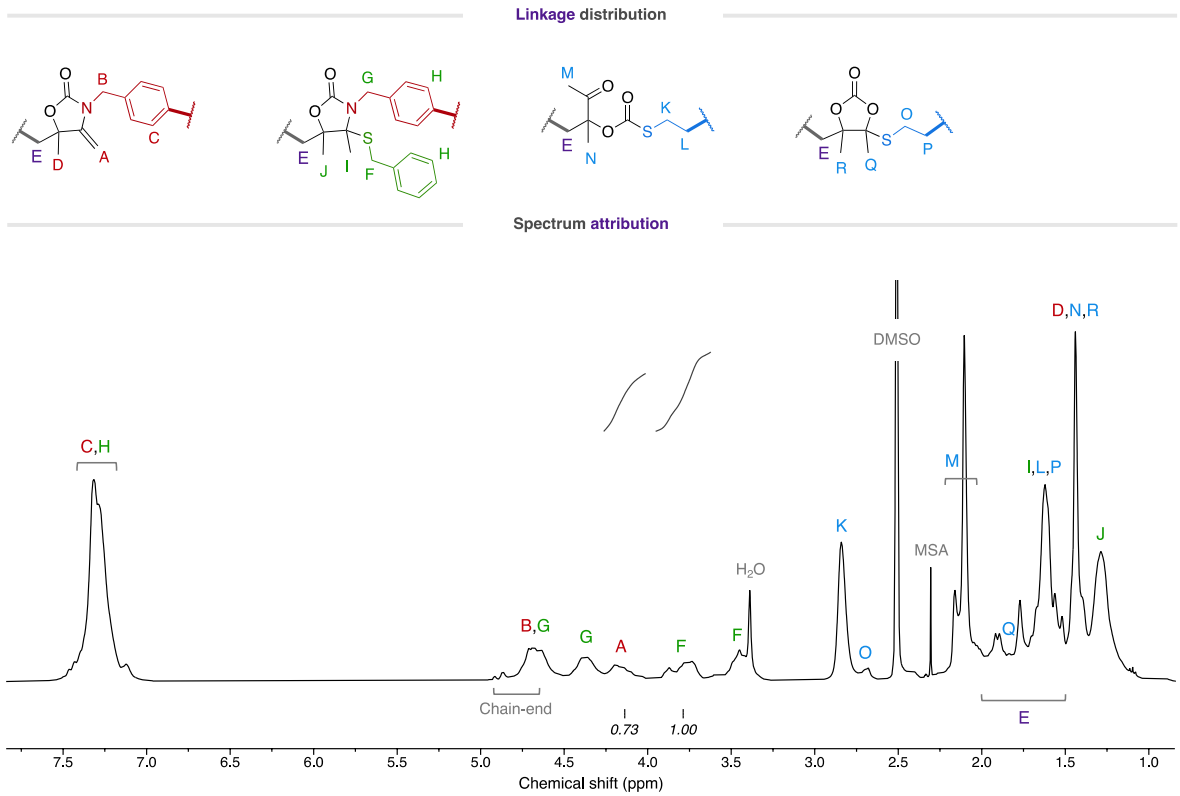

Figure S102 – ^{1}H-NMR spectrum of pure polymer functionalized with benzyl mercaptan (400 MHz, DMSO-d_6).

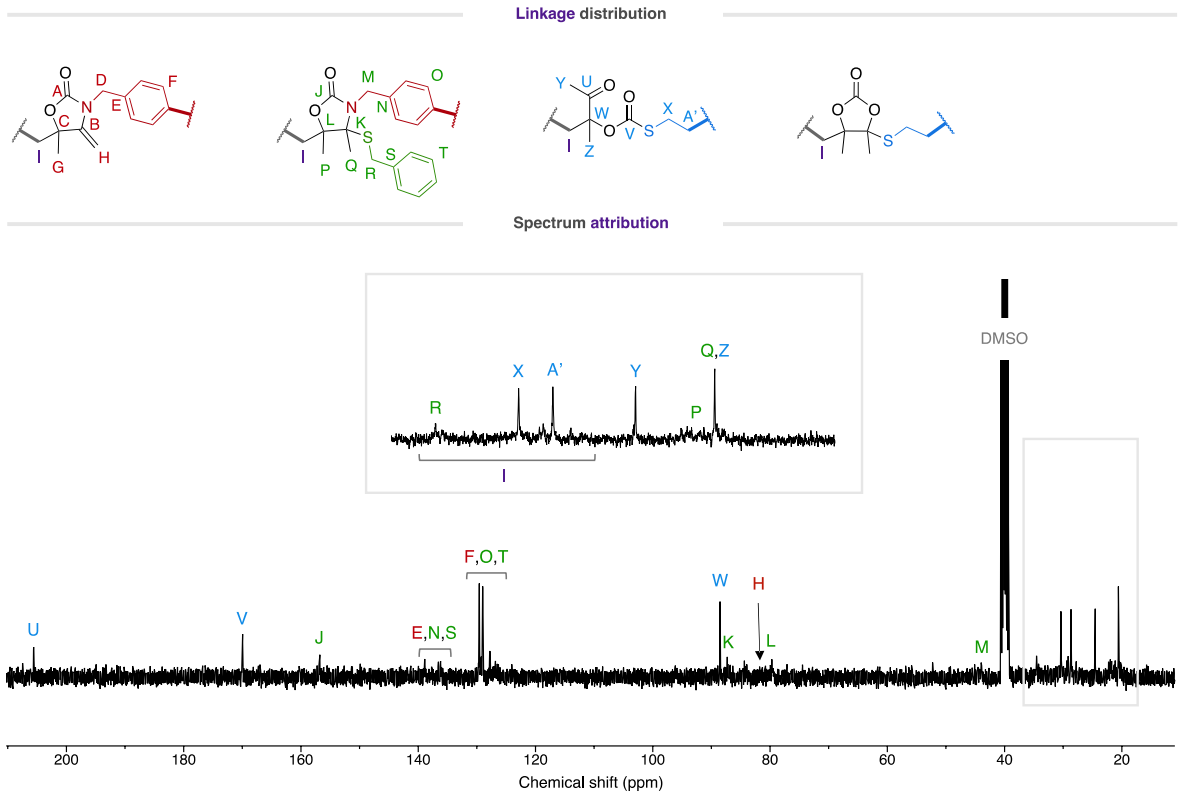

Figure S103 – ^{13}C-NMR spectrum of pure polymer functionalized with benzyl mercaptan (400 MHz, DMSO-d_6).

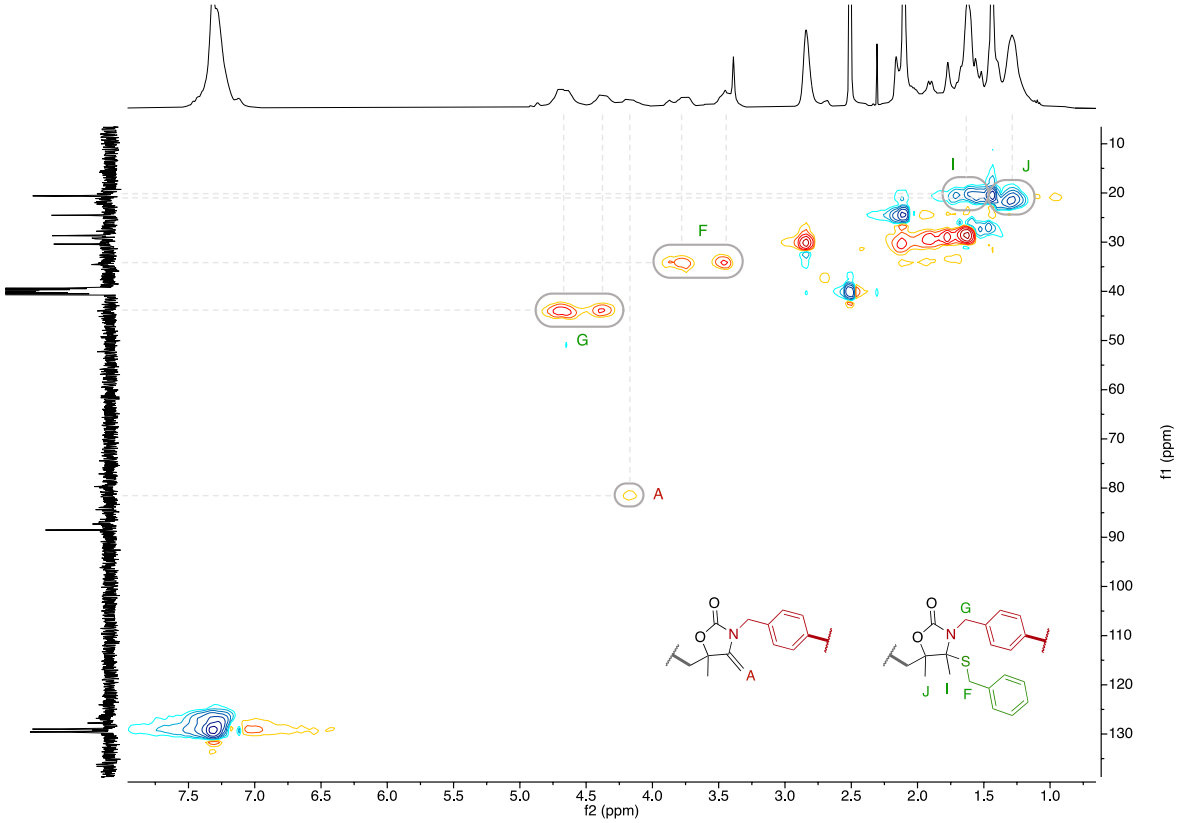

Figure S104 – ^{1}H-^{13}C HSQC NMR spectrum of pure polymer functionalized with benzyl mercaptan (400 MHz, DMSO-d_6).

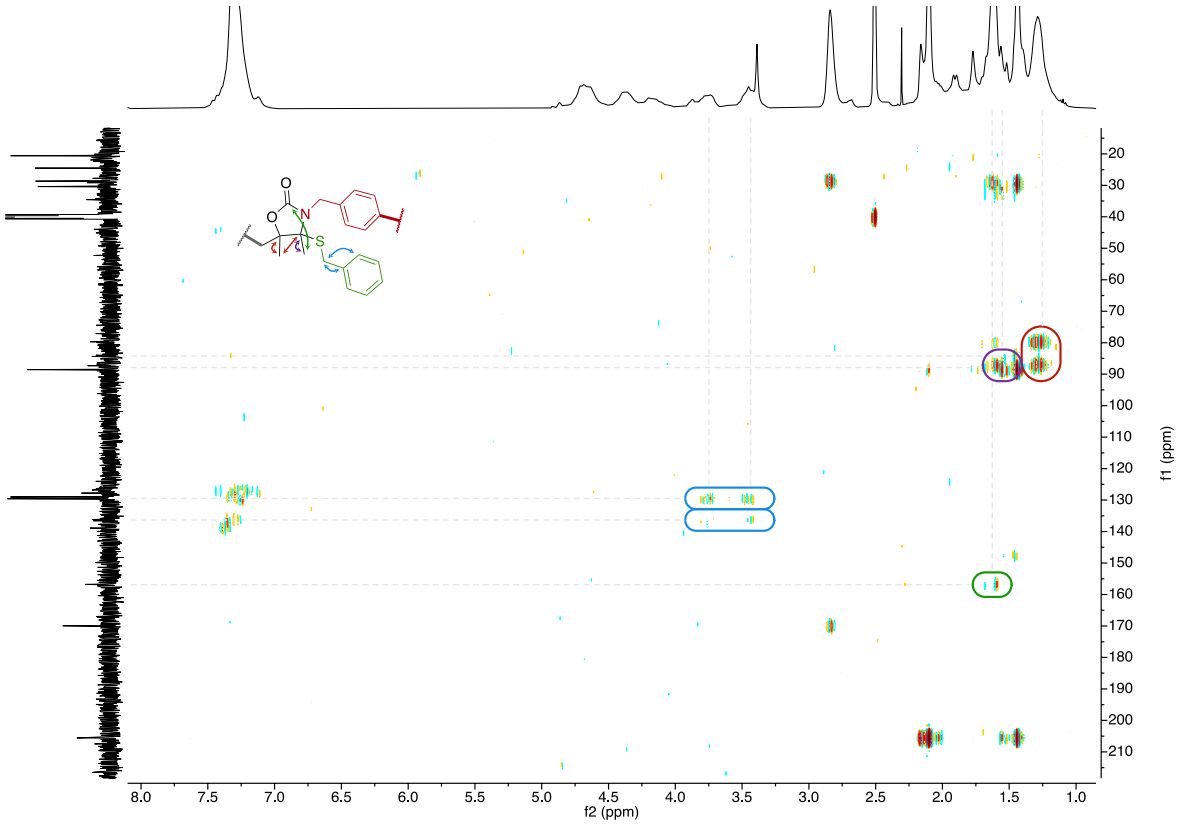

Figure S105 – ^{1}H-^{13}C HMBC NMR spectrum of pure polymer functionalized with benzyl mercaptan (400 MHz, DMSO-d_6).

P(A3T1)C dehydrated functionalized with furanmethanethiol

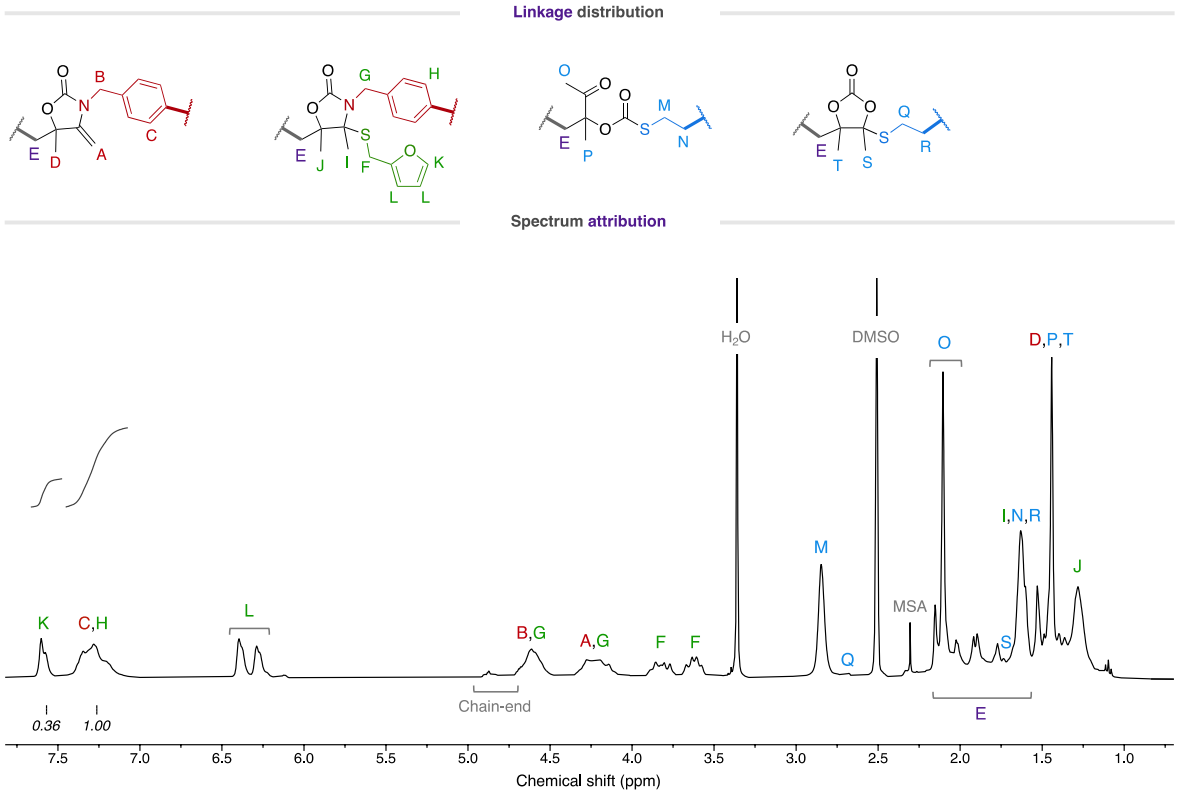

Figure S106 – ^{1}H-NMR spectrum of pure polymer functionalized with furanmethanethiol (400 MHz, DMSO-d_6).

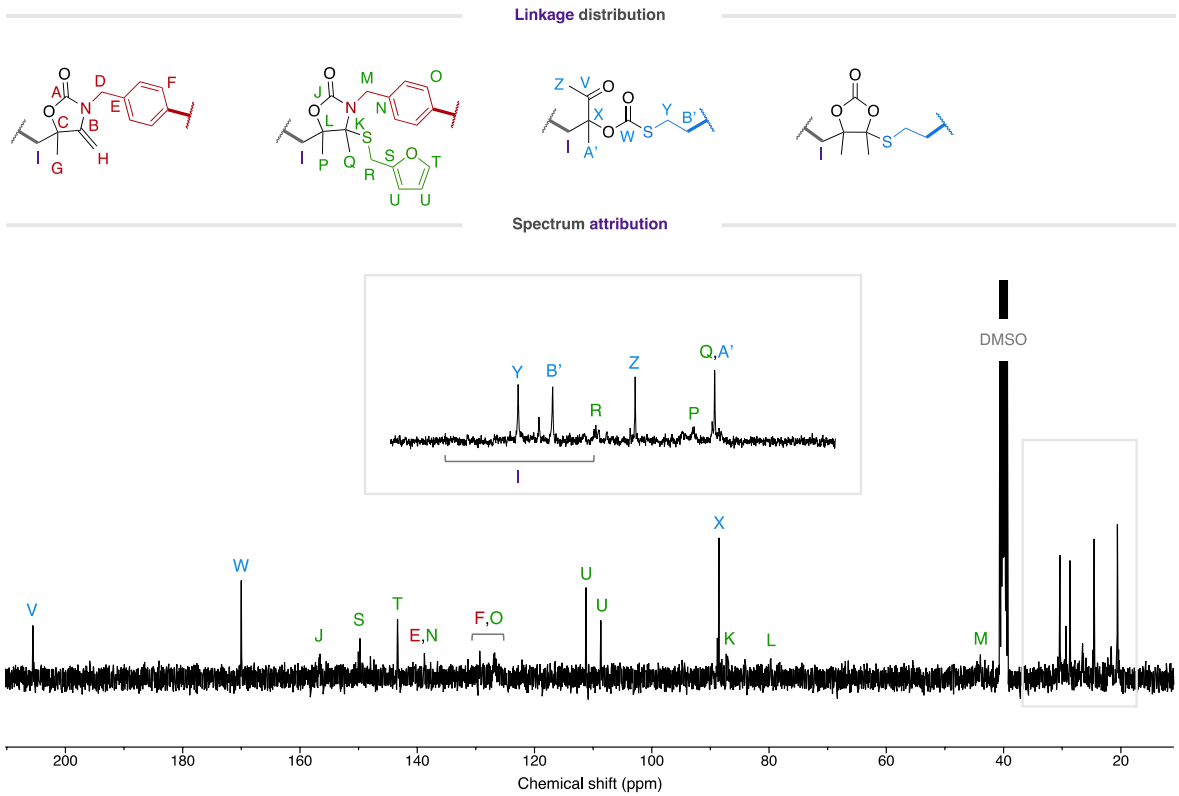

Figure S107 – ^{13}C-NMR spectrum of pure polymer functionalized with furanmethanethiol (400 MHz, DMSO-d_6).

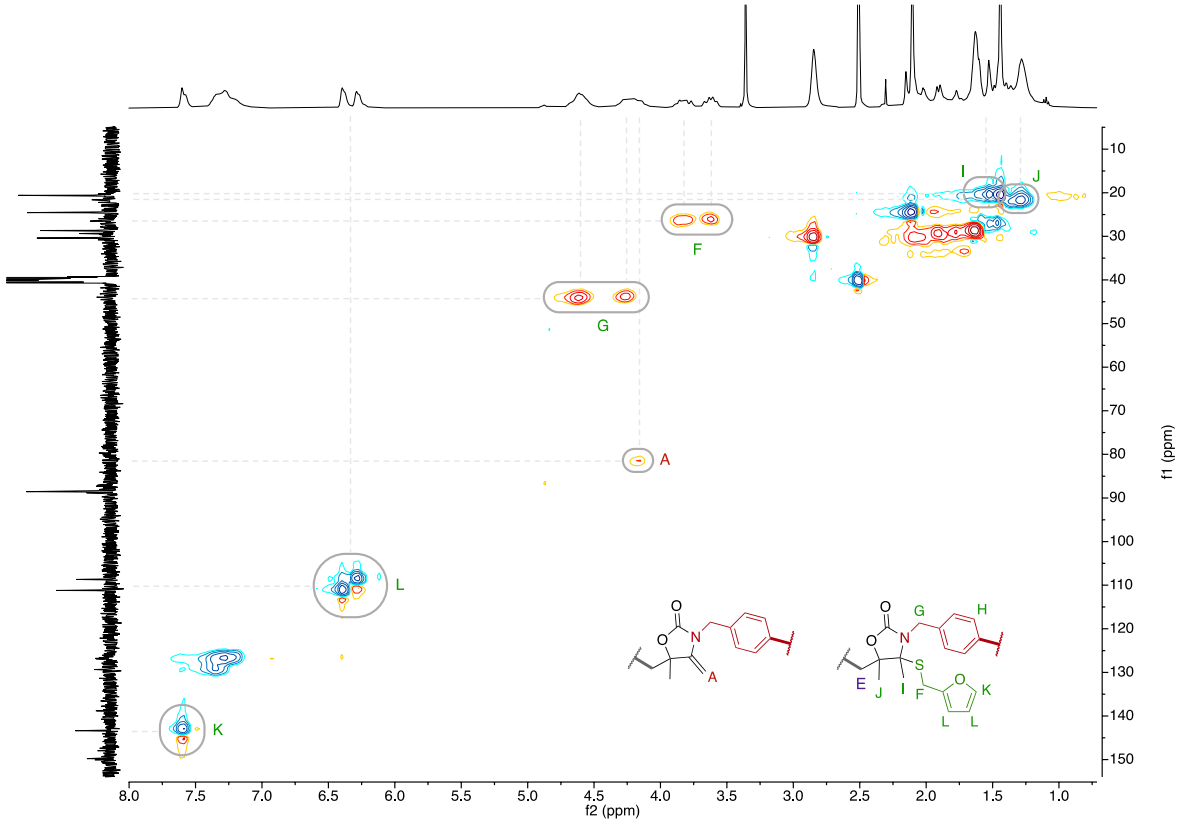

Figure S108 – ^{1}H-^{13}C HSQC NMR spectrum of pure polymer functionalized with furanmethanethiol (400 MHz, DMSO-d_6).

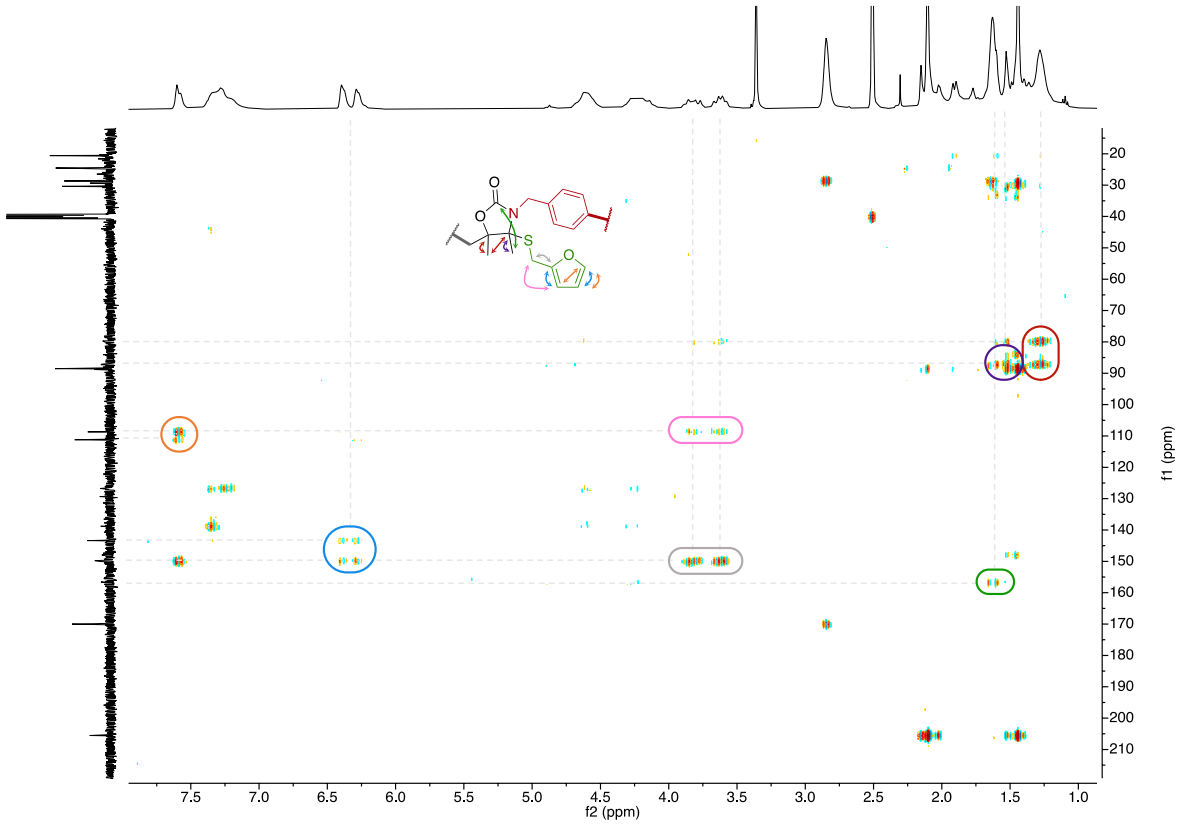

Figure S109 – ^{1}H-^{13}C HMBC NMR spectrum of pure polymer functionalized with furanmethanethiol (400 MHz, DMSO-d_6).

P(A3T1)C dehydrated functionalized with n-octanethiol

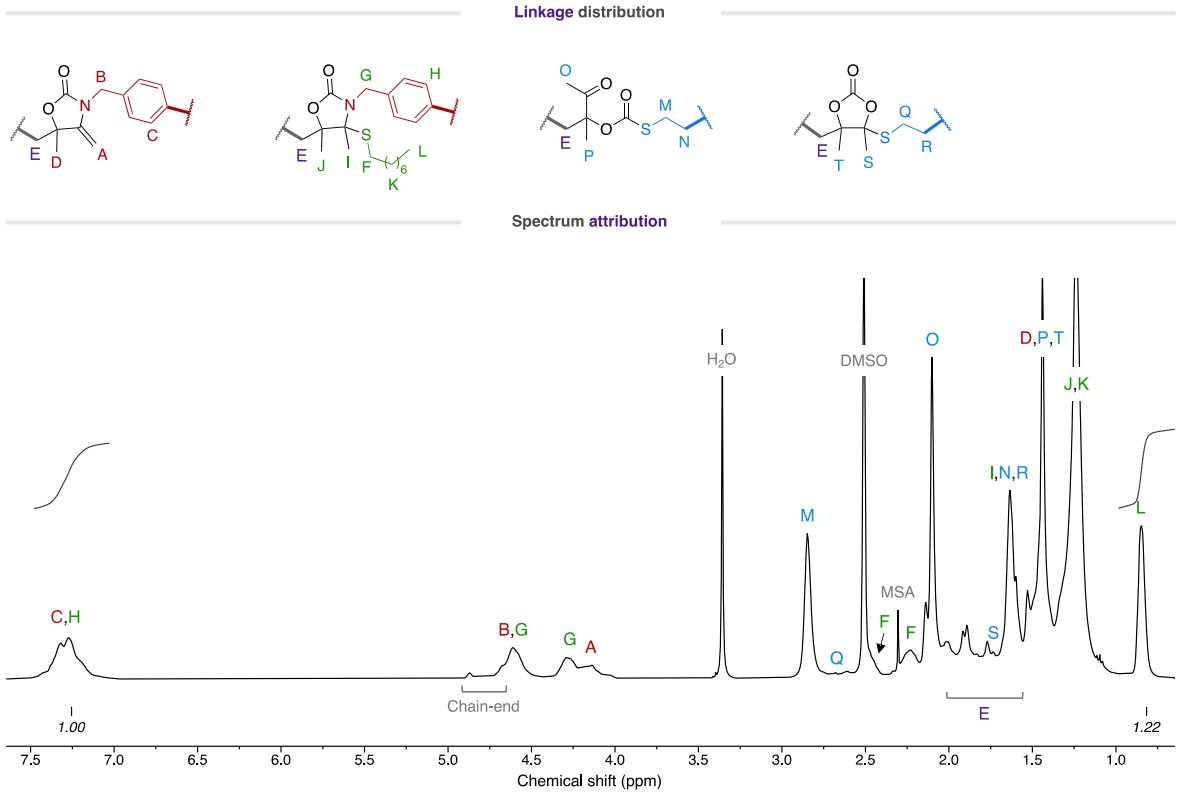

Figure S110 – ^{1}H-NMR spectrum of pure polymer functionalized with n-octanethiol (400 MHz, DMSO-d_6).

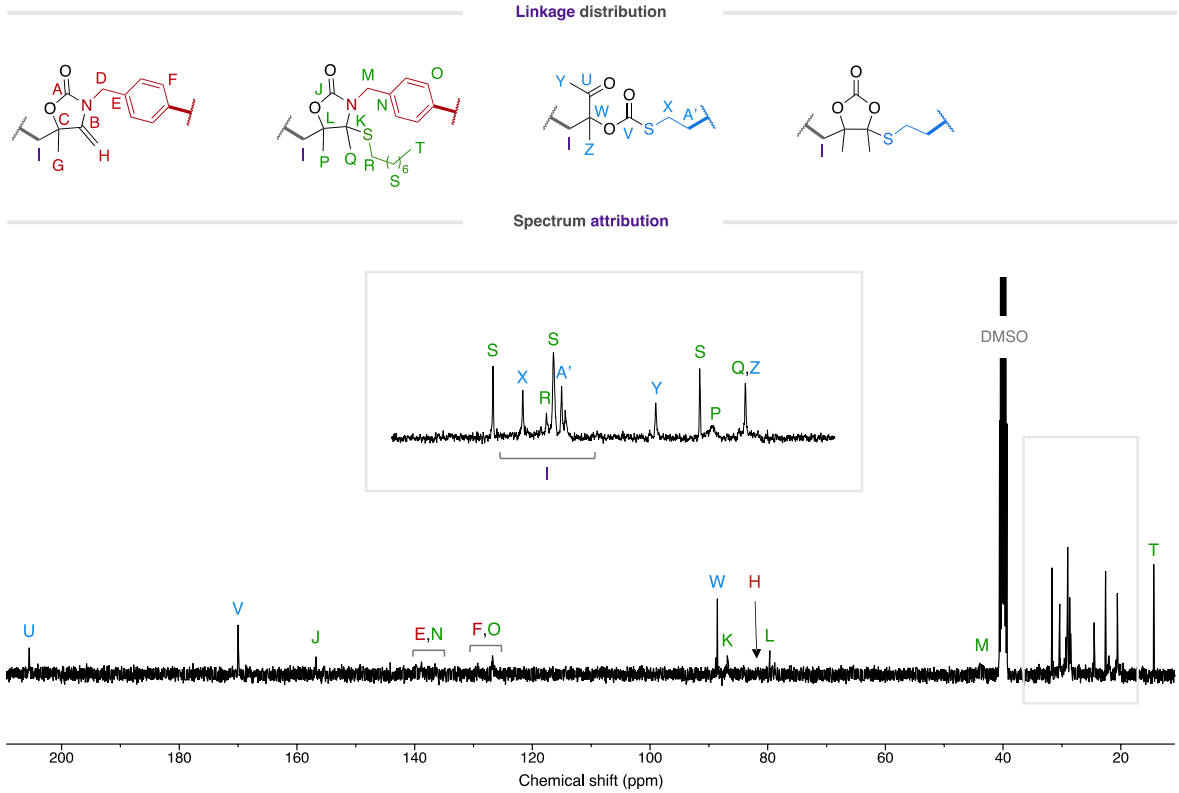

Figure S111 – ^{13}C-NMR spectrum of pure polymer functionalized with n-octanethiol (400 MHz, DMSO-d_6).

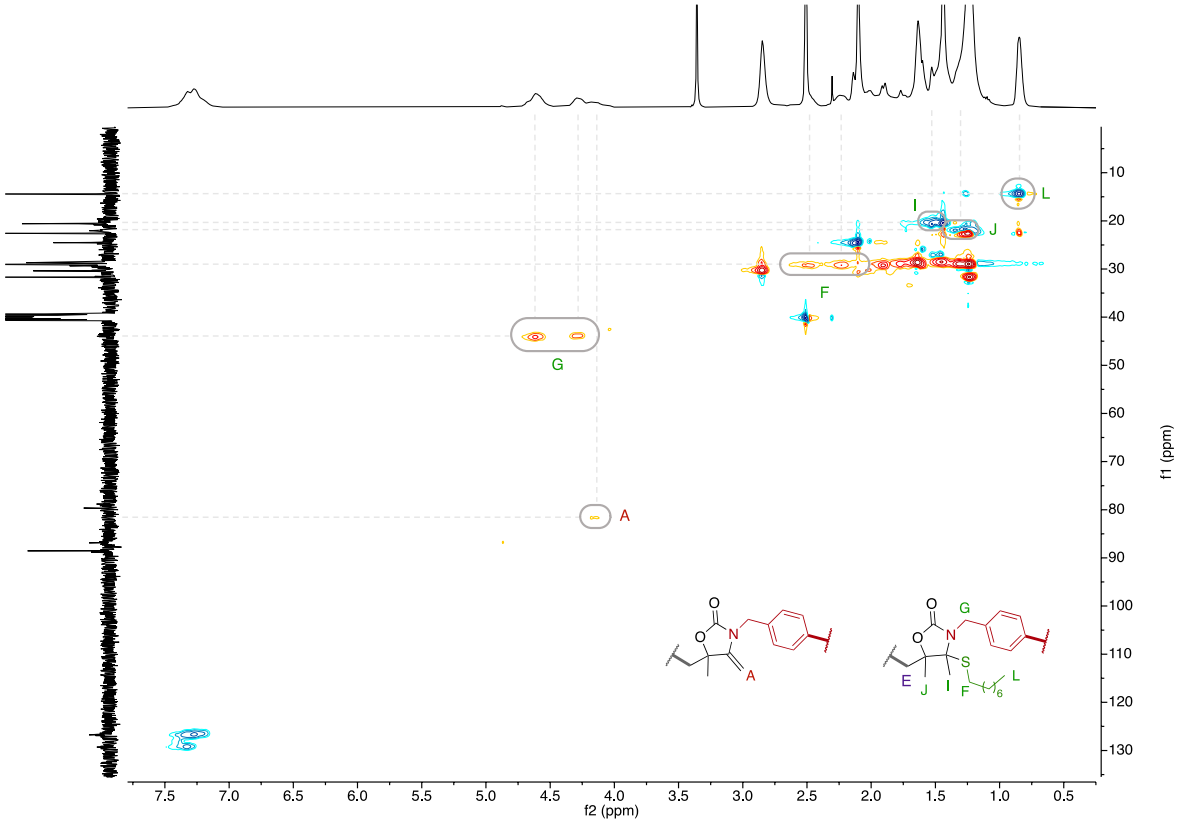

Figure S112 – ^{1}H-^{13}C HSQC NMR spectrum of pure polymer functionalized with n-octanethiol (400 MHz, DMSO-d_6).

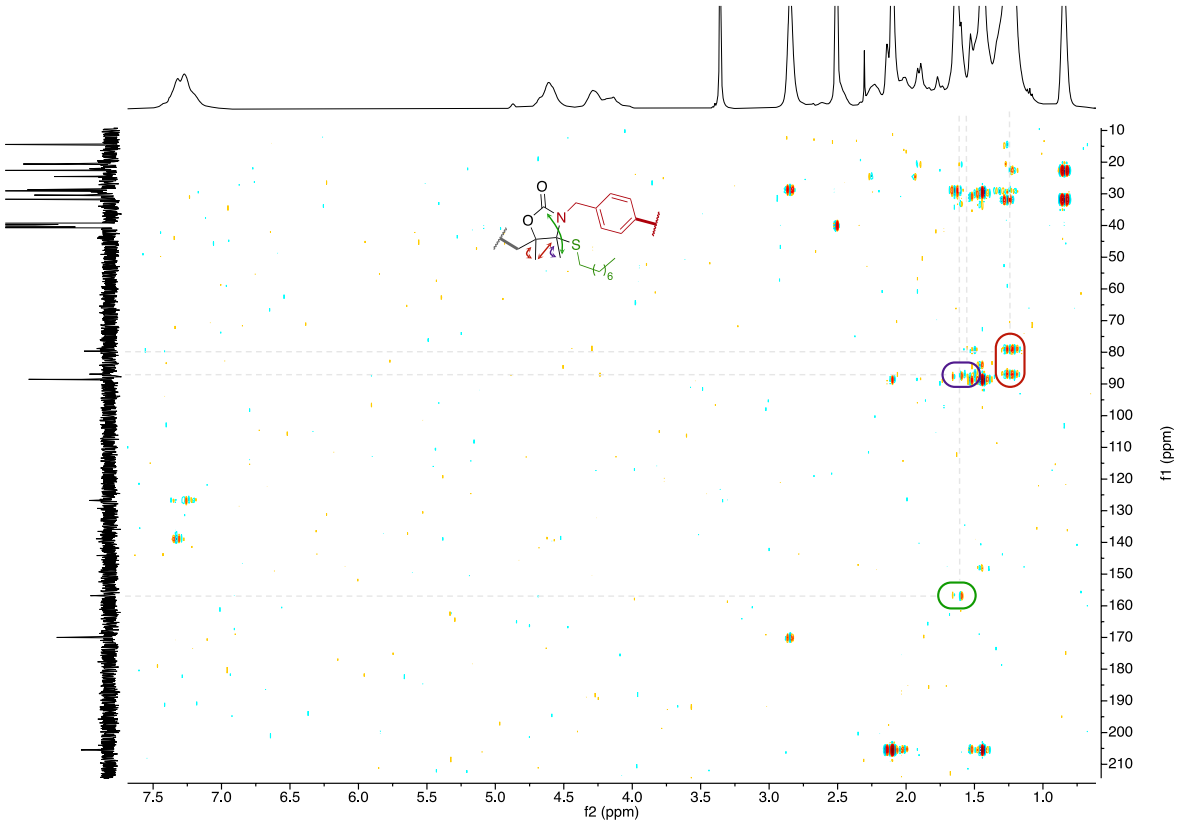

Figure S113 – ^{1}H-^{13}C HMBC NMR spectrum of pure polymer functionalized with n-octanethiol (400 MHz, DMSO-d_6).

P(A3T1)C dehydrated functionalized with methyl 3-mercaptopropionate

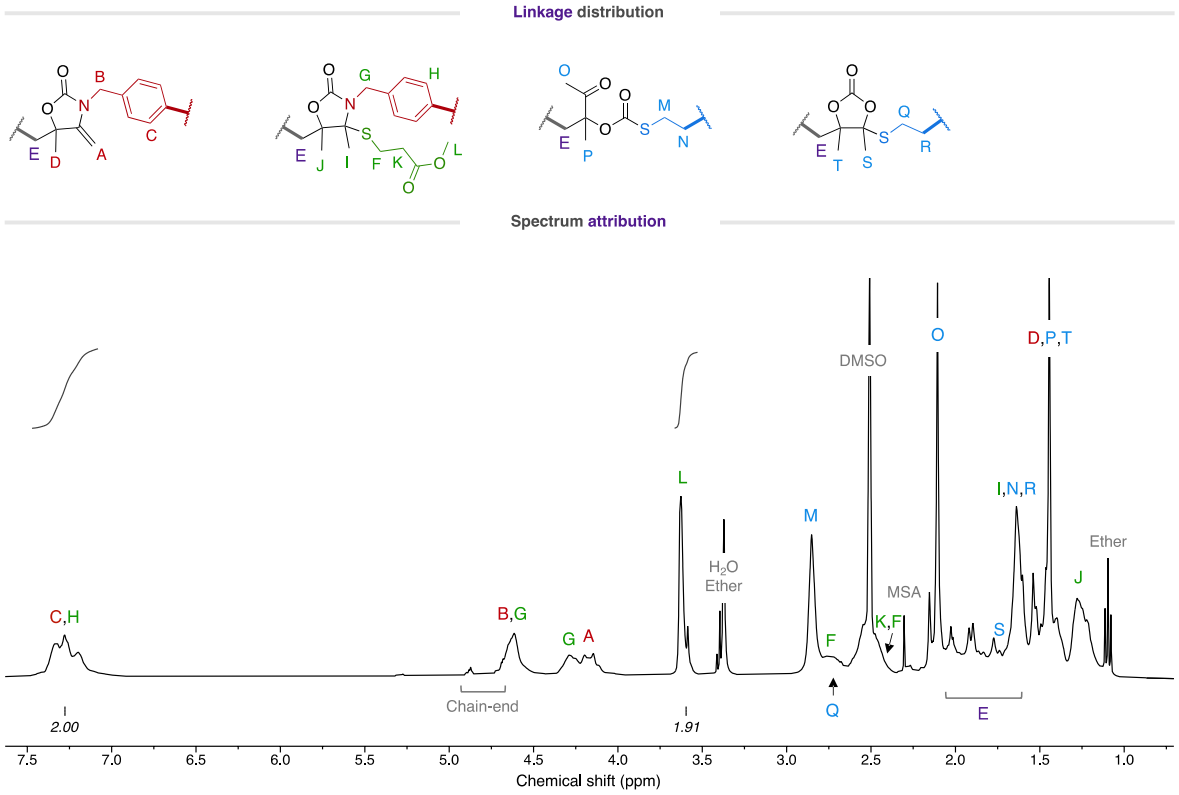

Figure S114 – ^{1}H-NMR spectrum of pure polymer functionalized with methyl 3-mercaptopropionate (400 MHz, DMSO-d_6).

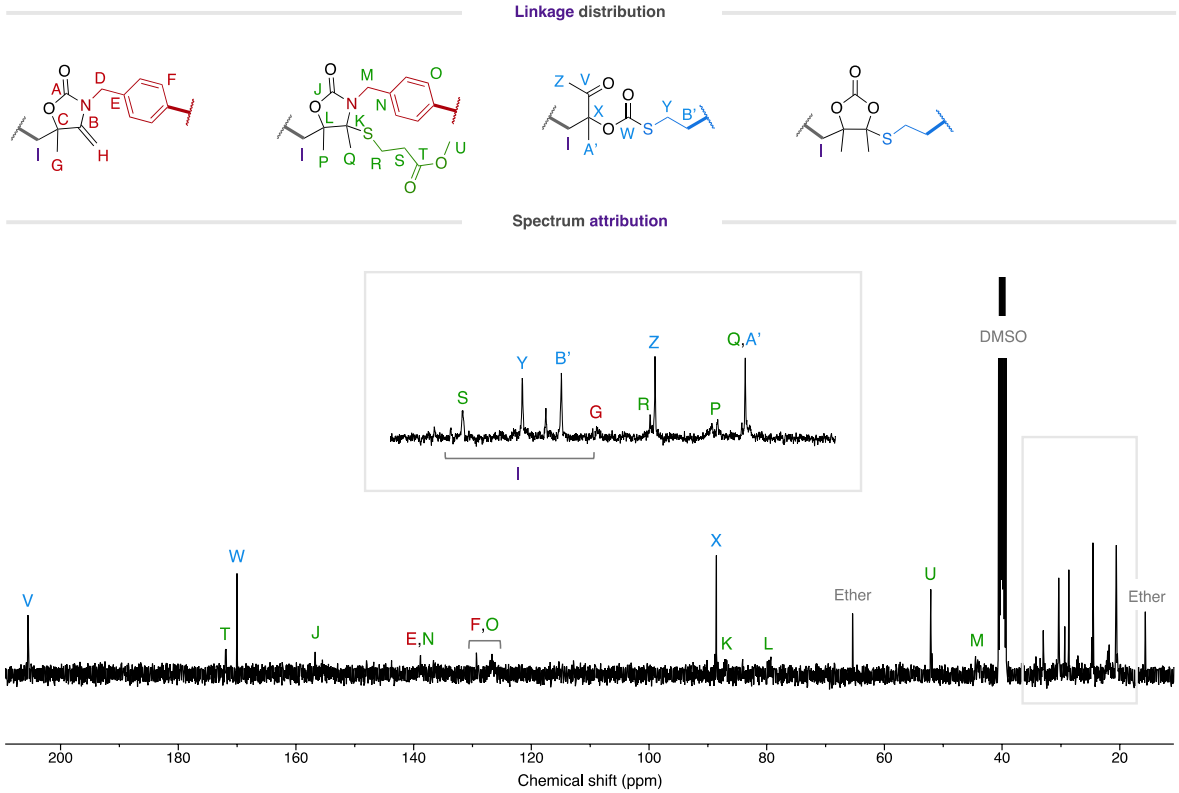

Figure S115 – ^{13}C-NMR spectrum of pure polymer functionalized with methyl 3-merceptopropionate (400 MHz, DMSO-d_6).

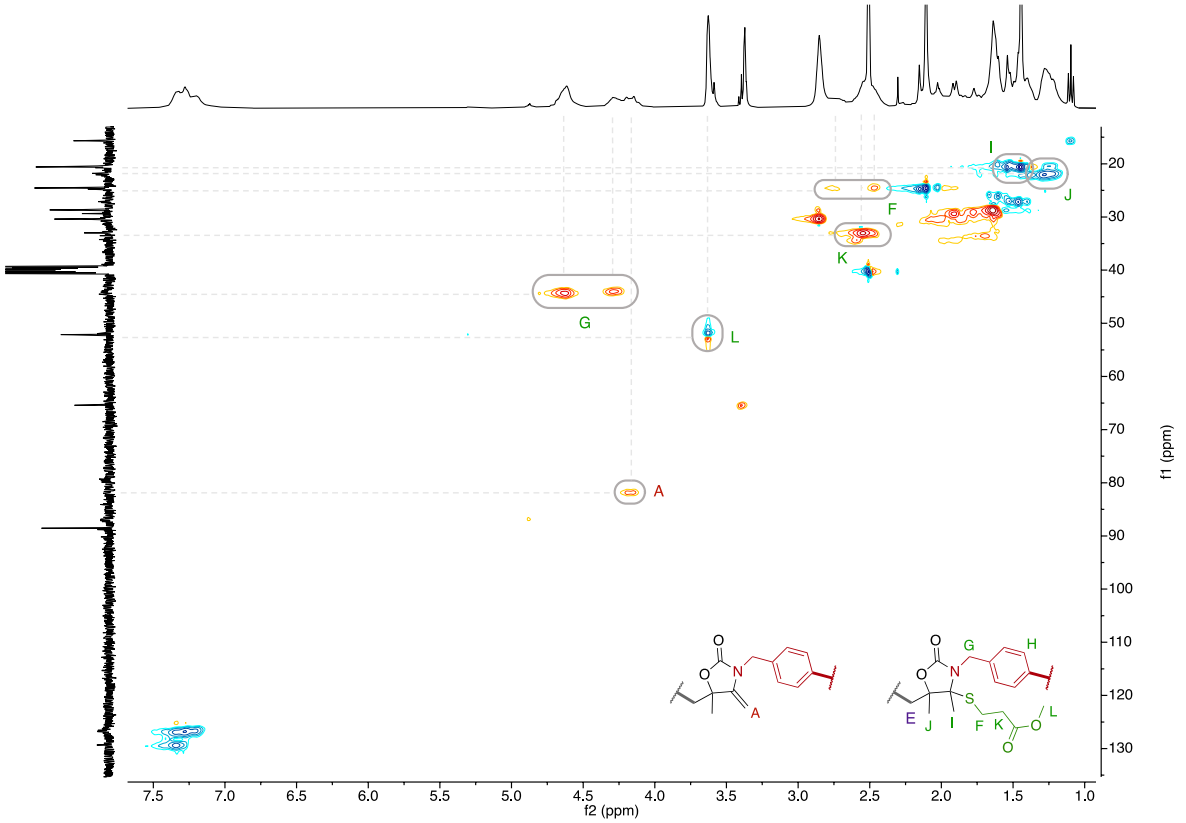

Figure S116 – ^{1}H-^{13}C HSQC NMR spectrum of pure polymer functionalized with methyl 3-mercaptopropionate (400 MHz, DMSO-d_6).

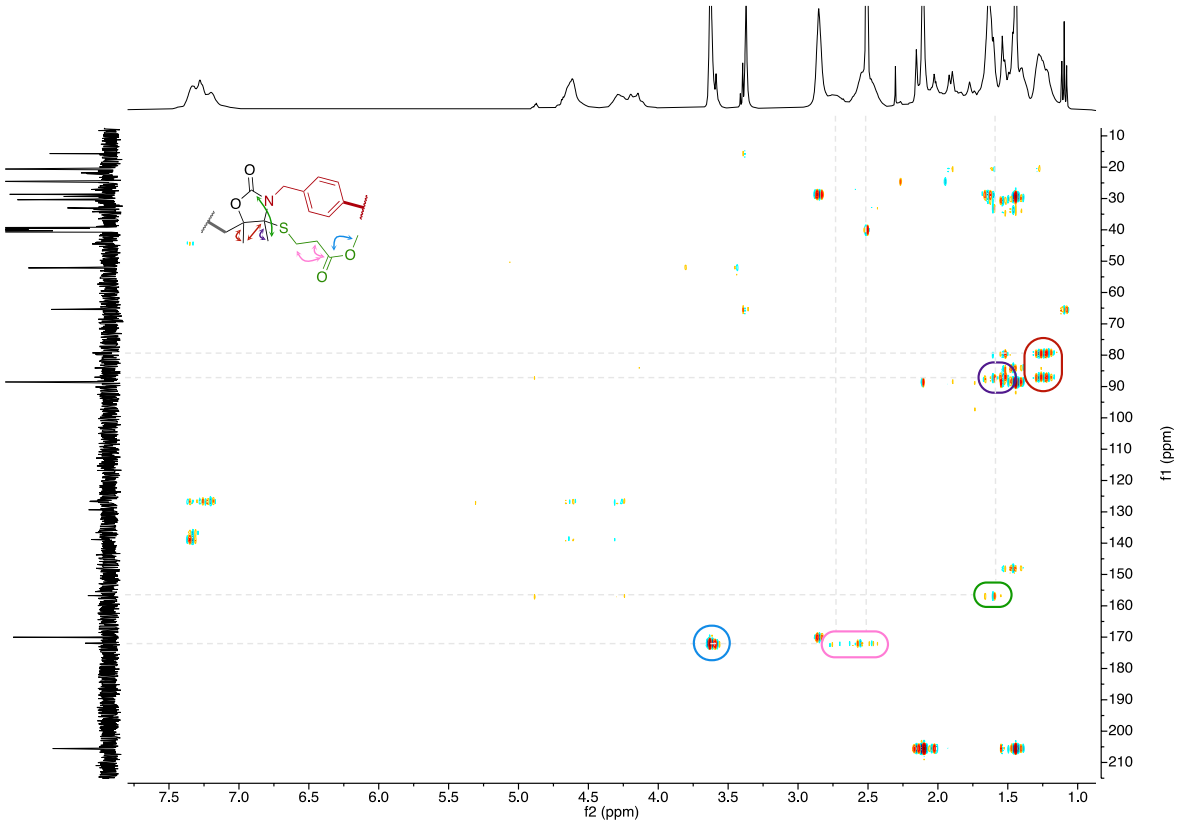

Figure S117 – ^{1}H-^{13}C HMBC NMR spectrum of pure polymer functionalized with methyl 3-mercaptopropionate (400 MHz, DMSO-d_6).

16. Characterization of polymer P(A1T3)C

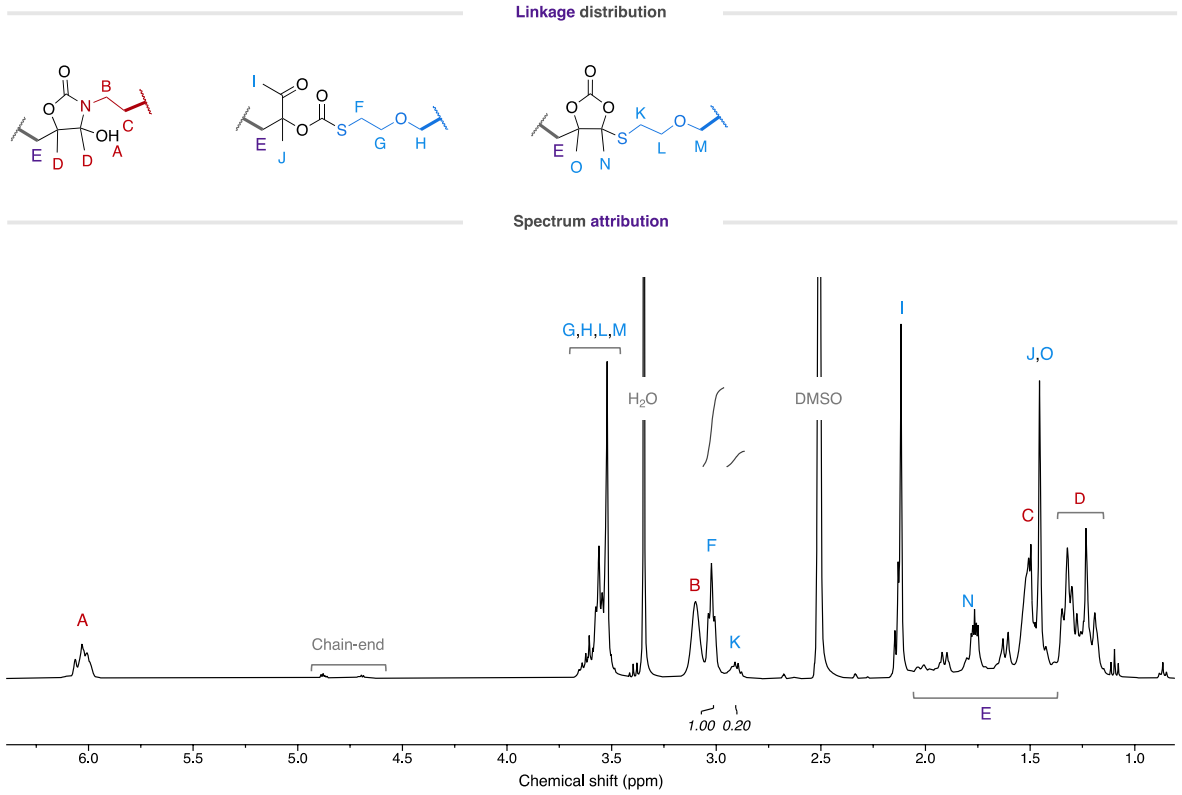

Figure S118 – ^{1}H-NMR spectrum of P(A1T3)C (400 MHz, DMSO-d_6).

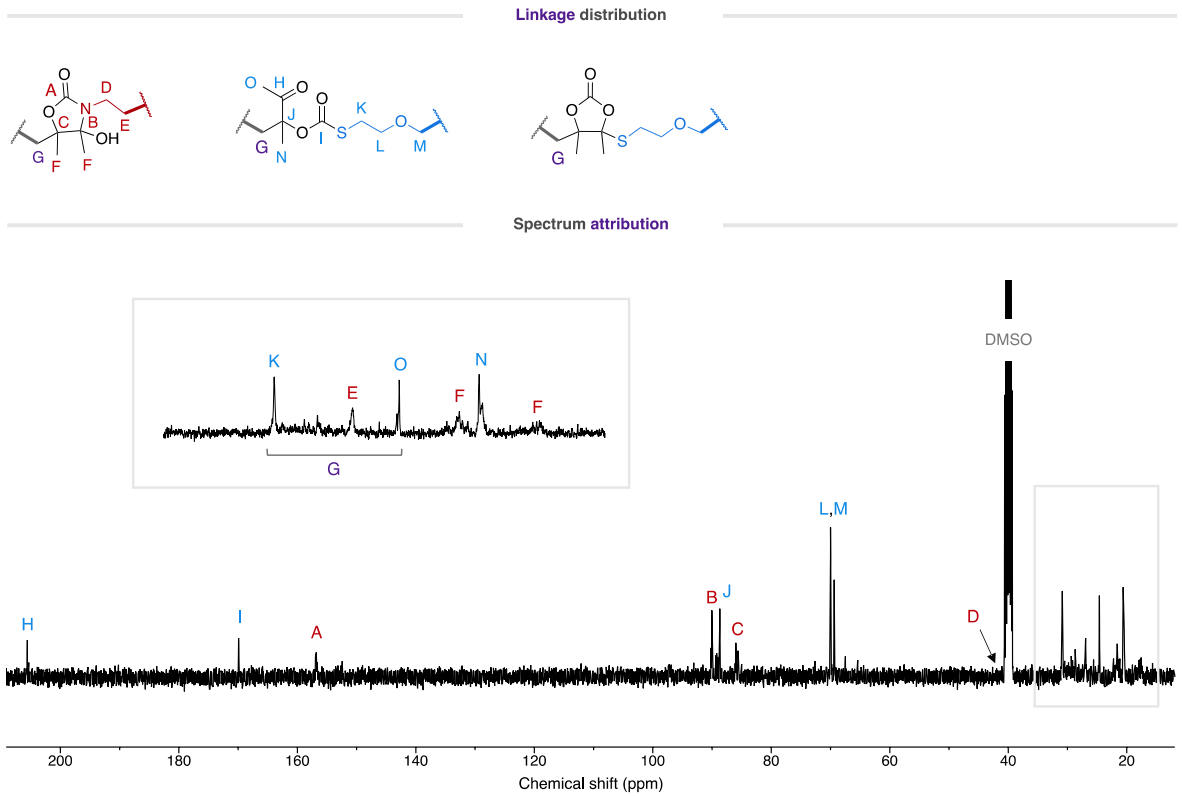

Figure S119 – ^{13}C-NMR spectrum of P(A1T3)C (400 MHz, DMSO-d_6).

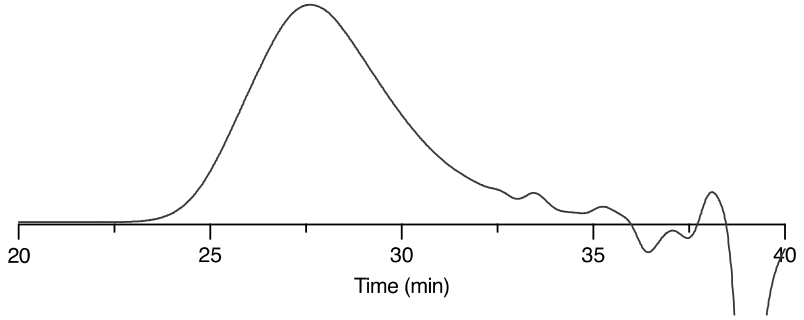

Figure S120 – SEC chromatogram (before purification) of P(A1T3)C.

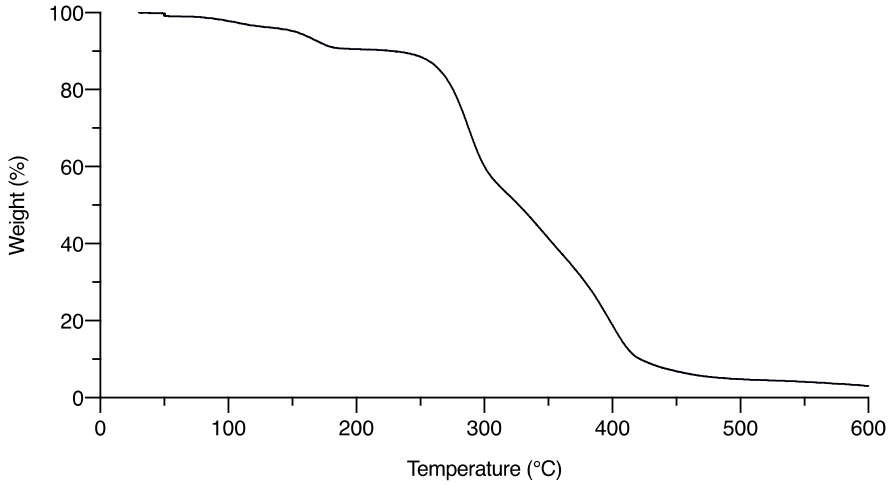

Figure S121 – TGA plot of P(A1T3)C.

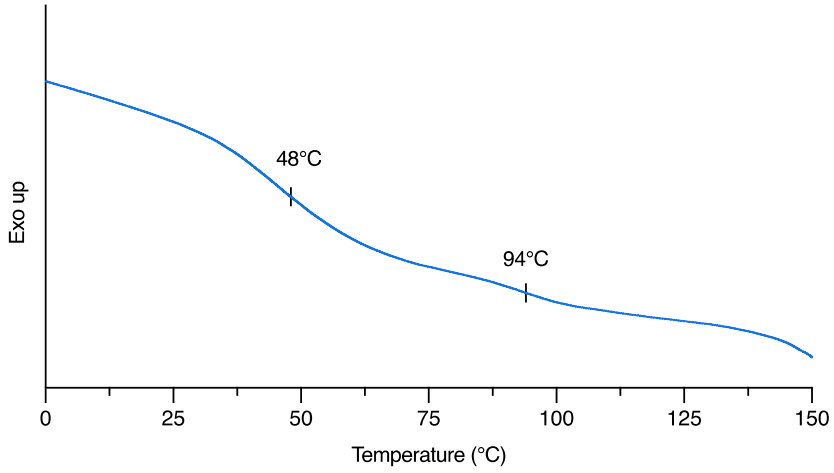

Figure S122 – Reversing heat flow by modulated DSC of P(A1T3)C.

17. Setup for the lap-shear tests experiments

As some specimens have shown high brittleness, some of the samples were breaking before the test when fixing them in the pneumatic clamps. To avoid this problem, a homemade setup made of a hook was developed, thus giving freedom to the sample when placing it in the clamps.

Figure S123 – Homemade setup for the lap-shear tests on prepared specimens.

18. References

1 S. Gennen, B. Grignard, T. Tassaing, C. Jérôme and C. Detrembleur, *Angewandte Chemie International Edition*, 2017, **56**, 10394–10398.

2 T. Habets, F. Siragusa, B. Grignard and C. Detrembleur, *Macromolecules*, 2020, **53**, 6396–6408.

3 A. A. OSWALD, F. NOEL and A. J. STEPHENSON, *The Journal of Organic Chemistry*, 1961, **26**, 3969–3974.

4 W. E. Thompson, R. J. Warren, I. B. Eisdorfer and J. E. Zarembo, *Journal of Pharmaceutical Sciences*, 1965, **54**, 1819–1821.

5 B. Chenon and C. Sandorfy, *Canadian Journal of Chemistry*, 1958, **36**, 1181–1206.